8-2019

Possible Schemes for a Single Photon Switch

Hemlin Swaran Rag
University of Arkansas, Fayetteville

Possible Schemes for a Single Photon Switch

A dissertation submitted in partial fulfillment
of the requirements for the degree of
Doctor of Philosophy in Physics

by

Hemlin Swaran Rag
Pondicherry University
Master of Science in Physics, 2010
University of Arkansas
Master of Science, 2015

August 2019
University of Arkansas

This dissertation is approved for recommendation to the Graduate Council.

Julio Gea-Banacloche, Ph.D.
Dissertation Director

Surendra Singh, Ph.D.
Committee Member

Reeta Vyas, Ph.D.
Committee Member

Pradeep Kumar, Ph.D.
Committee Member

Mark Arnold, Ph.D.
Committee Member

Abstract

I consider the effectiveness of a single control photon to route a target photon using two processes: the first one uses the transient excitation of a two-level system and the second one which uses the permanent population transfer in a three-level Λ-system to route the target photon. In the absence of a single control photon and when the system has additional decay channels, I find ways to optimize the success probability of routing with an increasing number of photons in the control field.

Acknowledgements

I am fortunate that I got Dr. Julio as my adviser and I am deeply indebted to him for accepting, training, and guiding me. I sincerely thank him for his encouragement and constant support. His amazing intuition and unparalleled ability to spot errors spearheaded my research in the right direction and helped me in shaping my projects into the current form. For all your help and support, I don't think I have enough words to thank you. Dr. Julio, you were phenomenal, and I truly enjoyed working with you.

I want to express my gratitude to Dr. Singh for his outstanding classes, his willingness to discuss and clarify my doubts and questions. Thank you, Dr. Singh and Dr. Vyas for your caring and moral support. Further, I want to thank my other committee members Dr. Mark Arnold and Dr. Pradeep Kumar for their comments and feedback.

I can't forget the help and motivation that I received from my gurus Dr. Satya, Dr. Alok, and Dr. Muruganandam; this thesis is meaningless without thanking them.

I am, really, lucky to have Bala as my roommate. He was always there whenever I needed help. Also, I want to thank my fellow graduate students Ambuj, Desalegn, Venkat, Bill, and my friends from India for their timely help and backing.

Finally, I am grateful to Achan, Amma, Chechi, Aami, and Razia for their unconditional love and care. Without you guys, this thesis wouldn't be possible.

Contents

List of Figures

Chapter 1

Introduction

A tunable light-matter interaction is at the heart of almost all modern optical technologies, including lasers, LED, and optical clocks. An enhanced, yet controllable, and low-loss interaction is required in most of these technologies. However, due to high loss, free space based light-matter interaction has limitations. This has been overcome, over the years, by mediating this interaction in a high-finesse cavity, or using superconducting microwave circuits[1, 2, 3, 4, 5, 6, 7, 8, 9]. The cavity-assisted interaction has not only improved optical technologies but also contributed significantly to our fundamental understanding of atomic systems; nevertheless cavity-mediated interaction is limited by the narrow bandwidth of the output photons [10, 11]. Moreover, it is challenging to make a high finesse cavity and it is extremely difficult to keep the atom inside the cavity.

On the other hand, superconducting microwave circuits, alternatively known in the community as circuit QED (quantum electrodynamics), is also a promising avenue. This new solid state approach, where an artificial atom and the coupling strengths of its various levels to the microwave resonator are engineered, provides an architecture for reliable and scalable quantum computing. Since we engineer the quantum system, various parameters can be tweaked and tuned to enhance the quantum effects and limit the environmental effects. As a result, circuit QED, the front runner in current day quantum technology, has gained a lot of attention and support from the industry side. However, the circuit QED set up requires a very low temperature (temperature of the order of millikelvin), and extremely precise fabrication techniques to limit the effect of external noise. Furthermore, there are a

few practical challenges such as the fact that conversion of a microwave photon to an optical photon is required for long range communication, and improving the atomic coherence of the artificial atom.

Another possibility is to use an atomic system that is coupled to a low-loss nanophotonic waveguide. Recently, considerable efforts have gone into developing such cavity-free systems. These waveguide based systems are promising as they offer low-loss and ultra strong coupling between the atom and the waveguide mode [12, 13, 14, 15, 16, 17, 18]. Also, it is fairly easy to integrate these nanophotonic waveguide systems on a chip, and therefore, they are certainly scalable. Here, I will use the techniques of waveguide QED that have been developed recently to discuss a possible scheme of photon routing.

Photons are excellent carriers of information, as they interact very weakly with each other in free-space, they are ideal for quantum information processing and long distance communication. Therefore, photon routers, which are required to take the information encoded photons in various direction for writing, reading, and manipulating the data, play a vital role in optical based quantum information processing and networks. Keeping that in mind, I study a simple routing scheme that could be potentially realized in a simple experimental setup.

Various schemes are available for routing a single-photon [19, 20, 21, 22, 23]. Most of these schemes involve a strong control field to route a single target photon. However, my objective is to achieve the routing with minimum resources. In particular, I want to see, is it possible to route a photon using a single control photon?. If not, how does the success probability increase with increasing number of photons?.

In the following chapters, I will use the techniques of waveguide QED to address this

question. In the first chapter, starting with the derivation of the Hamiltonian, I will introduce the pure-state analysis techniques to study the interaction of a single-photon multimode Fock state with a two-level system (TLS) in a waveguide. The single-photon-TLS result is absolutely paramount for all the routing schemes that we will see in this thesis. Although I will limit my discussion to a single-sided waveguide, I will also make remarks on extending this work to a bidirectional setup. In the latter part of the chapter, we will see how to extend this model to an atomic system with more than two levels and the interaction involving multiple fields, and how to use those systems effectively for routing a single photon. Firstly, I will discuss a routing scheme which involves the interaction of a target and a control photon with a three-level V-system, and we will see that, under ideal conditions, the success of this transient excitation scheme critically depends on the efficient excitation of the V-system by the control photon; which in turn depends on the control photon pulse shape. The second chapter will focus on how the transient excitation, which in turn characterizes the routing probability, increases with increasing number of control photons in the presence of external decay. The final chapter, on the other hand, explores the possibility of a routing scheme which relies on permanent population transfer on a Λ-system.

Chapter 2

Waveguide QED

In this chapter, I intend to discuss the interaction of a multimode photon field with a two-level atomic system (TLS) in a one dimensional geometry. Here, I will use pure state analysis (unitary frame work – no external loss in the system) to obtain most of the results. I have organized this chapter in the following way: the chapter starts with a brief derivation of interaction Hamiltonian of a TLS and quantized field in a single-sided geometry, and subsequently I will show how to handle analytically a single photon interaction in this one dimensional geometry. Further, I will make a couple of remarks on interaction in a bidirectional geometry. In the later part, I will use the single photon, in a single-sided setup, result to build a conditional phase gate using a three level V-system and two different photons in a unidirectional setup, and finally I will discuss how one can effectively use all these results to build a photon router.

2.1 Hamiltonian

The Hamiltonian of a TLS interacting with a single set of quantized modes can be written as (neglecting the vacuum part)

$$\begin{aligned} H_{system} &= H_{atom} + H_{field} + H_I, \\ H_{field} &= \sum_k \hbar\omega_k a_k^\dagger a_k. \end{aligned} \tag{2.1}$$

The atomic Hamiltonian (H_{atom}), and the free field Hamiltonian (H_{field}) give a trivial evolution to the system; the interesting dynamics of the system comes from the interaction Hamiltonian (H_I). Therefore, I will choose the interaction picture to study this system.

Here, the dominant term in the interaction part comes from the dipole interaction, so I have neglected all higher order interactions.

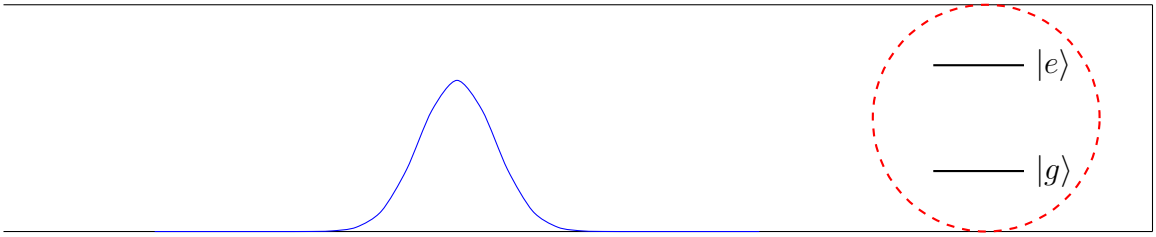

Figure 2.1: A cartoon of a single photon wavepacket that is interacting with a TLS in a single-sided setup. In a single-sided setup, the waveguide is terminated by a perfect mirror and the atome need to belocated close to the mirror: the distance beween the atom and the mirror should be smaller than the photon wavepacket size.

The interaction Hamiltonian, H_I, in terms of dipole operator $\overrightarrow{d} = -e\overrightarrow{r}$ ($-e$ is the charge of the electron and $\overrightarrow{r}$ is its coordinate relative to the atom), and electric field operator at the position of the atom $\overrightarrow{E}$ is

$$\begin{aligned} H_I &= -\overrightarrow{d}.\overrightarrow{E}, \\ H_I &= e\overrightarrow{r}.\overrightarrow{E}. \end{aligned} \tag{2.2}$$

It is useful to represent this Hamiltonian in a basis: a natural choice would be the bare atomic states, namely $|g\rangle$ (ground state), and $|e\rangle$ (excited state) as they form a complete set. Using the fact that the dipole operator has odd parity, one readily obtains

$$H_I = (\langle g|\, e\overrightarrow{r}\, |e\rangle\, |g\rangle\, \langle e| + \langle e|\, e\overrightarrow{r}\, |g\rangle\, |e\rangle\, \langle g|).\overrightarrow{E}. \tag{2.3}$$

2.2 Field quantization

The electric field is quantized in a box (of volume $V = AL$) with periodic boundary conditions. Further, without loss of generality, I have assumed $\langle g|\, e\overrightarrow{r}\, |e\rangle$, $\langle e|\, e\overrightarrow{r}\, |g\rangle$ are real and equal, and the temporal modes that are excited have the same polarization [24]. If we take our atom to be at the origin, the electric field, $E(0,t)$, is

$$\begin{aligned} E(z,t) &= E^{(+)}(z,t) + E^{(-)}(z,t), \\ E^{(+)}(z,t) &= i\sum_n \sqrt{\frac{\hbar\omega_n}{2\epsilon_0 V}} a_n e^{-i\omega_n(t-z/c)}, \\ E^{(+)}(0,t) &= i\sum_n \sqrt{\frac{\hbar\omega_n}{2\epsilon_0 V}} a_n e^{-i\omega_n t}. \end{aligned} \tag{2.4}$$

Although discrete modes are useful in numerical calculation, analytical calculations are typically easier with continuum modes. Taking $L \to \infty$, one can recast these discrete mode equations into continuum mode equations. Under this limit, the density of modes (ρ_ω) can be used to convert summation to an integral ($\sum_n = \int \rho_\omega \, d\omega$). Note that the density of modes depend on the choice of the boundary condition and dimension of the system. For this one-dimensional problem, the field operators, with the choice of periodic boundary conditions, transform to continuum-mode operators according to [25]

$$\begin{aligned} &\omega_n L = 2n\pi c, \\ &\mathrm{d}\omega(L/2\pi c) = \mathrm{d}n, \\ &\sum_n = \frac{L}{2\pi c}\int \mathrm{d}\omega, \\ &a_\omega = -\sqrt{\frac{L}{2\pi c}}\, a_n \\ &E^{(+)}(0,t) = -i\sqrt{\frac{\hbar}{4\epsilon_0 A\pi c}}\int \sqrt{\omega}\, a_\omega e^{-i\omega t}\mathrm{d}\omega. \end{aligned} \tag{2.5}$$

The minus sign in the definition of a_ω is arbitrary as the operators can be defined up to a phase factor. To be precise, the integral over ω should be running between $(0 \to \infty)$; instead of between $(-\infty \to \infty)$. A couple of assumptions are made to take the integral limit to $-\infty$, which I will clarify shortly. Finally, taking into account the time evolution of the atomic operator $\sigma_0 = |e\rangle \langle g|$

$$\sigma(t) = \sigma_0 \, e^{-i\omega_0 t}, \tag{2.6}$$

where ω_0 is the atomic transition frequency, the Hamiltonian takes the form

$$\begin{aligned} H_I &= \frac{-i\hbar\sqrt{\frac{\hbar\omega_p}{4\epsilon_0 A\pi c}}\,\langle b|\, e\overrightarrow{X}\,|a\rangle}{\hbar}\int \sigma^\dagger a_\omega e^{-i(\omega-\omega_0)t}\mathrm{d}\omega + \frac{i\hbar\sqrt{\frac{\hbar\omega_p}{4\epsilon_0 A\pi c}}\,\langle b|\, e\overrightarrow{X}\,|a\rangle}{\hbar}\int \sigma a_\omega^\dagger e^{i(\omega-\omega_0)t}\mathrm{d}\omega, \\ H_I &= -i\hbar g\int \sigma^\dagger a_\omega e^{-i(\omega-\omega_0)t}\mathrm{d}\omega + i\hbar g\int \sigma a_\omega^\dagger e^{i(\omega-\omega_0)t}\mathrm{d}\omega. \end{aligned} \tag{2.7}$$

In writing Eq.(2.7), the terms that oscillate with a frequency $\omega + \omega_0$ are neglected; such an approximation, in literature, is called the rotating wave approximation (RWA). Although RWA is well justified in the optical regime, one needs to be extremely careful when applying this approximation to a lower frequency regime. In RWA, only the field frequencies that are close to the atomic transition frequency ω_0 are important; therefore, it is safe to extend the integral limit to $-\infty$, and extending the limit without RWA can lead to spurious effect [26]. Furthermore, I will assume the initial state of the field to have a wavepacket structure whose carrier frequency is ω_p. In such a case, frequencies that contribute, significantly, to the integral in Eq.(2.5) are those which are close to ω_p, and it justifies the replacement of $\sqrt{\omega}$ with $\sqrt{\omega_p}$.

If the carrier frequency is not in resonance with the transition frequency (i.e

$\omega_p - \omega_0 = \Delta$ (detuning)), the interaction Hamiltonian, in terms of detuning, is

$$H_I = -i\hbar g \int \sigma^\dagger a_{\omega'} e^{-i(\omega'+\Delta)t} \mathrm{d}\omega' + i\hbar g \int \sigma a^\dagger_{\omega'} e^{i(\omega'+\Delta)t} \mathrm{d}\omega'. \tag{2.8}$$

At this point, the frequencies ω' are small quantities, that is , they represent the deviation from the central pulse frequency ω_p. In other words, ω' in this equation is equal to $\omega - \omega_p$ in the notation of Eq.(2.7). Furthermore, $g = \sqrt{\frac{\hbar\omega_p}{4\epsilon_0 A\pi c\hbar^2}} \langle g| \, e\overrightarrow{r} \, |e\rangle$ characterizes the coupling strength of the interaction between the field and the TLS. By defining a new multimode operator [27] in terms of the "slowly-varying" field operator

$$A_0(t) = \frac{1}{\sqrt{2\pi}} \int a_{\omega'} e^{-i\omega' t} \mathrm{d}\omega', \tag{2.9}$$

the Hamiltonian takes the compact form:

$$H_I = -i\hbar g \sigma^\dagger \sqrt{2\pi} A_0(t) e^{-i\Delta t} + i\hbar g \sigma \sqrt{2\pi} A_0^\dagger(t) e^{i\Delta t}. \tag{2.10}$$

It is worth spending time to understand the action of this multimode field operator ($A_0(t)$), which satisfies the equal time commutation relation

$$\left[A_0(t), A_0^\dagger(t')\right] = \delta(t - t'), \tag{2.11}$$

on an initial field state as it will be recurring in later chapters . On a mutimode 'N' photons Fock state

$$|N\rangle \equiv \frac{1}{\sqrt{N!}} \left(\int \tilde{f}(\omega) a^\dagger_\omega \mathrm{d}\omega \right)^N |0\rangle \,, \tag{2.12}$$

where $\tilde{f}(\omega')$ gives the initial pulse profile of photon

$$f(t) = \frac{1}{\sqrt{2\pi}} \int \tilde{f}(\omega) e^{-i\omega t} \mathrm{d}\omega, \tag{2.13}$$

the action of $A_0(t)$ leads to

$$A_0(t)\,|N\rangle = \sqrt{N} f(t)\,|N-1\rangle\,. \tag{2.14}$$

This can be easily verified using Eq.(2.12) and Eq.(2.13).

2.3 Single photon-TLS interaction

In this section, I will focus on the interaction of a TLS with a single photon Fock state in a unidirectional waveguide as shown in Figure 2.1. Extension of this result to a bi-directional waveguide is straightforward and will be commented on at the end. Various approaches are available to handle this problem, including the Heisenberg Langevin formalism [28, 29], diagrammatic summation techniques, scattering matrix formalism, green function approach, Lehmann-Symanzik-Zimmermann reduction approach, input-output formalism, Bethe anzatz [30, 31, 32, 33, 34, 35, 36, 37, 38, 39, 40, 41, 42], stochastic and genaralized master equation method [43, 44, 45, 46], and pure-state wavefunction analysis[47, 48]. It is remarkable that most of these techniques were developed very recently. To deal with with single photon-TLS interaction, I will use pure-state analysis[27, 47, 49].

Consider the case in which the atom is initially in the ground state; the total state vector can be written as

$$|\psi\rangle = |\psi_g\rangle\,|g\rangle + |\psi_e\rangle\,|e\rangle\,, \tag{2.15}$$

where, the initial field state, $|\psi_g(0)\rangle = |1\rangle$, is a single photon Fock state (see for instance Eq.(2.12)) and $|\psi_e(0)\rangle = |0\rangle$, the vacuum. Using the Schrodinger equation,

$\imath\hbar\partial/\partial t\,|\psi\rangle = H_I\,|\psi\rangle$ the equations of motion for $|\psi_g\rangle$ and $|\psi_e\rangle$ are then

$$\frac{\partial}{\partial t}\,|\psi_e\rangle = -g\sqrt{2\pi}A_0(t)e^{-i\Delta t}\,|\psi_g\rangle\,, \tag{2.16a}$$

$$\frac{\partial}{\partial t}\,|\psi_g\rangle = g\sqrt{2\pi}A_0^\dagger(t)e^{i\Delta t}\,|\psi_e\rangle\,. \tag{2.16b}$$

Formally integrating Eq.(2.16b) and substituting in Eq.(2.16a) will result in

$$|\psi_g(t)\rangle = |\psi_g(0)\rangle + g\sqrt{2\pi}\int_0^t A_0^\dagger(t')e^{i\Delta t'}\,|\psi_e(t')\rangle\,\mathrm{d}t', \tag{2.17a}$$

$$\frac{\partial}{\partial t}\,|\psi_e\rangle = -\sqrt{2\pi g^2}e^{-i\Delta t}f(t)\,|0\rangle - 2\pi g^2\int_0^t e^{i\Delta(t-t')}A_0(t)A_0^\dagger(t')\,|\psi_e(t')\rangle\,\mathrm{d}t'. \tag{2.17b}$$

The last expression of Eq.(2.17b) can be put in normal order by using Eq.(2.11), which gives

$$\frac{\partial}{\partial t}\,|\psi_e(t)\rangle = -\sqrt{2\gamma}e^{-i\Delta t}f(t)\,|0\rangle - \gamma\,|\psi_e(t)\rangle - 2\gamma\int_0^t e^{i\Delta(t-t')}A_0^\dagger(t')A_0(t)\,|\psi_e(t')\rangle\,\mathrm{d}t', \tag{2.18}$$

where I have used the spontaneous decay rate, $\gamma = \pi g^2$, to simplify the expression. Furthermore, it can be integrated formally by introducing an integrating factor $e^{-\gamma t}$:

$$|\psi_e(t)\rangle = -\sqrt{2\gamma}\int_0^t e^{-\gamma(t-t')-i\Delta t'}f(t')\,\mathrm{d}t'\,|0\rangle - 2\gamma\int_0^t \mathrm{d}t'\int_0^{t'}\mathrm{d}t''\,e^{-\gamma(t-t')}A_0^\dagger(t'')A_0(t')\,|\psi_e(t'')\rangle \tag{2.19}$$

Equation (2.19) can be taken as the starting point of a recursive solution that will eventually terminate if the initial state $\psi_g(0)$ has a finite number of photons. Normal ordering of multimode field operators, at each iteration, ensure the termination of the series. For a single photon input state, a single iteration is sufficient to get the solution. After a single iteration, Eq. (2.19) reads

$$|\psi_e(t)\rangle = -\sqrt{2\gamma}\int_0^t e^{-\gamma(t-t')-i\Delta t'}f(t')\,\mathrm{d}t'\,|0\rangle\,. \tag{2.20}$$

Note that one may need to perform N iteration for a N-photon input state. For a small number of photons, it may be possible to get an expression for the probability amplitude of the excited state and that for the ground state. However, it gets harder with increasing numbers of photons. Since the pulse will reach the position of the atom at time $t = 0$, the probability amplitude of the excited state is zero for $t < 0$. Therefore lowering the lower limit of integration is not going to contribute to the integral, and we can safely extend it to $-\infty$.

$$|\psi_e(t)\rangle = -\sqrt{2\gamma} \int_{-\infty}^{t} e^{-\gamma(t-t')-i\Delta t'} f(t') \, \mathrm{d}t' \, |0\rangle \tag{2.21}$$

Now the single photon transient excitation probability, $P_e(t) = \langle\psi_e(t)|\psi_e(t)\rangle$, can be obtained easily from Eq.(2.20), and can be shown that, when optimized, the transient excitation probability, even at the level of single photon, can reach 1; also, the pulse shape is an important quantity that has strong influence on transient probability. As it requires a thorough discussion, I will devote an entire chapter to transient excitation probability.

Finally, following a straightforward substitution of Eq.(2.20) in Eq.(2.17a), one gets the scattered field state as

$$|\psi_g(t)\rangle = |\psi_g(0)\rangle - 2\gamma \int_{-\infty}^{t} A_0^\dagger(t') dt' \int_{-\infty}^{t'} e^{-\gamma(t'-t'')+i\Delta(t'-t'')} f(t'') \, \mathrm{d}t'' \, |0\rangle \, . \tag{2.22}$$

In many scattering problems, one might be interested in the scattered field state a long time after the interaction. The asymptotic single photon field state, that can be easily obtained from Eq.(2.22) by simply taking the integral limit to infinity, for zero detuning ($\Delta = 0$) is

$$\begin{aligned} |\psi_g(\infty)\rangle &= \int_{-\infty}^{\infty} A_0^\dagger(t) f(t) dt \, |0\rangle - 2\gamma \int_{-\infty}^{\infty} A_0^\dagger(t') dt' \int_{-\infty}^{t'} e^{-\gamma(t'-t'')} f(t'') \, \mathrm{d}t'' \, |0\rangle \, , \\ |\psi_g(\infty)\rangle &= \int_{-\infty}^{\infty} A_0^\dagger(t) \left(f(t) - 2\gamma G(t) \right) dt \, |0\rangle \, , \end{aligned} \tag{2.23}$$

where, I have introduced a new function

$$G(t) = \int_{-\infty}^{t} e^{-\gamma(t-t')} f(t') \, \mathrm{d}t'. \tag{2.24}$$

It is clear that $|\psi_g(\infty)\rangle$ corresponds to a single photon state with a new pulse shape, $f(t) - 2\gamma G(t)$. Consequently, the effect of a TLS on a single photon input state, in a single-sided setup is to modify the pulse shape. By computing the overlap between the input and output state, one gets a useful measure to quantify this pulse distortion. In literature, this overlap has been termed as fidelity, which is

$$e^{-i\phi}\sqrt{F} = \int_{-\infty}^{\infty} f^*(t) \left(f(t) - 2\gamma G(t)\right) dt. \tag{2.25}$$

2.4 Adiabatic regime

For a large enough coupling, that is when $\gamma T \gg 1$ (T is the pulse duration), following a repeated integration by parts of Eq.(2.24), $G(t)$ can expressed as a series [47] :

$$G(t) = \sum_{i=0} \frac{(-1)^i}{\gamma^{i+1}} f^{(i)}(t). \tag{2.26}$$

Here $f^{(i)}(t)$ stands for the i^{th} derivative of $f(t)$. When the coupling is large, it is sufficient to take only the 0^{th} order term in the series. In such case, the fidelity will be

$$\begin{aligned} e^{-i\phi}\sqrt{F} &= \int_{-\infty}^{\infty} f^*(t) \left(f(t) - 2\gamma f(t)/\gamma\right) dt, \\ e^{-i\phi}\sqrt{F} &= -\int_{-\infty}^{\infty} |f(t)|^2 dt, \\ e^{-i\phi}\sqrt{F} &= -1. \end{aligned} \tag{2.27}$$

It is interesting to note that in the adiabatic regime, or strong-coupling regime the pulse is not distorted after the interaction, but it acquires a phase of π after the interaction. As far

as this thesis is concerned, this result is crucial, and I will be invoking it in later sections. In many cases, knowing the spectrum of the scattered field will be very useful; this can be obtained by a straightforward Fourier transform of Eq.(2.23). The spectrum, with detuning, is

$$\begin{aligned} |\psi_b(\infty)\rangle &= \int_{\infty}^{\infty} a_\omega^\dagger \tilde{f}(\omega) \mathrm{d}\omega \, |0\rangle - 2\gamma \int_{\infty}^{\infty} a_\omega^\dagger \, \frac{\tilde{f}(\omega)}{\gamma - i(\Delta - \omega)} \mathrm{d}\omega \, |0\rangle \,, \\ |\psi_b(\infty)\rangle &= -\int_{\infty}^{\infty} \frac{\gamma + i(\Delta - \omega)}{\gamma - i(\Delta - \omega)} \tilde{f}(\omega) \; \hat{a}_\omega^\dagger \; \mathrm{d}\omega \, |0\rangle \,. \end{aligned} \tag{2.28}$$

Therefore, as a result of the adiabatic interaction with the TLS, the input pulse spectrum $\tilde{f}(\omega)$ is modified as $\dfrac{\gamma + i(\Delta - \omega)}{\gamma - i(\Delta - \omega)} \tilde{f}(\omega)$.

2.5 Bidirectional waveguide

This is a simple extension of the unidirectional waveguide setup: a new operator, say $B(t)$, that represents the modes traveling in the opposite direction, needs to be incorporated to the interaction part of Hamiltonian (Eq.(2.10)). For simplicity, I will consider the symmetric case in which all these modes couple to the atom with the same coupling constant. The bidirectional Hamiltonian, with zero detuning ($\Delta = 0$), will be

$$H_I = -i\hbar g \sigma^\dagger \sqrt{2\pi}[A_0(t) + B_0(t)] + i\hbar g \sigma \sqrt{2\pi}[A_0^\dagger(t) + B_0^\dagger(t)]. \tag{2.29}$$

The simple transformations $C(t) = [A_0(t) + B_0(t)]/\sqrt{2}$ and $D(t) = [A_0(t) - B_0(t)]/\sqrt{2}$ can put the above Hamiltonian in the same form as the unidirectional case Eq.(2.10):

$$H_I = -i\hbar g \sigma^\dagger 2\sqrt{\pi} C_0(t) + i\hbar g \sigma 2\sqrt{\pi} C_0^\dagger(t). \tag{2.30}$$

This has the same structure of Eq.(2.10) except for a factor of $\sqrt{2}$. Therefore, just by

defining $\gamma_b = 2\pi g^2$, the same final sate of the field (Eq.(2.22)), with $A_0(t)$ replaced by $C_0(t)$ throughout, will be applicable here. It is easy to verify the action of $C_0(t)$ on the input state, $|\psi_g(0)\rangle = |M, N\rangle$, gives

$$C_0(t)\,|M,N\rangle = \frac{f(t)}{\sqrt{2}}\left(\sqrt{M}\,|M-1,N\rangle + \sqrt{N}\,|M,N-1\rangle\right). \tag{2.31}$$

Here, the M right-traveling photons and N left-traveling photons are considered to have the same pulse shape, $f(t)$. For a single photon input state $|\psi_g(0)\rangle = |1,0\rangle$ the final field state is

$$\begin{aligned}
|\psi_g(t)\rangle &= |1,0\rangle - 2\gamma_b \int_{-\infty}^{t} C_0^\dagger(t')dt' \int_{-\infty}^{t'} e^{-\gamma_b(t'-t'')} C_0(t'')\,\mathrm{d}t''\,|1,0\rangle\,, \\
|\psi_g(t)\rangle &= \int_{-\infty}^{\infty} A_0^\dagger(t) f(t) dt\,|0,0\rangle - \gamma_b \int_{-\infty}^{t} dt' \int_{-\infty}^{t'} e^{-\gamma_b(t'-t'')}[A_0^\dagger(t') + B_0^\dagger(t')] f(t'')\,\mathrm{d}t''\,|0,0\rangle\,.
\end{aligned} \tag{2.32}$$

In the last step Eq.(2.31) is used to simplify the action of $C_0(t)$ on the initial state. The asymptotic limit is particularly useful here to look at the transport property of photons in this bidirectional geometry. In the asymptotic limit, Eq.(2.32) takes a neat form:

$$|\psi_g(\infty)\rangle = \int_{-\infty}^{\infty} (f(t) - \gamma_b G(t)) A_0^\dagger(t) dt\,|0,0\rangle - \gamma_b \int_{-\infty}^{\infty} G(t) B_0^\dagger(t) dt'\,|0,0\rangle\,. \tag{2.33}$$

As expected, the single photon, after scattering, can be found in either right-traveling mode or left-traveling mode with some probability. However, in the strong coupling regime where $\gamma_b G(t) \approx f(t)$, Eq.(2.33) simplifies as

$$|\psi_g(\infty)\rangle = -\int_{-\infty}^{\infty} f(t) B_0^\dagger(t) dt'\,|0,0\rangle\,. \tag{2.34}$$

This means that, under adiabatic condition, the photon after interaction will be found in

the left traveling modes: the TLS acts like an atomic mirror in the strong coupling regime and the photon gets reflected from it. This complete reflection of the photon is the bidirectional analogy of the π phase shift that we obtained in the unidirectional setup.

Here, the coupling strength has been assumed to be same for both sets of traveling modes, and this is expected in this kind of symmetric scenario. Although this assumption made the calculation much simpler, it may not be true for chiral waveguides, where the coupling strength depends on the direction of the modes; in such scenarios, we need to perform calculations by taking both the modes (left and right propagating modes) into account. The symmetric case has been thoroughly investigated in [47].

2.6 Three level V-system

The remarkable π phase shift of single photon, in a single sided geometry, opened up the possibility of building a conditional phase gate (CPHASE): a gate where the phase of a photon (target) is influenced by another photon (control). In the CPHASE gate, the role played by both the control and the target photons are, in fact, interchangeable. However, in a photon routing scheme, which uses a control photon to rout the target photon, we should be able to distinguish both the control and the target photons. Unfortunately, the TLS cannot distinguish two different photons; we require a system with more than two levels to distinguish two photons. On the other hand, three-level system, a straightforward extension of TLS, can distinguish two different photons acting on its two separate transitions. In practice, there are three different ways to consider a three-level system: lambda (Λ), ladder, and V-system. My objective here is to carefully analyze the potential of the V-system, together with two different photons in a single sided geometry, in which

the ground state is shared by two excited states, to act as a conditional phase gate.

The depiction of a three-level V-system, interacting resonantly with two different photons, is shown in Figure (2.2); where I represented the target (control) photon with red (blue) color. In this setup, the V-system, in the absence of the control photon, will act like a TLS. In such case, the target that is interacting adiabatically with the V-system will acquire π-phase. However, if we can invert the atom using the control photon, when the target arrives at the atom, the atom will be transparent to the target and thus it will acquire no phase. This is the key idea of this scheme and success of this scheme depends on the perfect excitation of the atom by the control photon. The following section will focus on theoretical analysis of this system and its feasibility to act as a CPHASE gate.

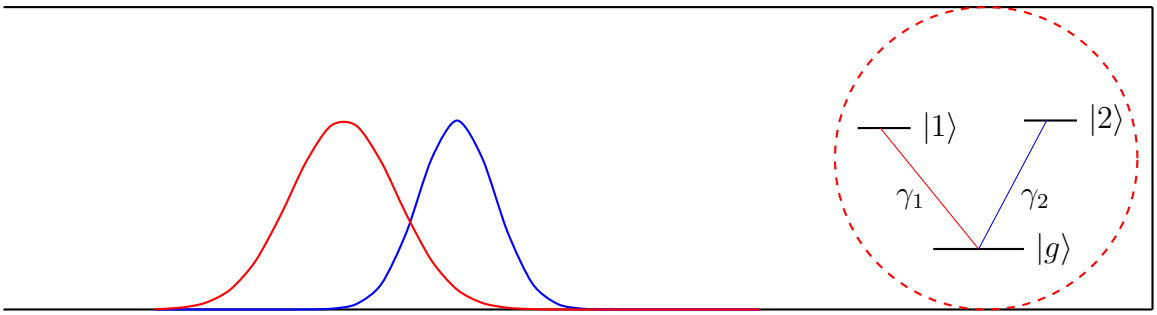

Figure 2.2: Depiction of three level V-system, interacting with two different photons, in a single sided geometry. The control photon is labeled with blue and the target is labeled with red color.

.

2.7 V-system Hamiltonian

The Hamiltonian of this system is a straightforward extension of Eq.(2.10). With an additional multimode operator A_{02} that corresponds to the annihilation operator of the

control photon which would be distinguished, for instance, either by its resonant frequency, or its polarization, the Hamiltonian of the system is

$$H_I = i\hbar\sqrt{2\gamma_1}\,\sigma_1^\dagger A_{01}(t) - i\hbar\sqrt{2\,\gamma_2}\,\sigma_2^\dagger A_{02}(t) + H.C. \tag{2.35}$$

Where I have used γ_1, γ_2 to represent the coupling strength of $|g\rangle \to |1\rangle$ and $|g\rangle \to |2\rangle$ transitions respectively. The action of this Hamiltonian on a most general atom-field state, $|\psi\rangle = |\psi_g\rangle\,|g\rangle + |\psi_1\rangle\,|1\rangle + |\psi_2\rangle\,|2\rangle$, and tracing over the atomic states will result in the following field state equations:

$$\begin{aligned} |\dot{\psi_g}\rangle &= \sqrt{2\gamma_1}A_{01}^\dagger(t)\,|\psi_1\rangle + \sqrt{2\gamma_2}A_{02}^\dagger(t)\,|\psi_2\rangle \\ |\dot{\psi_1}\rangle &= -\sqrt{2\gamma_1}A_{01}\,|\psi_g\rangle \\ |\dot{\psi_2}\rangle &= -\sqrt{2\gamma_2}A_{02}\,|\psi_g\rangle \end{aligned} \tag{2.36}$$

In what follows, I will choose two initial input photons, $|\psi_g(0)\rangle = |1,1\rangle$, acting resonantly on the separate legs of this V-system. For brevity, I will follow a simple notation where the position of photon in the input state matches with the corresponding transition in the atomic system. This makes the calculations easier to keep in track, and the action of multimode field operators on the input two photons state will be, simply, then

$$\begin{aligned} A_{01}\,|1,1\rangle &= f_1\,|0,1\rangle\,, \\ A_{02}\,|1,1\rangle &= f_2\,|1,0\rangle\,. \end{aligned} \tag{2.37}$$

I will use the same approach that I used in section 2.3 to get the asymptotic field state $|\psi_g(\infty)\rangle$; the simple strategy is to formally integrate the ground state field state, that is

$$|\psi_g(t)\rangle = |\psi_g(0)\rangle + \int_0^t dt'\sqrt{2\gamma_1}A_{01}^\dagger\,|\psi_1(t')\rangle + \int_0^t dt'\sqrt{2\gamma_2}A_{02}^\dagger\,|\psi_2(t')\rangle\,, \tag{2.38}$$

and substitute this equation in the remaining excited field state equations. After the substitution, the excited field state equations can be integrated to obtain closed form expressions, which are

$$\begin{aligned}
|\psi_1(t)\rangle = &-\sqrt{2\gamma_1}e^{-\gamma_1 t}\int_0^t dt'\ e^{\gamma_1 t'} f_1(t')\,|0\ 1\rangle + 2\gamma_2\sqrt{2\gamma_1}e^{-\gamma_1 t} \\
&\int_0^t dt'\ e^{\gamma_1 t'}\int_0^{t'} dt''\ A^\dagger_{02}(t'')f_1(t')e^{-\gamma_2 t''}\int_0^t dt'''\ e^{\gamma_2 t'''}f_2(t''')\,|0\ 0\rangle\,, \\
|\psi_2(t)\rangle = &-\sqrt{2\gamma_2}e^{-\gamma_2 t}\int_0^t dt'\ e^{\gamma_2 t'} f_2(t')\,|1\ 0\rangle + 2\gamma_1\sqrt{2\gamma_2}e^{-\gamma_2 t} \\
&\int_0^t dt'\ e^{\gamma_2 t'}\int_0^{t'} dt''\ A^\dagger_{01}(t'')f_2(t')e^{-\gamma_1 t''}\int_0^t dt'''\ e^{\gamma_1 t'''}f_1(t''')\,|0\ 0\rangle\,.
\end{aligned} \tag{2.39}$$

Substitution of these equations back into Eq.(2.38) followed by a single iteration will yield the final field state. Finally, by projecting the final field state onto the time state vector

$$|t_1,t_2\rangle = \int d\omega_1 \int d\omega_2 e^{i(\omega_1 t_1+\omega_2 t_2)}a^\dagger_{\omega_1}a^\dagger_{\omega_2}\,|0,0\rangle$$

we get the asymptotic field wavefunction as

$$\begin{aligned}
\langle t_1,t_2|\psi_g(\infty)\rangle = &\left(f_1(t_1)-2\gamma_1 G_1(t_1)\right)\left(f_2(t_2)-2\gamma_2 G_2(t_2)\right) - 4\gamma_1\gamma_2\left[e^{-\gamma_1(t_1-t_2)}\right. \\
&\left. G_1(t_2)G_2(t_2)\Theta\left(t_1-t_2\right) + e^{-\gamma_2(t_2-t_1)}G_1(t_1)G_2(t_1)\Theta\left(t_2-t_1\right)\right].
\end{aligned} \tag{2.40}$$

Where I have used $G_i(t)=\int_{-\infty}^t e^{-\gamma_i(t-t')}f_i(t')dt'$ to write the asymptotic field wavefunction in a compact form. Furthermore, I can rewrite this equation into a symmetric form by introducing a new notation where I will denote the smallest of t_1, t_2 by $t_<$. By letting $\gamma_>$ which is equal to γ_2 if $t_2>t_1$, and equal to γ_1 if $t_1>t_2$, Eq.(2.40) reads as

$$\langle t_1,t_2|\psi_g(\infty)\rangle = \prod_{i=1}^{2}\left(f_i(t_i)-2\gamma_i G_i(t_i)\right) - 4\gamma_1\gamma_2 e^{-\gamma_>|t_1-t_2|}G_1(t_<)G_2(t_<). \tag{2.41}$$

2.8 CPHASE gate

The final state, Eq.(2.41), is all that we needed to study the potential of this system to act as a CPHASE gate. In the absence of the control photon, this equation will be reduced to $(f_1(t) - 2\gamma_1 G_1(t))$. In such occasion, as I remarked earlier, the target photon of pulse profile, $f_1(t)$, which is interacting resonantly with the V-system, will only see a TLS and acquire the π- phase in the strong coupling regime (see Eq.(2.27). I want to control this phase by sending a control photon in a way that the target will not interact with the V-system: the control and the target are timed in a manner that the control will switch off the interaction of the target photon with the V-system. To make this happen, when the target will reach the atom, the control should invert the atom completely. In terms of fidelity, it means that I need to project the asymptotic field state onto the interacted control and the unmodified target photon, and I require this fidelity to be as close to one to realize a CPHASE gate. In mathematical terms, in the absence of control, I have

$$e^{-i\phi}\sqrt{F} = \int_{-\infty}^{\infty} f_1^*(t)\left(f_1(t) - 2\gamma_1 G_1(t)\right) dt = -1, \tag{2.42}$$

and in the presence of control, I require

$$e^{-i\phi}\sqrt{F} = \int_{-\infty}^{\infty}\int_{-\infty}^{\infty} \left[f_1^*(t_1)\left(f_2(t_2) - 2\gamma_2 G_2(t_2)\right)^* \langle t_1, t_2|\psi_g(\infty)\rangle\right] dt_1 dt_2 = 1. \tag{2.43}$$

Here, the fidelity serves as a good measure to characterize the performance of this gate. The effectiveness of this system as a CPHASE is reduced to the question: How well one can make the fidelity (Eq.2.43) close to one?. Moreover, the closeness of this fidelity, at the single photon level, critically depends on the ability of the control photon to excite the

atom completely. Unfortunately, not all single photon pulses can invert the atom with unit probability; the only single photon pulse profile which can perform the magic is the rising exponential pulse [50, 51] provided that the pulse duration is inverse of the coupling rate of the transition – a result that immediately follows from Eq.(2.21). Therefore, I will restrict my discussion to a case where the target has the familiar gaussian pulse shape ($f_1(t) = e^{-t^2/4T_1^2}/\sqrt{T_1\sqrt{2\pi}}$) and the control has this special rising exponential pulse profile ($f_2(t) = e^{t/T_2}\sqrt{2/T_2}$) with the pulse duration $T_2 = 1/\gamma_2$ to take the atomic system to state $|2\rangle$ with unit probability. With these pulse profiles, Eq.(2.42) and Eq.(2.43) are analytically solvable, and are expressible, as a series in terms of $1/\gamma_1 T_1$, and T_1/T_2:

$$\int_{-\infty}^{\infty} f_1^*(t)\left(f_1(t) - 2\gamma_1 G_1(t)\right) dt = -1 + \frac{1}{2(\gamma_1 T_1)^2} - \frac{3}{8(\gamma_1 T_1)^4} + O(1/(\gamma_1 T_1)^6), \tag{2.44}$$

$$\int_{-\infty}^{\infty}\int_{-\infty}^{\infty}\left[f_1^*(t_1)\left(f_2(t_2) - 2\gamma_2 G_2(t_2)\right)^* \langle t_1, t_2|\psi_g(\infty)\rangle\right] dt_1 dt_2 = 1 - 4\sqrt{\frac{2}{\pi}}\left(\frac{T_1}{T_2}\right) + \frac{2}{\gamma_1 T_1}\left(\frac{T_1}{T_2}\right) + 4\left(\frac{T_1}{T_2}\right)^2 - \frac{16}{3}\sqrt{\frac{2}{\pi}}\left(\frac{T_1}{T_2}\right)^3. \tag{2.45}$$

These fidelity expressions indicate that I can make them arbitrarily close to the required values by appropriately choosing the coupling strengths and the pulse durations. For instance, we could choose the duration of the target photon pulse (T_1) in such a way that $\gamma_1 T_1 \gg 1$ and at the same time it is much smaller compared to the control photon pulse duration (T_2); that is $T_2 \gg T_1$. This means that we need to choose T_1 in a manner that the target is essentially confine to the region where the control photon provides maximum excitation. As a remark, I want to mention that if I use an optimized gaussian pulse,

instead of a rising exponential pulse as the control photon, which can provide a maximum excitation of 87%, the overlap integral Eq. (2.45) will only be be as large as 0.63. The rising exponential pulse, the time reversed version of decaying exponential pulse, with its ability to invert the atom with unit probability makes it an ideal candidate for the control photon; yet, shaping a single photon with the rising exponential shape is by no means an easy task, and it is part of ongoing research activities[50, 51, 52, 53, 54, 55, 56, 57, 58, 59].

The coherent control of the phase of the target photon and thus obtaining the CPHASE gate is not the end of the story. It is possible to build a photon router, which is essential for future quantum networks and computers, by simply incorporating this single-sided V-system to an interferometer setup. I will discuss more on this topic in the following section. Finally, I want to emphasize that the success of this scheme critically depends on the shape of the control photon and careful timing of the control and target photons.

2.9 Photon routing

In this section, I want to discuss the possibility of building a photon router by coherently controlling the phase of the target photon. The idea here is to simply incorporate the single sided V-system setup to an arm of the Michelson ineterferometer.

We could route the photon by incorporating the single-sided V-system to the Michelson interferometer. Replacing one of the mirrors in the arm of the Michelson interferometer by the single-sided V-system, and accordingly feeding the control photon, we should be able to control the emergent port of the target photon. See, for instance, Figure 2.3 and Figure 2.4 for a possible realization of this scheme. It may be possible to use other interferometers for routing the target photon, but the scheme that uses Michelson interferometer looks

relatively simple. Finally, I want to emphasize that this schemes may not be as simple as I described; it may, still, require additional optical elements, such as optical circulator, for ensuring the unidirectionality of the modes.

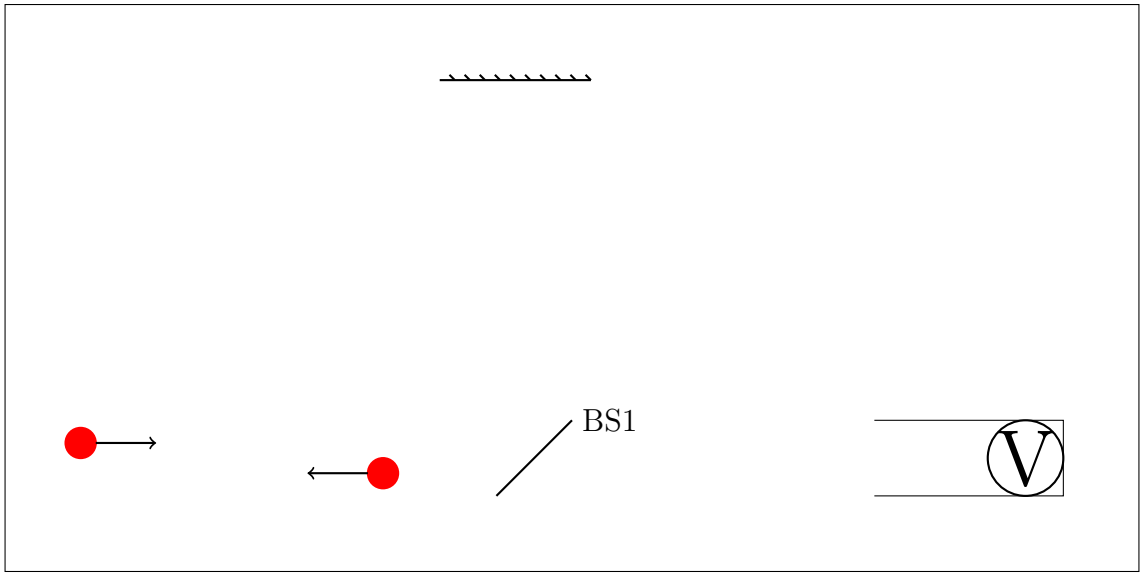

Figure 2.3: The behavior of a target photon (shown in red color) in a modified Michelson interferometer. In the absence of control photon, the V-system act as a mirror and impart a π shift to the target photon, and hence the emergent port of the target photon will be the same as the one it enters the interferometer.

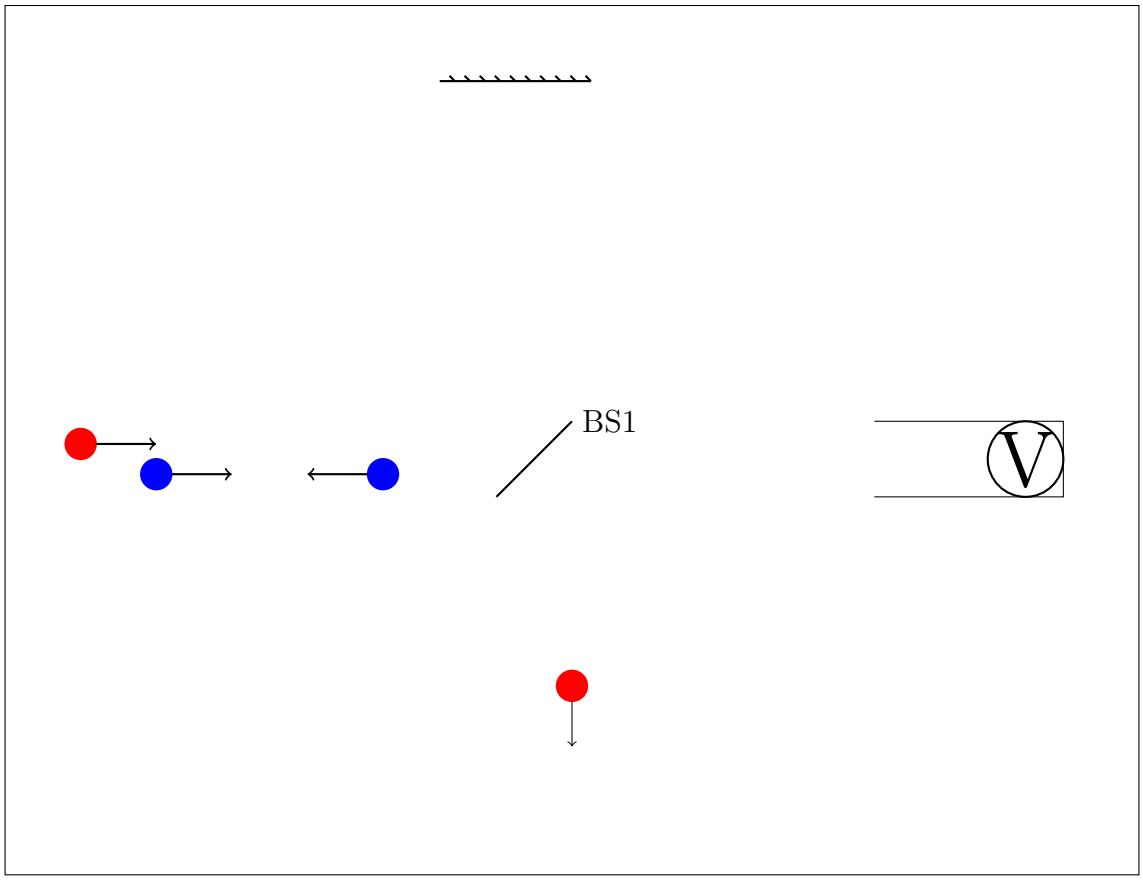

Figure 2.4: The behavior of a target photon (shown in red color), in the presence of control photon, in a modified Michelson interferometer. In the presence of control photon, the V-system will not impart π phase to the target, and therefore, the target will emerge out of the port that is orthogonal to the port through which it enters.

2.10 Conclusion and Remarks

I have given a detailed description of the quantized-light matter interaction in a waveguide and showed how to handle the system analytically when the number of photons are few. Although my primary focus was on the interaction in a single-sided setup, I have discussed the bi-directional scenario for a symmetric case. Further, as an extension to the simple case, I studied the interaction of two different photons with the V-system, and explored the possibility of building a conditional phase (CPHASE) gate with this interaction. Finally, I

also pointed a way to build a photon routing scheme using the single-sided V-system and utilizing the quantum coherence in the Michelson interferometer.

The central result of this chapter is the π phase imparted on a photon by the TLS in a single-sided adiabatic interaction, and most of the subsequent results are based on the coherent control of this phase using another control photon. I have used a three-level scheme for the coherent control of this phase and analytically characterized its potential to act as the CPHASE gate. It is seen that the success of this gate and the photon routing scheme critically depend on the control photon transient excitation probability, which in turn depends, at the single photon level, on the shape of the control photon pulse[60].

The method that I used here, pure state analysis, is robust in getting the final field state and the excitation probability of the TLS. Although, the focus was on asymptotic field state, the theory is dynamical and it is possible to get the system properties at any arbitrary time. It is also straightforward to extend the single photon results of this chapter to N-photon state [29, 47].

In spite of the fact that this method is simple, it may, still, require to do complicated manipulations to get the expectation value of interesting quantities; also, the approach is based on the unitary evolution, so decay into external modes (modes other than waveguide modes) is not possible to incorporate in this method; also, multimode coherent state calculations are difficult in this formalism.

In principle, this photon routing scheme should work in the ideal scenario namely: there is no external decay in the system, the control photon has the right shape for the perfect excitation of atomic system and the coupling strength of each levels have right magnitude to take the Eq.(2.44), and Eq.(2.45) to the desired value. However, in reality, it may be

difficult to achieve the perfect conditions; therefore, in the next chapter, I will analyze the problem in which the conditions are relaxed, and characterize the transient excitation probability, under external decay, with increasing number of photons.

Chapter 3

Transient excitation probability

3.1 Introduction

From the perspective of a single photon logic gate, or a switch, it is evident from the previous discussion that the transient excitation probability plays a crucial role in our scheme. Earlier works[50, 51] showed that, apart from the transverse-mode profile of the field, the temporal profile of the field has significant influence on the excitation probability. In addition, a thorough understanding of transient excitation probability will be useful to gain insights into atom-based single photon sources. Therefore, it is worth exploring, in great detail, the effect of pulse shapes on transient excitation probability

As I mentioned earlier, the transient excitation probability of a TLS can even reach unity, which is contrary to its steady-state counter part. The steady-state probability can reach a maximum value of 0.5, and that is why there are no two level lasers. To achieve unit excitation in the transient regime, one needs a very intense and short pulse, and this inversion is limited by the upper level decay time. The steady state value, however, can be achieved with CW (Continuous Wave) laser.

In the last chapter, I limited my discussion to a single photon, or maximum up to two photon interaction, and those results are applicable when the system has no external decay. I will relax these conditions in this chapter and study the transient excitation probability of TLS, under external decay, with increasing numbers of photons. I will use Heisenberg-Langevin (HL) formalism to study the system. This formalism is very useful as it allows to incorporate external decay into the system. Apart from this, the formalism is

very robust when it comes to multiphoton fields such as coherent states.

The chapter is organized in such a way that it starts with a brief derivation of optical Bloch equations for multimode fields. Subsequently, I will use these equations to study the excitation probability, and I will demonstrate how this probability scales with increasing numbers of photons. Being an operator method, getting the state of the output field in this HL formalism is slightly involved. Therefore, I will make a quick digression, at an appropriate place, and show how to obtain the output field state's wavefunction in this formalism.

3.2 Optical bloch equations

The derivation of optical Bloch equations directly follows from the Hamiltonian:

$$H = -i\hbar g \int \sigma^\dagger a_\omega e^{-i\omega t} d\omega + i\hbar g \int a_\omega^\dagger e^{i\omega t} \sigma d\omega - i\hbar G \int \sigma^\dagger b_\Omega e^{-i\Omega t} d\Omega + i\hbar G \int b_\Omega^\dagger e^{i\Omega t} \sigma d\Omega \quad (3.1)$$

This Hamiltonian is a straightforward extension of Eq.(2.8) with an additional operator, b_Ω, that represents the annihilation operator of the bath mode at frequency Ω. Further, I have taken the coupling strength of the TLS to the pulse mode (a_ω) to be g, and that of bath mode is G. In what follows, I will use Heisenberg equation of motion (for any operator A, the equation is given by $\dot{A} = i/\hbar\,[H, A]$) to get the equations of motion for the field operators a_ω and b_Ω; they are

$$\begin{aligned} \dot{a}_\omega &= g\sigma e^{i\omega t}, \\ \dot{b}_\Omega &= G\sigma e^{i\Omega t}. \end{aligned} \quad (3.2)$$

Formal integration of these equations leads to

$$\begin{aligned} a_\omega(t) &= a_\omega(0) + g\int_0^t \sigma(t')e^{\iota\omega t'}dt', \\ b_\Omega(t) &= b_\Omega(0) + G\int_0^t \sigma(t')e^{\iota\Omega t'}dt'. \end{aligned} \tag{3.3}$$

Similarly, we can obtain the equations for the atomic operators, which, after the substitution of Eq. (3.3), are reduced to

$$\begin{aligned} \dot{\sigma_z}(t) =& -2\pi g^2\left(\sigma_z + \mathbb{I}\right) - 2\pi G^2\left(\sigma_z + \mathbb{I}\right) - 2g\left(\int \sigma^\dagger a_\omega(0)e^{-\iota\omega t}d\omega + \int a_\omega^\dagger(0)\sigma e^{\iota\omega t}d\omega\right) \\ & - 2G\left(\int \sigma^\dagger b_\Omega(0)e^{-\iota\Omega t}d\Omega + \int b_\Omega^\dagger(0)\sigma e^{\iota\Omega t}d\Omega\right), \\ \dot{\sigma}^\dagger(t) =& -(\pi g^2 + \pi G^2)\sigma^\dagger(t) + g\int a_\omega^\dagger(0)\sigma_z(t)e^{\iota\omega t}d\omega + G\int b_\Omega^\dagger(0)\sigma_z(t)e^{\iota\Omega t}d\Omega, \\ \dot{\sigma}(t) =& -(\pi g^2 + \pi G^2)\sigma(t) + g\int \sigma_z(t)a_\omega(0)e^{-\iota\omega t}d\omega + G\int \sigma_z(t)b_\Omega(0)e^{-\iota\Omega t}d\Omega. \end{aligned} \tag{3.4}$$

Here, I will denote the pulse mode coupling rate by, $\Gamma_P = 2\pi g^2$, and that of bath mode operator by, $\Gamma_B = 2\pi G^2$. This coupling rates are slightly different from the one that I defined in the earlier chapter; they differ by a factor of 2. Using the familiar multimode field operator $A_0(t)$, Eq.(3.4) takes the form:

$$\begin{aligned} \dot{\sigma_z}(t) =& -\left(\Gamma_p + \Gamma_B\right)\left(\sigma_z + \mathbb{I}\right) \\ & - 2\sqrt{\Gamma_p}\sigma^\dagger(t)A_0(t) - 2\sqrt{\Gamma_p}A_0^\dagger(t)\sigma(t) - 2G\left(\int \sigma^\dagger b_\Omega(0)e^{-\iota\Omega t}d\Omega + \int b_\Omega^\dagger(0)\sigma e^{\iota\Omega t}d\Omega\right) \\ \dot{\sigma}^\dagger(t) =& -\left(\Gamma_p + \Gamma_B\right)\frac{\sigma^\dagger(t)}{2} + \sqrt{\Gamma_p}A_0^\dagger(t)\sigma_z(t) + G\int b_\Omega^\dagger(0)\sigma_z(t)e^{\iota\Omega t}d\Omega \\ \dot{\sigma}(t) =& -\left(\Gamma_p + \Gamma_B\right)\frac{\sigma(t)}{2} + \sqrt{\Gamma_p}\sigma_z(t)A_0(t) + G\int \sigma_z(t)b_\Omega(0)e^{\iota\Omega t}d\Omega \end{aligned} \tag{3.5}$$

In the following sections, I will assume that the bath is in the vacuum state: there is no excitation in the bath initially. Furthermore, I will consider two scenarios in the case of

pulse mode: in one case, I will assume that the pulse mode is initially in a Fock state with definite photon number, and in the second situation I will choose the initial state of pulse mode to be a multimode coherent state with an average photon number. In all these scenarios, I will assume the initial state of the atom is the ground state.The expectation value of Eq.(3.4) for a specific initial state will give equations that look similar to the familiar optical Bloch equations.

3.3 Multimode coherent state

As an example, I will choose the initial state where the atomic system is in the ground state ($|g\rangle$), the pulse mode is in a multimode coherent state ($|\alpha\rangle$) with an average number of photon $\bar{n}$, and the bath is considered to have no excitation ($|0\rangle$). To get the expectation value of these operators, one must know the action of the multimode field operator, $A_0(t)$, on a multimode coherent state. Note that the same way as we define a coherent state for a single mode field, we can express a multimode coherent state as the coherent superposition of multimode Fock states ($|N\rangle$):

$$\begin{aligned} |\alpha\rangle &= e^{-|\alpha|^2/2} \sum_{N=0}^{\infty} \frac{(\alpha)^N}{\sqrt{N!}} |N\rangle \,, \\ |\alpha\rangle &= e^{-|\alpha|^2/2} \sum_{N=0}^{\infty} \frac{(\alpha)^N}{N!} \left(\int dt' f(t') A^\dagger(t') \right)^N |0\rangle \,. \end{aligned} \tag{3.6}$$

The best way to understand the action of a multimode field operator on this coherent state, with average number of photons, $\bar{n} = |\alpha|^2$ (for simplicity, we can take α to be real), is by analyzing the action of $A_0(t)$ on each term of the coherent state. In particular, the

action of $A_0(t)$ on $N = 0$ term gives

$$A_0(t)e^{-|\alpha|^2/2}\,|0\rangle = 0.$$

Similarly, the action on $N = 1$ term leads to

$$A_0(t)e^{-|\alpha|^2/2}\,\alpha \int dt_1 f(t_1)A_0^\dagger(t_1)\,|0\rangle = 0,$$

$$A_0(t)A_0^\dagger(t_1) = \delta(t-t_1) + A_0^\dagger(t_1)A_0(t),$$

$$e^{-|\alpha|^2/2}\,\alpha \int dt_1 f(t_1)\left(\delta(t-t_1) + A_0^\dagger(t_1)A_0(t)\right)|0\rangle = e^{-|\alpha|^2/2}\,\alpha f(t)\,|0\rangle\,.$$

Extending this procedure to n^{th} term, one arrives at

$$e^{-|\alpha|^2/2}\,\frac{\alpha}{(n-1)!}\,f(t)\left(\int dt_2 f(t_2)A_0^\dagger(t_2)\right)^{(n-1)}|0\rangle\,.$$

In summary, the action of $A_0(t)$ on multimode coherent state is

$$A_0(t)\,|\alpha\rangle = \left(0 + e^{-|\alpha|^2/2}\,\alpha f(t) + .. + e^{-|\alpha|^2/2}\,\frac{\alpha f(t)}{(n-1)!}\left(\int dt_2 f(t_2)A_0^\dagger(t_2)\right)^{(n-1)} + ..\right)|0\rangle\,,$$

$$A_0(t)\,|\alpha\rangle = \alpha f(t)e^{-|\alpha|^2/2}\sum_{m=0}^{\infty}\frac{\alpha^m}{m!}\left(\int dt_2 f(t_2)A_0^\dagger(t_2)\right)^m|0\rangle\,,$$

$$A_0(t)\,|\alpha\rangle = \alpha f(t)\,|\alpha\rangle\,.$$

Therefore, it is clear that the multimode coherent state is an eigenstate of multimode annihilation operator with eigenvalue, $\alpha f(t)$. Where, α is related to the average number of photons ($\bar{n}$) in the multi mode coherent state. Since the expectation value of bath mode noise operator is zero, it is straightforward to write down the optical Bloch equations; they

are

$$\begin{aligned}
\langle \dot{\sigma_z}(t)\rangle &= -\left(\Gamma_p+\Gamma_B\right)\left(\langle\sigma_z(t)\rangle+\mathbb{I}\right)-2f(t)\sqrt{\bar{n}\Gamma_p}\left(\langle\sigma(t)\rangle+\left\langle\sigma^\dagger(t)\right\rangle\right),\\
\left\langle\dot{\sigma^\dagger}(t)\right\rangle &= -\left(\Gamma_p+\Gamma_B\right)\frac{\left\langle\sigma^\dagger(t)\right\rangle}{2}+f(t)\sqrt{\bar{n}\Gamma_p}\left\langle\sigma_z(t)\right\rangle,\\
\left\langle\dot{\sigma(t)}\right\rangle &= -\left(\Gamma_p+\Gamma_B\right)\frac{\langle\sigma(t)\rangle}{2}+f(t)\sqrt{\bar{n}\Gamma_p}\left\langle\sigma_z(t)\right\rangle.
\end{aligned} \tag{3.7}$$

It is possible to simplify these equations further by noting that, for real $f(t)$ and on resonance (as I have assumed here), the expectation value of coherence [1] (σ) and its hermitian conjugate are equal. This will help to define a new operator (Σ) in terms of the expectation value of the sum of the coherence and its conjugate, $\Sigma = \left\langle\sigma+\sigma^\dagger\right\rangle$. Using this new operator, we can express Eq.(3.7) as

$$\begin{aligned}
\langle \dot{\sigma_z}(t)\rangle &= -\left(\Gamma_p+\Gamma_B\right)\left(\langle\sigma_z(t)\rangle+\mathbb{I}\right)-2f(t)\sqrt{\bar{n}\Gamma_p}\;\Sigma(t),\\
\dot{\Sigma}(t) &= -\frac{1}{2}\left(\Gamma_p+\Gamma_B\right)\Sigma(t)+2f(t)\sqrt{\bar{n}\Gamma_p}\;\left\langle\sigma_z(t)\right\rangle.
\end{aligned} \tag{3.8}$$

Although, these equations are hard to integrate analytically, for an arbitrary $f(t)$, it is easy to solve them numerically. Further, to compute $P_e(t) = \left(\langle\sigma_z\rangle+\mathbb{I}\right)/2$, the excitation probability of the atom, we can alternately represent Eq.(3.8) in terms of $P_e(t)$:

$$\begin{aligned}
\dot{P}_e(t) &= -\left(\Gamma_p+\Gamma_B\right)P_e(t)-f(t)\sqrt{\bar{n}\Gamma_p}\;\Sigma(t),\\
\dot{\Sigma}(t) &= -\frac{1}{2}\left(\Gamma_p+\Gamma_B\right)\Sigma(t)+4f(t)\sqrt{\bar{n}\Gamma_p}\;P_e(t)-2f(t)\sqrt{\bar{n}\Gamma_p}.
\end{aligned} \tag{3.9}$$

3.4 Fock state

In a way that is similar to the multimode coherent state, we can obtain equations for a N-photon Fock state. However, for this initial condition, we need to solve $2N$ coupled

[1] This is something like the electric dipole moment for an electric-dipole-allowed transition.

differential equations:

$$\begin{aligned}\dot{P}_{e,n} &= -\left(\Gamma_P + \Gamma_B\right) P_{e,n} - f(t)\sqrt{n\Gamma_P}\ \Sigma_{n-1},\\ \dot{\Sigma}_{n-1} &= -\frac{1}{2}\left(\Gamma_P + \Gamma_B\right)\ \Sigma_{n-1} + 4f(t)\sqrt{n\Gamma_P}\ P_{e,n-1} - 2f(t)\sqrt{n\Gamma_P}.\end{aligned} \tag{3.10}$$

Where, n runs from 1 to N, and $P_{e,n}$ represents n-photon excitation probability. The explicit form of $P_{e,N}$ and Σ_N, which I used to write Eq.(3.10), are given by

$$P_{e,N} = \left(\langle N, g|\, \sigma_z(t)\, |N, g\rangle + \mathbb{I}\right)/2,$$

$$\Sigma_{N-1} = \langle N-1, g|\, \sigma(t)\, |N, g\rangle + \langle N, g|\, \sigma^\dagger(t)\, |N-1, g\rangle\,.$$

Again, solving this set of equations for an arbitrary pulse profile is hard. However, it is still possible to obtain a closed form expression in some special cases. I will discuss more on mutiphoton excitation probability in the later part and want to focus on the single photon case in the following section.

3.5 Fock state: single photon

For a single photon Fock state, Eq.(3.10) has a simple structure, and it is relatively straightforward to get the analytical expression for the excitation probability [61]. Here, I want to present an alternate way to obtain the same result; this will also help to establish the connection between HL formalism, and the approach that I used in the first chapter.

Let the initial state be $|g, 1, 0\rangle$, where the atomic system, field, and the bath are in ground state, single photon Fock state, vacuum respectively. As time progresses, this state will evolve to a different state as the Hamiltonian, Eq. (3.1), will induce an unitary evolution to the system. For any arbitrary time, the evolved state, $|\phi(t)\rangle$ in the Schrödinger

picture is

$$|\phi(t)\rangle = e^{-iHt/\hbar}\,|g,1,0\rangle\,. \tag{3.11}$$

To get the excitation probability amplitude, one needs to compute the overlap of this evolved state and $|e,0,0\rangle$. Mathematically, the probability amplitude is

$$\begin{aligned}\langle e,0,0|\phi(t)\rangle &= \langle e,0,0|\, e^{-itH/\hbar}\,|g,1,0\rangle\,,\\ &= \langle g,0,0|\,\sigma(0)e^{-iHt/\hbar}\,|g,1,0\rangle\,.\end{aligned}$$

Where $\sigma(0)$ is the Schrödinger picture lowering operator. Also, notice that the action of the unitary operator ($U = e^{-iHt/\hbar}$) on the vacuum of the composite system $|g,0,0\rangle$:

$$e^{-iHt/\hbar}\,|g,0,0\rangle = |g,0,0\rangle\,.$$

Therefore, by suitable incorporation of the identity ($UU^\dagger = \mathbb{I}$), the probability amplitude will be

$$\langle g,0,0|\,\sigma(t)\,|g,1,0\rangle\,.$$

Here, $\sigma(t)$ represents Heisenberg operator, and the formal solution of this operator is readily available from Eq.(3.5). The probability amplitude is then

$$\begin{aligned}\langle e,0,0|\phi_{out}(t)\rangle &= \langle g,0,0|\,\sigma(t)\,|g,1,0\rangle\\ \langle e,0,0|\phi_{out}(t)\rangle &= \sqrt{\Gamma_P}\int_{-\infty}^{t} dt'\, e^{-(\Gamma_P+\Gamma_B)(t-t')/2}\,\langle g,0,0|\,\sigma_z(t')A_0(t')\,|g,1,0\rangle\\ &\quad + G\int_{-\infty}^{t} dt'\, e^{-(\Gamma_P+\Gamma_B)(t-t')/2}\int \langle g,0,0|\,\sigma_z(t)b_\Omega(0)e^{\iota\Omega t}d\Omega\,|g,1,0\rangle\\ \langle e,0,0|\phi_{out}(t)\rangle &= -\sqrt{\Gamma_P}\int_{-\infty}^{t} dt'\, e^{-(\Gamma_P+\Gamma_B)(t-t')/2}f(t').\end{aligned}$$

Where, I have used the fact that $\langle g,0,0|\,\sigma_z(t)\,|g,0,0\rangle = -1$. Finally, the single photon

excitation probability is

$$P_{e,1}(t) = |\langle e,0,0|\phi_{out}(t)\rangle|^2 = \Gamma_P \left(\int_{-\infty}^{t} dt' \, e^{-(\Gamma_P+\Gamma_B)(t-t')/2} f(t') \right)^2 . \tag{3.12}$$

At this point, it is worth comparing the excitation probability expressions that we obtained using both methods. In fact, when the external decay is absent ($\Gamma_B = 0$), Eq.(3.12) is identical to the the probability expression one obtains using Eq.(2.20) (the only difference is that the coupling strength γ defined in chapter 2 is $\Gamma_P/2$)

3.6 Ouput wavefunction

Although HL formalism is in Heisenberg picture, it is, still, possible to obtain the wavefunction of the output field state. The crucial piece that is missing in the discussion is the output field operator which is essential for obtaining the output wavefunction. Clearly, for any arbitrary time, the state of the system (in the Schrödinger picture) is

$$|\phi_{out}(t)\rangle = \int a_\omega^\dagger f(\omega,t) d\omega \, |g,0,0\rangle + \int \xi(\Omega,t) b_\Omega^\dagger d\Omega \, |g,0,0\rangle + f_e(t) \, |e,0,0\rangle . \tag{3.13}$$

Where the first term corresponds to the scenario in which the photon is in the pulse mode, second term represents the case in which it is in the bath mode, and the last term gives the probability amplitude of the atom in the excited state. Eventually, the excited state probability amplitude will decay for a time long enough after the interaction, the asymptotic state $|\phi_{out}(t)\rangle$ is given by

$$|\phi_{out}(t)\rangle = \int a_\omega^\dagger f(\omega,t) d\omega \, |g,0,0\rangle + \int \xi(\Omega,t) b_\Omega^\dagger d\Omega \, |g,0,0\rangle . \tag{3.14}$$

Notice that the action of a_ω on this state, followed by a projection onto $|g,0,0\rangle$, gives

the asymptotic field state $f(\omega, t)$. To do this in the Heisenberg picture, we need operator, and one can obtain it in the following way.

As we already know, from Eq.(3.3), how the field operator a_ω evolves with time:

$$a_\omega(t) = a_\omega(0) + g \int_{-\infty}^{t} \sigma(t') e^{i\omega t'} dt'$$

Fourier transforming this expression with respect to a new variable τ gives

$$\frac{1}{\sqrt{2\pi}} \int d\omega e^{-i\omega\tau} \left(a_\omega(0) + g \int_{-\infty}^{t} \sigma(t') e^{i\omega t'} dt' \right) = A_0(\tau) + \sqrt{\Gamma_P} \int_{-\infty}^{t} \sigma(t') \delta(t' - \tau).$$

In the asymptotic limit, the integration limit can be taken to infinity which gives the out put field operator A_{out}:

$$A_{out}(\tau) = A_0(\tau) + \sigma(\tau)\sqrt{\Gamma_P}. \tag{3.15}$$

Equation.(3.15) is in agreement with the output field operator given in [26]. Once the output field operator is known, it is relatively easy to get the output field wavefunction. A single photon scattered field state would be ideal to illustrate this method: If the field contains a single photon, then $\langle g, 0, 0| A_0(t) |g, 0, 0\rangle$ gives the initial field wavefunction f(t); so, by Eq.(3.15), the scattered field wavefunction will be

$$\langle g, 0, 0| A_{out}(t) |g, 1, 0\rangle = \langle g, 0, 0| A_0(t) |g, 1, 0\rangle + \sqrt{\Gamma_P} \ \langle g, 0, 0| \sigma(t) |g, 1, 0\rangle ,$$

$$\langle g, 0, 0| A_0(t) |g, 1, 0\rangle + \sqrt{\Gamma_P} \ \langle g, 0, 0| \sigma(t) |g, 1, 0\rangle = f(t) + \sqrt{\Gamma_P} \langle g, 0, 0| \sigma(t) |g, 1, 0\rangle .$$

The formal solution of $\sigma(t)$ can be obtained from Eq.(3.4). We then have

$$f(t) + \sqrt{\Gamma_P} \langle g, 0, 0| \sigma(t) |g, 1, 0\rangle = f(t) + \sqrt{\Gamma_P} \int_{-\infty}^{t} dt' \Big[e^{-(\Gamma_P + \Gamma_B)(t-t')/2} \langle g, 0, 0| \sqrt{\Gamma_P} \sigma_z(t') A_0(t') |g, 1, 0\rangle \Big] ,$$

Since $\langle g, 0, 0| \sigma_z(t') |g, 0, 0\rangle = -1$, the single photon output wavefunction, in presence of

external decay, is

$$f(t) - \Gamma_P \int_{-\infty}^{t} dt' e^{-(\Gamma_P+\Gamma_B)(t-t')/2} f(t'). \tag{3.16}$$

This expression, with no external decay ($\Gamma_B = 0$), is the same as the one I derived in the first chapter (see Eq.2.23). Extending this method to more than one photon is also possible, but I will not be pursing it here.

3.7 Single photon fock state excitation probability

Coming back to the discussion of the single photon excitation probability, it is interesting to note that the form of the single photon excitation probability (see Eq.(3.12)) provides a simple proof that the only single photon pulse that can achieve the unit excitation is the pulse with rising exponential shape. To prove this, note that Eq.(3.12) can be expressed as

$$P_{e,1}(t) = \frac{\Gamma_P}{\Gamma_P + \Gamma_B} \left(\int_{-\infty}^{t} u(t') f(t') dt' \right)^2, \tag{3.17}$$

where, $u(t')$ is defined as

$$u(t') = \sqrt{\Gamma_P + \Gamma_B} e^{-(\Gamma_P+\Gamma_B)(t-t')}. \tag{3.18}$$

From Eq.(3.17), after a straightforward application of Cauchy-Schwartz inequality, it follows immediately that

$$\begin{aligned} P_{e,1}(t) &\leq \frac{\Gamma_P}{\Gamma_P + \Gamma_B} \int_{-\infty}^{t} u(t')^2 dt' \int_{-\infty}^{t} f(t')^2 dt', \\ P_{e,1}(t) &\leq \frac{\Gamma_P}{\Gamma_P + \Gamma_B} \int_{-\infty}^{t} f(t')^2 dt'. \end{aligned} \tag{3.19}$$

The last steps follows from the fact that $u(t')$ is normalized in the interval $(-\infty, t]$. It is evident from this inequality that a pulse ($f(t)$) which is normalized in the interval $(-\infty, \infty)$ can never give unit excitation under the presence of external dissipation.

However, in the absence of external decay, the pulse can give unit excitation if the pulse is entirely contained in the interval $(-\infty, t]$. Therefore, the right pulse shape to get unit excitation is the one which has the shape identical to that of $u(t')$; except for an overall minus sign. For a pulse that matches the shape of $u(t')$ (rising exponential pulse), the maximum excitation probability, from Eq.(3.17), is then

$$P_{e,max} = \frac{\Gamma_P}{\Gamma_P + \Gamma_B}. \tag{3.20}$$

An alternate example would be to consider the familiar gaussian pulse, $f(t) = e^{-t^2/T^2}/\sqrt{T\sqrt{\pi/2}}$, substitution of this pulse form in Eq.(3.12) results in the exact expression

$$P_e(t) = \frac{\sqrt{2\pi}\Gamma_P T}{4} e^{-(\Gamma_P+\Gamma_B)t+(\Gamma_P+\Gamma_B)^2T^2/8} \left(1 + \mathrm{erf}\left(\frac{t}{T} - \frac{\Gamma_P + \Gamma_B}{4}\right)\right). \tag{3.21}$$

The maximum excitation probability can be obtained from this expression by optimizing it with respect to time, t, and pulse duration, T. However, analytical optimization of Eq.(3.21) is difficult, and one may resort to numerical optimization. Numerically (I have used Mathematica), it is possible to show that the maximum of this function happens when $t_{opt} \approx 0.731T$, and the corresponding pulse duration is $T_{opt} = 1.368/(\Gamma_P + \Gamma_B)$. The optimized Gaussian excitation probability is then

$$P_{e,max} = 0.801\frac{\Gamma_P}{\Gamma_P + \Gamma_B}. \tag{3.22}$$

Although it is possible to perform the integral in Eq.(3.12) for a family of pulses, the final maximization may, still, involve numerical optimization. The optimized excitation probability for typical pulse profiles is given in Table 3.1. The detailed calculations and

optimization for these pulses are available in our paper[61].

Table 3.1: Optimized excitation probability for various pulse profiles. Here, Θ represents the usual Heaviside theta function

Pulse	Form	$P_{e,max}$
Rising exp pulse	$\Theta(t_0 - t)\sqrt{2/T}e^{(t-t_0)/T}$	1.000 $\Gamma_P/(\Gamma_P + \Gamma_B)$
Square pulse	$\Theta(t)\Theta(T - t)/\sqrt{T}$	0.815 $\Gamma_P/(\Gamma_P + \Gamma_B)$
Gaussian pulse	$e^{-t^2/T^2}/\sqrt{T\sqrt{\pi/2}}$	0.801 $\Gamma_P/(\Gamma_P + \Gamma_B)$
Decaying exp pulse	$\Theta(t)e^{-t/T}\sqrt{2/T}$	0.541 $\Gamma_P/(\Gamma_P + \Gamma_B)$

Improving the optimized excitation beyond these values requires the pulses to have additional parameters that can be tuned. A simple and practical way of getting pulses with an extra tunable parameter would be to consider an output pulse from a driven atom-cavity setup, where the cavity decay rate will become an additional parameter of the input pulse. It turns out that the decaying pulse from such a cavity-atom set up can certainly boost the excitation probability; also, the output pulse from this cavity-atom system which is driven by a gaussian pulse can significantly improve the excitation probability [61]. The exact form of these pulses can be found in [49]; it is then a matter of substituting them in Eq.(3.12) and optimizing it numerically. The behavior of excitation probability as a function of the ratio of coupling rates (Γ_P/Γ), where Γ_P, $\Gamma = \Gamma_P + \Gamma_B$ are pulse mode coupling rate and total coupling rate respectively, is shown in Figure 3.1.

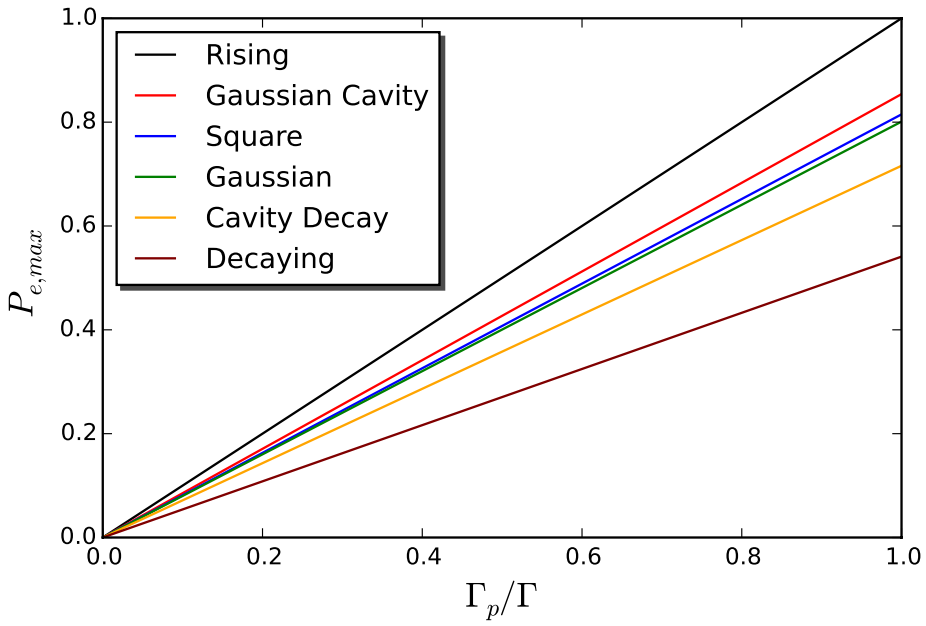

Figure 3.1: The single-photon fock state excitation probability as a function of ratio of coupling rates. Here Γ_P represents the pulse mode coupling rate and the total coupling rate, $\Gamma_P + \Gamma_B$, is represented by Γ.

3.8 Excitation probability: single-photon coherent state

The single-photon coherent state is a misnomer: the right way of putting it would be a coherent state with an average number of one photon. It is intuitive that the single-photon coherent state excitation probability will be a lot smaller than the single-photon Fock state as the single photon coherent state has a substantial probability of containing no photons (i.e, the vacuum state). In fact, there is a simple way to show that the single-photon coherent state excitation probability will always be strictly less than 0.632.

The single-photon coherent state, when expressed in terms of Fock states, has a probability $P(n) = e^{-1}/n!$ to have n photons. Therefore, this coherent state has an identical probability $1/e$ of having no photon (in which case there will be no excitation), and a single-photon in it. Further, it has a probability $1 - 2/e$ of having more than one photon.

The best way to understand the bound on the single-photon coherent state excitation probability ($P_{e,\bar{1}}$) is by expressing it in terms of n-photon excitation probability ($P_{e,n}$):

$$P_{e,\bar{n}=1} = e^{-1}P_{e,1} + \sum_{n=2}^{\infty} \frac{e^{-1}}{n!} P_{e,n}. \tag{3.23}$$

Since the probability of having more than one photon in a coherent state is non zero, it is evident that the summation term in Eq.(3.23) is strictly grater than zero. Therefore, it is easy to deduce that $P_{e,\bar{n}=1} > e^{-1}P_{e,1}$. Additionally, there is always a possibility of having no excitation, because $P(0) \neq 0$, and hence the chance of getting some excitation cannot exceed $1 - P(0)$. Therefore, the single-photon excitation probability is bounded by

$$e^{-1}P_{e,1} < P_{e,\bar{n}=1} < 1 - e^{-1}. \tag{3.24}$$

Here, I want to emphasize that this expression is true for any arbitrary pulse shape, so it is clear that a large excitation is impossible with a single-photon coherent state; one needs to consider a multiphoton coherent state to approach unit excitation. Unlike in the case of single-photon Fock state, getting an analytical expression for the coherent state excitation probability is not possible (although the Bloch equations look deceptively simple); except for a square pulse; in other cases, one needs to solve Eq.(3.9) numerically to get the excitation probability. The behavior of the optimized "single-photon coherent state" excitation probability as a function of ratio of coupling for various pulses is shown in Figure 3.2.

In quantum optics, the coherent states are considered to be states that are very close to classical states and they serve as a great tool to study quantum-classical correspondence. Therefore, it is not surprising that Eq.(3.9) is formally identical to semiclassical optical

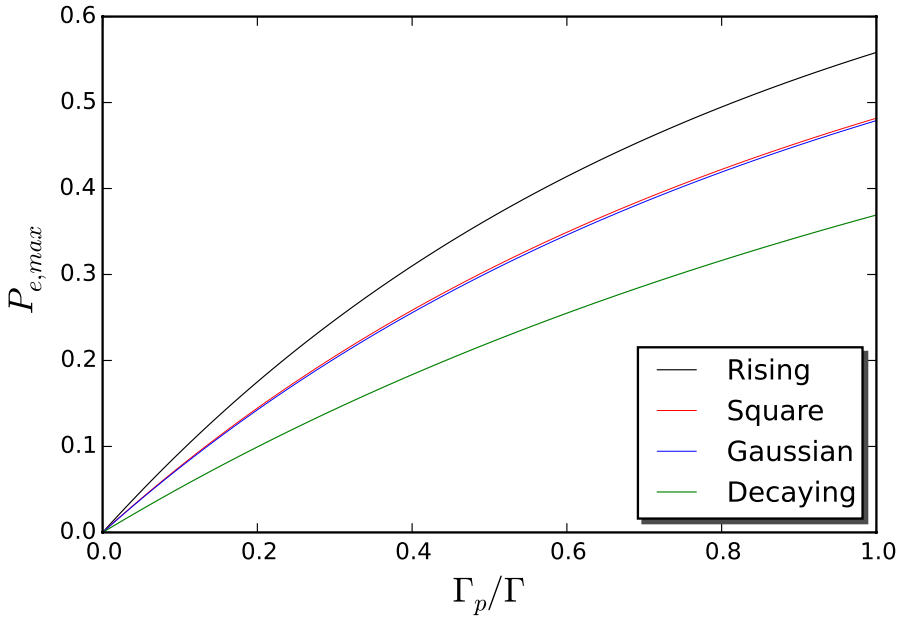

Figure 3.2: The optimized "single-photon coherent state" excitation probability as a function of the ratio of couplings. Here Γ_P represents the pulse mode coupling rate and the total coupling rate, $\Gamma_P + \Gamma_B$, is represented by Γ.

Bloch equations. Also, under appropriate limits, one expects that these equations yield the same semiclassical predictions; we will explore a few of them in the following discussion.

A good starting point, before stepping to solve it exactly, is to consider the special case where the damping terms can be neglected ($\Gamma_P + \Gamma_B \approx 0$). In such case, we can re-scale the equations:

$$\begin{aligned} \dot{P}_e(t) &= -f(t)\sqrt{\bar{n}\Gamma_p}\ \Sigma(t), \\ \dot{\Sigma}(t) &= 4f(t)\sqrt{\bar{n}\Gamma_p}\ P_e(t) - 2f(t)\sqrt{\bar{n}\Gamma_p}, \end{aligned} \tag{3.25}$$

using a simple transformation $\tau = \int_0^t f(t')dt'$, into a simple linear differential equations:

$$\begin{aligned} \frac{d}{d\tau}P_e &= -\sqrt{\bar{n}\Gamma_p}\ \Sigma, \\ \frac{d}{d\tau}\Sigma &= 4\sqrt{\bar{n}\Gamma_p}\ P_e - 2\sqrt{\bar{n}\Gamma_p}. \end{aligned} \tag{3.26}$$

Where I used the chain rule, $\frac{d}{d\tau} = \frac{d}{dt}\frac{dt}{d\tau}$ of derivative to simplify the expression. Notice that the two equations in Eq.(3.26) lead to a single expression:

$$\frac{d^2 P_e}{d\tau^2} = -4\bar{n}\Gamma_p P_e + 2\bar{n}\Gamma_p. \tag{3.27}$$

Equation (3.27) is the familiar oscillator equation, and the general solution of this equation includes ' sin' and ' cos' functions. However, in this particular case (with the initial condition, $P_e(0) = 0$), the solution is

$$\begin{aligned} P_e(\tau) &= \frac{1}{2} - \frac{1}{2}\cos(2\sqrt{\bar{n}\Gamma_P}\tau), \\ P_e(t) &= \frac{1}{2} - \frac{1}{2}\cos\left(2\sqrt{\bar{n}\Gamma_P}\int_0^t f(t')dt'\right). \end{aligned} \tag{3.28}$$

It is obvious from Eq.(3.28) that the atomic system can achieve a full inversion by using a 'π' pulse; that is

$$2\sqrt{\bar{n}\Gamma_P}\int_0^t f(t')dt' = \pi \tag{3.29}$$

It is worth noting that this condition is an outcome of the assumption that I made earlier: $\Gamma_P + \Gamma_B = 0$. However, the presence of Γ_P in the Eq.(3.29) makes it hard to justify such assumption. Nevertheless, it is expected that this result may approximately hold for a sufficiently intense ($\bar{n} \gg 1$) and short pulse ($(\Gamma_P + \Gamma_B)T \ll 1$). I will discuss more on this topic in a later section (3.10).

3.8.1 Square pulse: An exactly solvable model

Here, I will take a square pulse, which in this case is exactly solvable, as an example and obtain the exact analytic expression for the excitation probability. Instead of working with

Eq.(3.25), I will use Eq.(3.8) to get the analytic excitation probability. Letting, $f(t) = 1/\sqrt{T}$, $0 < t < T$ and $\Gamma = \Gamma_P + \Gamma_B$, I will rewrite Eq.(3.8) in terms of a new parameter, $\Omega_0 = 2\sqrt{\bar{n}\Gamma_P/T}$ as

$$\begin{aligned} \langle \dot{\sigma_z}(t) \rangle &= -\Gamma \langle (\sigma_z(t) + \mathbb{I}) \rangle - \Omega_0 \Sigma(t), \\ \dot{\Sigma}(t) &= -\frac{1}{2}\Gamma\Sigma(t) + \Omega_0 \langle \sigma_z(t) \rangle . \end{aligned} \tag{3.30}$$

This set of coupled linear equations is solvable in many ways. Here I will use the techniques of Laplace transform to obtain the solution. Applying Laplace transform with the initial condition, $\langle \sigma_z(0) \rangle = -1$, and $\Sigma(0) = 0$, will result

$$\begin{aligned} s\Sigma(s) &= -\frac{\Gamma}{2}\Sigma(s) + \Omega_0 \langle \sigma_z(s) \rangle , \\ s \langle \sigma_z(s) \rangle + 1 &= -\Gamma y(s) - \frac{\Gamma}{s} - \Omega_0 \Sigma(s). \end{aligned} \tag{3.31}$$

A simple manipulation of these algebraic equations will give us

$$\langle \sigma_z(s) \rangle = -\frac{(s+\Gamma)(s+\Gamma/2)}{s((s+\Gamma)(s+\Gamma/2) + \Omega_0^2)} \tag{3.32}$$

At this stage, to get the time domain version of $\sigma_z(t)$, one needs to perform an inverse Laplace transform of Eq.(3.32). The standard approach here is to convert this into a familiar form whose inverse Laplace transform is already known. Using the method of partial fraction it is relatively simple to show

$$\langle \sigma_z(s) \rangle = -\frac{\Gamma^2}{\Gamma^2 + 2\Omega_0^2}\frac{1}{s} - \frac{2\Omega_0^2}{\Gamma^2 + 2\Omega_0^2}\left[\frac{s + 3/4\ \Gamma}{(s + 3/4\ \Gamma)^2 + \Omega^2} + \frac{3\ \Gamma}{4\ \Omega}\frac{\Omega}{((s + 3/4\ \Gamma)^2 + \Omega^2)}\right]. \tag{3.33}$$

Where I used, $\Omega = \sqrt{\Omega_0^2 - \Gamma^2/16}$, in the last step to simplify the expression. Furthermore, the Eq.(3.33) is in a familiar form, and its is fairly straightforward to obtain its inverse

Laplace transform:

$$\langle\sigma_z(t)\rangle = -\frac{\Gamma^2}{\Gamma^2+2\Omega_0^2} - \frac{2\Omega_0^2}{\Gamma^2+2\Omega_0^2}e^{-3\Gamma t/4}\left[\cos(\Omega t)+\frac{3\Gamma}{4\Omega}\sin(\Omega t)\right]. \tag{3.34}$$

Finally, the excitation probability, $P_{e,\bar{n}}(t) = (1+\langle\sigma_z(t)\rangle)/2$, is given by

$$P_{e,\bar{n}}(t) = \frac{\Omega_0^2}{\Gamma^2+2\Omega_0^2}\left[1-e^{-3\Gamma t/4}\left(\cos(\Omega t)+\frac{3\Gamma}{4\Omega}\sin(\Omega t)\right)\right]. \tag{3.35}$$

It is not hard to show that the maximum of this function happens when $t = t_{max} = \pi/\Omega$, a kind of 'π' pulse condition that can only happen if the constraint, $\pi/\Omega \leq T$ holds. It follows immediately from this constraint that, T has to be chosen appropriately:

$$\begin{aligned} \pi^2 &\leq \Omega^2 T^2 \\ \pi^2 &\leq \left(4\Gamma_P\bar{n}/T - \Gamma^2/16\right)T^2 \end{aligned} \tag{3.36}$$

Solving this, simple, quadratic equation for T yields

$$-\sqrt{\frac{64\bar{n}^2\Gamma_P^2}{\Gamma^2}-\pi^2} \leq \frac{\Gamma T}{4} - \frac{8\bar{n}\Gamma_P}{\Gamma} \leq \sqrt{\frac{64\bar{n}^2\Gamma_P^2}{\Gamma^2}-\pi^2}. \tag{3.37}$$

Substituting $t = \pi/\Omega$ in Eq.(3.35) will provide

$$P_{e,\bar{n}} = \frac{4\bar{n}\Gamma_P/T}{\Gamma^2+8\bar{n}\Gamma_P/T}\left(1+exp\left[-\frac{3\pi\Gamma}{\sqrt{64\bar{n}\Gamma_P}/T-\Gamma^2}\right]\right). \tag{3.38}$$

This is a strictly decreasing function of T, and which, therefore, has a maximum at the smallest value of T that respects the constrain, Eq.(3.37). The final expression is a complicated function of $\bar{n}\Gamma_P/\Gamma$, but for $\bar{n}=1$, and $\Gamma_P = \Gamma$ case, the value of $P_{e,\bar{1}}$ is 0.433.

Surprisingly, it turns out that it is possible to do better than this, at least in the $\bar{n}=1$ case, by by choosing a pulse shorter than π/Ω. For such pulses, the excitation probability will be an increasing function and it reaches its maximum when $t = T$. The resulting

expression for such pulse is given by

$$P_{e,\bar{n}=1} = \frac{4\Gamma_P}{\Gamma^2 T + 8\Gamma_P}\left[1 - e^{-3\Gamma T/4}\left(\cos(\Omega T) + \frac{3\Gamma}{4\Omega}\sin(\Omega T)\right)\right]. \tag{3.39}$$

This is a two parameter function, and we can choose the parameters to be Γ_P/Γ and ΓT. Although it may be challenging to optimize it analytically, it is possible to optimize numerically by fixing the first parameter and find the value of the second parameter that maximizes $P_{e,\bar{n}}$. For the special case $\Gamma = \Gamma_P$, the optimal T is found to be $T = 1.487/\Gamma$, and the resulting excitation probability for the square pulse is

$$(P_{e,\bar{n}=1})_{max} = 0.482. \tag{3.40}$$

The results for other values of external loss are shown in Figure 3.2, which also includes numerical results for other pulse shapes. In contrast to the case of single-photon Fock state, in which case the optimized excitation probability has a simple and linear trend, the coherent state behavior is fairly more complex.

3.9 Multi-Photon wavepackets, and asymptotic results

We have seen that, at the single photon level, the unit atomic excitation is possible with a photon of right pulse shape, but a deterministic single photon source with appropriate pulse shape is notoriously hard to realize. Therefore, it would be useful to quantify this excitation, in the absence of perfect pulse shape, when the field consists of more than one photon. With the advent of lasers, realizing multiphoton coherent states is certainly easy. On the other hand, generating multiphoton Fock states is extremely hard. Accordingly, I will consider coherent states first, in which case the equations that I need to solve are

Eq.(3.9).

As I mentioned earlier, Eq.(3.9) may not permit an analytical solution, except for a square pulse. However, it is possible to get an approximate solution in two opposite limits. If the pulse is very broad compared to the overall decay time, $(\Gamma_P + \Gamma_B)^{-1}$, the equations can be solved adiabtically by setting the left hand side of Eq.(3.9) equal to zero:

$$P_{e,\bar{n}}(t) = \frac{4\bar{n}\Gamma_P}{(\Gamma_P + \Gamma_B)^2 + 8\bar{n}\Gamma_P f(t)^2} f(t)^2 \tag{3.41}$$

As it is evident from Eq.(3.41), the adiabatic excitation probability is always less than 1/2; the value that it takes in the limit when $\bar{n} \to \infty$. This well-known phenomenon, in which a sufficiently long and intense field will drive the population inversion of a two level medium to zero, is known as "bleaching", and the medium will be transparent in such occasion.

An alternate limit where it is possible to achieve unit excitation is by considering a sufficiently intense and very short pulse. It is worth noting that such unit excitation or near unit excitation is transient as it can be achieved for only a very short time, which is limited by the lifetime of atomic levels. The usefulness of this transient excitation relies on the timescales that are involved.

As in in the previous section, I want to explore the effect of pulse shape on the excitation probability and see how $P_{e,\bar{n}}$ approaches 1 as $\bar{n}$ increases. As a convenient starting point, I will choose the square pulse solution (Eq.(3.35)) which has a local maximum at $t = t_{max} = \pi/\Omega$, if the condition Eq.(3.37) is satisfied. In the large $\bar{n}$ limit, we

get this condition as

$$\frac{\pi^2\Gamma}{4\bar{n}\Gamma_P} + O\left(\frac{1}{\bar{n}}\right)^3 \leq \Gamma T \leq \frac{64\bar{n}\Gamma_P}{\Gamma} - \frac{\pi^2\Gamma}{4\bar{n}\Gamma_P} + O\left(\frac{1}{\bar{n}}\right)^3 \tag{3.42}$$

Observe that in the large $\bar{n}$ limit, Eq.(3.38) becomes

$$P_{e,\bar{n}} \simeq 1 - \frac{3\pi\Gamma}{16}\sqrt{\frac{T}{\bar{n}\Gamma_P}} - \left(\frac{9\pi^2}{64} - \frac{1}{2}\right)\frac{\Gamma^2 T}{4\bar{n}\Gamma_P} + O\left(\frac{1}{\bar{n}}\right)^{3/2} \tag{3.43}$$

Optimization of Eq.(3.43) is crucial at this stage: If we don't optimize it with respect to T, $P_{e,\bar{n}}$ approaches 1 as $1/\sqrt{\bar{n}}$. However, a much favorable scaling is obtainable by choosing the smallest value of T allowed by the Eq.(3.42). Substituting $T = \pi^2/4\bar{n}\Gamma_P$, we get

$$P_{e,\bar{n}} \simeq 1 - \frac{3\pi^2\Gamma}{32\bar{n}\Gamma_P} - \left(\frac{9\pi^2}{64} - \frac{1}{2}\right)\left(\frac{\Gamma}{4\bar{n}\Gamma_P}\right)^2 + O\left(\frac{1}{\bar{n}}\right)^3 \tag{3.44}$$

For $\bar{n} = 1$ case, I showed an alternate approach, which led to a better optimized result, where the maximum happened to be at the end of the pulse, $t = T$. However for the multiphoton case, this alternate approach, in fact, will reduce to the exact same result Eq.(3.44).

As a final comment, I want to point out that, in contrast to the single photon case, the optimized pulse duration in the large $\bar{n}$ limit is, to the lowest order in $1/\bar{n}$, independent of external decay rate Γ_B, and we will see that this is even true for every other pulse shapes too.

3.10 Asymptotic result: perturbation theory approach

The above exactly-solvable square pulse result is very useful to get the asymptotic result for other pulse shapes. From Eq.(3.44), it is clear that, in order to get the first order

correction, in $1/\bar{n}$, to $P_{e,\bar{n}}$ we need to keep terms that are linear in Γ (here I have taken Γ, and Γ_P as independent variables). The simple strategy to get the first order correction in Γ is to use perturbation theory.

As a first step in this perturbation approach, it is ideal to express Eq.(3.9) in terms of some dimensionless variable. Assuming T to be a parameter that characterizes the pulse duration, we can define a new quantity $g(t) = \sqrt{T}f(t)$ (g has the same shape as f, but has no dimensions). Also, like earlier, defining $\Omega_0 = 2\sqrt{\bar{n}\Gamma_P/T}$, and a new dimensionless time $\tau = \Omega_0 t$, the dimensionless equations are then

$$\begin{aligned} \frac{dx}{d\tau} &= -\frac{\epsilon}{2}x + g(\tau)y - g(\tau), \\ \frac{dy}{d\tau} &= -\epsilon y - g(\tau)x. \end{aligned} \tag{3.45}$$

Where $\Sigma \equiv x$, $2P_{e,\bar{n}} \equiv y$, and $\epsilon = \Gamma/\Omega_0$. Further, assuming a formal power series solution for both x, and y in terms of the parameter ϵ, that is

$$x(t) = x^{(0)}(t) + \epsilon x^{(1)}(t) + \epsilon^2 x^{(2)}(t) + ...,$$

$$y(t) = y^{(0)}(t) + \epsilon y^{(1)}(t) + \epsilon^2 y^{(2)}(t) + ...$$

Substitution of these formal solutions back into Eq.(3.45) will immediately give the lowest order equations:

$$\begin{aligned} \frac{dx^{(0)}}{d\tau} &= -g(\tau)y^{(0)} - g(\tau), \\ \frac{dy^{(0)}}{d\tau} &= -g(\tau)x^{(0)}. \end{aligned} \tag{3.46}$$

These lowest order equations are identical to Eq.(3.26), and the solutions to these

equations are

$$\begin{aligned} x^{(0)}(\tau) &= -\sin(\theta(\tau)), \\ y^{(0)}(\tau) &= 1 - \cos(\theta(\tau)). \end{aligned} \tag{3.47}$$

Where $\theta(\tau) = \int_{-\infty}^{\tau} g(\tau')d\tau'$. Note that, for $\theta = \pi$, the 0^{th} order correction leads to perfect excitation of the atomic system. Proceeding further, we obtain the first order equations as

$$\begin{aligned} \frac{dx^{(1)}}{d\tau} &= g(\tau)y^{(1)} - \frac{1}{2}x^{(0)}(\tau) \\ \frac{dy^{(1)}}{d\tau} &= -g(\tau)x^{(1)} - y^{(0)}(\tau). \end{aligned} \tag{3.48}$$

The integration of these equations will become much easier when expressed in terms of the variable θ. Again, using the chain rule, these Eq.(3.48) becomes

$$\begin{aligned} \frac{dx^{(1)}}{d\theta} &= y^{(1)} - \frac{1}{2g(\tau)}x^{(0)}(\tau), \\ \frac{dy^{(1)}}{d\theta} &= -x^{(1)} - \frac{1}{g(\tau)}y^{(0)}(\tau). \end{aligned} \tag{3.49}$$

One gets a better appreciation of these equations by expressing them as a matrix differential equation. With $1/g(\tau) = d\tau/d\theta$, Eq.(3.49) is simply then

$$\frac{d}{d\theta}\begin{pmatrix} x^{(1)} \\ y^{(1)} \end{pmatrix} = \underbrace{\begin{pmatrix} 0 & 1 \\ -1 & 0 \end{pmatrix}}_{M}\begin{pmatrix} x^{(1)} \\ y^{(1)} \end{pmatrix} + \begin{pmatrix} F_1(\theta) \\ F_2(\theta) \end{pmatrix} \tag{3.50}$$

Where, $F_1(\theta) \equiv -\frac{1}{2}\frac{d\tau}{d\theta}x^{(0)}(\theta)$, and $F_2(\theta) \equiv -\frac{d\tau}{d\theta}y^{(0)}(\theta)$. The formal solution of Eq.(3.50) is given by

$$\begin{pmatrix} x^{(1)} \\ y^{(1)} \end{pmatrix} = \int_0^{\theta} d\theta' e^{M(\theta-\theta')}\begin{pmatrix} F_1(\theta) \\ F_2(\theta) \end{pmatrix}, \tag{3.51}$$

where, alternately, we can express this matrix M in terms of the Pauli matrices. Since $i\sigma_y = M$, using the well know identity, $e^{i(\theta-\theta')\sigma_y} = \mathbf{I}\cos(\theta-\theta') + i\sigma_y\sin(\theta-\theta')$, we get the

formal solution of $y^{(1)}(\theta)$ as

$$\begin{aligned} y^{(1)}(\theta) &= \int_0^\theta d\theta' \left(F_2(\theta')\cos(\theta-\theta') - F_1(\theta')\sin(\theta-\theta')\right) \\ y^{(1)}(\theta) &= -\int_0^\theta \frac{d\tau}{d\theta'}\left(y^{(0)}(\theta')\cos(\theta-\theta') - \frac{x^{(0)}(\theta')}{2}\sin(\theta-\theta')\right)d\theta' \end{aligned} \tag{3.52}$$

Even though the first order correction has a complicated form, it, still, allows us to express $P_{e,\bar{n}}$ in a compact form at the expected maximum $\theta = \pi$:

$$\begin{aligned} P_{e,\bar{n}}\mid_{\theta=\pi} &= \frac{1}{2}\left(y^{(0)} + \epsilon y^{(1)}\right), \\ P_{e,\bar{n}}\mid_{\theta=\pi} &= 1 - \frac{\epsilon}{2}\int_0^\pi \frac{1}{g(\tau(\theta'))}\left(-\cos(\theta')\left[1-\cos(\theta')\right] + \frac{1}{2}\sin^2(\theta')\right)d\theta', \\ 1 - P_{e,\bar{n}}\mid_{\theta=\pi} &= \epsilon\int_0^\pi \frac{\sin^4(\theta'/2)}{g(\tau(\theta'))}d\theta'. \end{aligned} \tag{3.53}$$

The last expression in Eq.(3.53) is very convenient to get the first order correction to the asymptotic excitation probability. As an example, I will consider the hyperbolic secant pulse, and demonstrate how to use Eq.(3.53) to get the first order correction.

3.10.1 Example: Hyperbolic secant pulse

The first step for implementing Eq.(3.53) is to get the expression for θ from the dimensionless pulse profile. For a hyperbolic secant pulse, $f(t) = \sqrt{1/T}sech(2t/T)$, one immediately finds, in terms of the dimensionless time ($\tau = \Omega_0 t$), the dimensionless pulse profile, $g(\tau) = sech(2\tau/(\Omega_0 T))$. At this point, it is a matter of straightforward integration to get θ:

$$\begin{aligned} \theta(\tau) &= \int_{-\infty}^t g(\tau')d\tau' \\ \theta(\tau) &= \frac{\Omega_0 T}{4}\left(\pi + \tan^{-1}(\tanh(\tau/(\Omega_0 T)))\right). \end{aligned} \tag{3.54}$$

Inverting this equation and writing τ as a function of θ, we have

$$\tau = \Omega_0 T \tanh^{-1}\left[\tan\left(\frac{4\theta - \pi\Omega_0 T}{4\Omega_0 T}\right)\right]. \tag{3.55}$$

The derivative $d\tau/d\theta = 1/g(\tau(\theta))$ is simply then

$$\frac{d\tau}{d\theta} = \cosh\left(2\tanh^{-1}\left[\tan\left(\frac{4\theta - \pi\Omega_0 T}{4\Omega_0 T}\right)\right]\right) \tag{3.56}$$

Defining $a = \Omega_0 T$, and using Eq.(3.56), we get Eq.(3.53) as

$$1 - P_{e,\bar{n}} \mid_{\theta=\pi} = \frac{\Gamma}{\Gamma_P \bar{n}}\left(\frac{a}{4}\int_0^{\pi} \cosh\left(2\tanh^{-1}\left[\tan\left(\theta/a - \pi/4\right)\right]\right)\sin^4(\theta'/2)d\theta'\right). \tag{3.57}$$

At this stage, one needs to numerically minimize Eq.(3.57) with respect to the parameter 'a' to get the optimized first order correction to $P_{e,\bar{n}}$. The minimum of the quantity in the bracket of Eq.(3.57)) is 0.88088, and it is obtained when $a = 2.5679$. The corresponding optimized pulse duration, $T_{opt} = a_{opt}^2/(4\bar{n}\Gamma_P)$ is $1.64854/(\bar{n}\Gamma_P)$. Finally, we obtain the maximum excitation for hyperbolic secant pulse as

$$P_{e,\bar{n}} \simeq 1 - 0.88088\frac{\Gamma}{\Gamma_P \bar{n}}. \tag{3.58}$$

The procedure for other pulse shapes to get the asymptotic form of $P_{e,\bar{n}}$ is exactly the same as that of hyperbolic secant pulse. A thorough investigation of asymptotic excitation probability for various other pulse shapes is available in [61], and I have summarized them in the table below, and graphically, for the $\Gamma_B = 0$ case, these results are presented in Figure 3.3.

Table 3.2: The asymptotic excitation probability for various pulse profiles as a function of the average number of photons and the coupling rates.

Pulse	T_{opt}	$P_{e,\bar{n}}$
Rising pulse	$\pi^2/(8\bar{n}\Gamma_P)$	$1-0.519432\,[\pi^2\Gamma/\,(8\bar{n}\Gamma_P)]$
Square pulse	$\pi^2/(4\bar{n}\Gamma_P)$	$1-[3\pi^2\Gamma/\,(32\bar{n}\Gamma_P)]$
Gaussian pulse	$1.45009/(\bar{n}\Gamma_P)$	$1-0.91597\,[\Gamma/\,(\bar{n}\Gamma_P)]$
Decaying pulse	$3.347/(\bar{n}\Gamma_P)$	$1-1.47895\,[\Gamma/\,(8\bar{n}\Gamma_P)]$

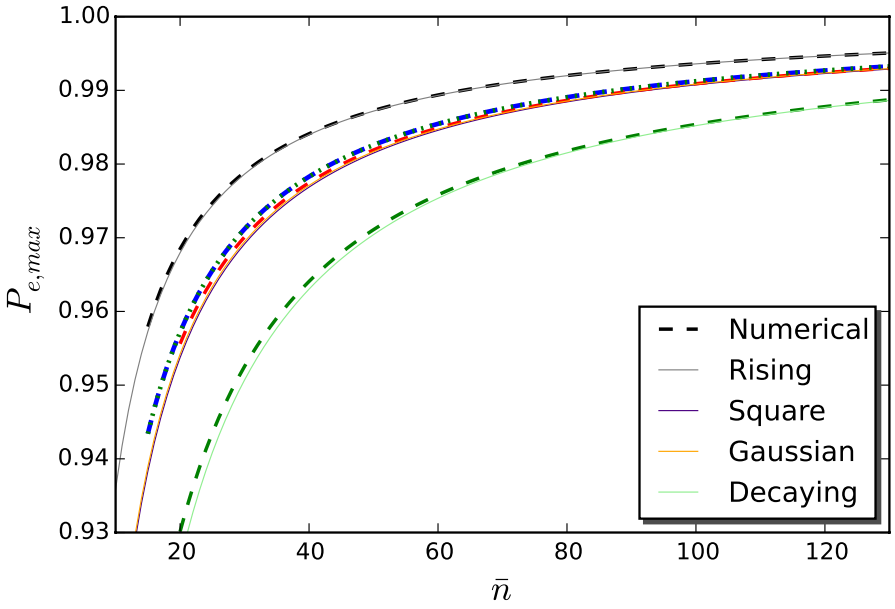

Figure 3.3: The optimized excitation probability for multiphoton coherent states, for various pulse shapes, as a function of the average number of photons ($\bar{n}$).

3.11 Multiphoton Fock states

Preparation of multiphoton Fock states, in contrast to coherent states, is very hard.

Nevertheless, I wish to consider this case for completeness. Before getting into the

discussion of asymptotic results, I want to start the section with the adiabatic result.

3.11.1 Fock states: adiabatic result

Like in the coherent state case, one can obtain the adiabatic results by equating the derivative of Eq.(3.10) to zero. We get then

$$P_{e,N} = -\frac{8\Gamma_P N}{\Gamma^2} f(t)^2 P_{e,N-1} + \frac{4\Gamma_P N}{\Gamma^2}. \tag{3.59}$$

Starting with the single photon ($N = 1$) result, we can recursively solve this equation to get the N-photon excitation probability:

$$\begin{aligned}
P_{e,1} &= \frac{4\Gamma_P}{\Gamma^2} f(t)^2, \\
P_{e,2} &= -4\left(\frac{4\Gamma_P}{\Gamma^2} f(t)^2\right)^2 + 2\left(\frac{4\Gamma_P}{\Gamma^2} f(t)^2\right), \\
P_{e,3} &= 24\left(\frac{4\Gamma_P}{\Gamma^2} f(t)^2\right)^3 - 12\left(\frac{4\Gamma_P}{\Gamma^2} f(t)^2\right)^2 + 3\left(\frac{4\Gamma_P}{\Gamma^2} f(t)^2\right) \\
&\quad . \\
&\quad . \\
P_{e,N} &= -\frac{1}{2}\sum_{n=1}^{N} \frac{N!}{(N-n)!}\left(-\frac{8\Gamma_P}{\Gamma^2} f(t)^2\right)^n .
\end{aligned} \tag{3.60}$$

3.11.2 An exactly solvable case

Although the system of $2N$ coupled differential equations, Eq.(3.10), is difficult to solve analytically, it is, surprisingly, possible to integrate them for some special pulses. One of them is the usual square pulse, in which case, and for small number of photons, one could easily integrate Eq.(3.10) recursively. Here, I want to consider an alternate case, the rising exponential pulse, and in this case, the same recursive approach leads to a closed form

expression for $P_{e,N}(t)$.

Consider a rising exponential pulse, with pulse duration $T = 1/\lambda$, $f(t) = \sqrt{\lambda}e^{\lambda t/2}$ for $t \leq 0$, and zero for $t > 0$. Recursively one finds

$$
\begin{aligned}
P_{e,1} =& \frac{4e^{\lambda t}\,\lambda\Gamma_P}{(\lambda+\Gamma)^2}, \\
P_{e,2} =& \frac{8e^{\lambda t}\,\lambda\Gamma_P}{(\lambda+\Gamma)^2} - \frac{64e^{2\lambda t}\,(\lambda\Gamma_P)^2}{(\lambda+\Gamma)^2\,(2\lambda+\Gamma)\,(3\lambda+\Gamma)}, \\
P_{e,3} =& \frac{12e^{\lambda t}\,\lambda\Gamma_P}{(\lambda+\Gamma)^2} - \frac{192e^{2\lambda t}\,(\lambda\Gamma_P)^2}{(\lambda+\Gamma)^2\,(2\lambda+\Gamma)\,(3\lambda+\Gamma)} + \frac{1536e^{3\lambda t}\,(\lambda\Gamma_P)^3}{(\lambda+\Gamma)^2\,(2\lambda+\Gamma)\,(3\lambda+\Gamma)^2\,(5\lambda+\Gamma)}, \\
P_{e,4} =& \frac{16e^{\lambda t}\,\lambda\Gamma_P}{(\lambda+\Gamma)^2} - \frac{384e^{2\lambda t}\,(\lambda\Gamma_P)^2}{(\lambda+\Gamma)^2\,(2\lambda+\Gamma)\,(3\lambda+\Gamma)} + \frac{6144e^{3\lambda t}\,(\lambda\Gamma_P)^3}{(\lambda+\Gamma)^2\,(2\lambda+\Gamma)\,(3\lambda+\Gamma)^2\,(5\lambda+\Gamma)} \\
& - \frac{49152e^{4\lambda t}\,(\lambda\Gamma_P)^4}{(\lambda+\Gamma)^2\,(2\lambda+\Gamma)\,(3\lambda+\Gamma)^2\,(5\lambda+\Gamma)\,(4\lambda+\Gamma)\,(7\lambda+\Gamma)}.
\end{aligned}
$$

From this recursive solutions, one immediately gets the N^{th} photon excitation probability as

$$
P_{e,N}(t) = \sum_{n=1}^{N}(-1)^{n+1}2^{3n-1}\,\frac{N!}{(N-n)!}\,\frac{(\lambda\Gamma_P)^n\,e^{n\lambda t}}{\prod_{m=1}^{n}(m\,\lambda+\Gamma)\,((2m-1)\lambda+\Gamma)} \tag{3.61}
$$

We can, further, reduce Eq.(3.61) to a more compact form. The final form, in terms of generalized hypergeometric function, is

$$
P_{e,N}(t) = \frac{4N\,e^{\lambda t}\,\lambda\Gamma_P}{(\lambda+\Gamma)^2}\mathbf{HypergeometricPFQ}\left[\{1, 1-N\}, \left\{2+\frac{\Gamma}{\lambda}, \frac{3}{2}+\frac{\Gamma}{2\lambda}\right\}, \frac{4\Gamma_P e^{\lambda t}}{\lambda}\right]. \tag{3.62}
$$

3.11.3 Fock states: perturbative solution

It is practically difficult, except for square and rising pulses, to get an exact analytical result for the excitation probability. Therefore, I will resort to the same kind of perturbative approach that I used for the coherent state.

Letting $g(t) = \sqrt{T} f(t)$, $\Omega_0 = 2\sqrt{N\Gamma_P T}$, $\tau = \Omega_0 t$, we can rewrite Eq.(3.10) as

$$\begin{aligned} \frac{d}{d\tau} y_n &= -\epsilon y_n - g(\tau)\sqrt{\frac{n}{N}} x_{n-1}, \\ \frac{d}{d\tau} x_{n-1} &= -\frac{\epsilon}{2} y_n + g(\tau)\sqrt{\frac{n}{N}} y_{n-1} - g(\tau)\sqrt{\frac{n}{N}}, \end{aligned} \tag{3.63}$$

where $x_n = \Sigma_n$, $y_n = 2P_{e,n}$, and $\epsilon = \Gamma/\Omega_0$. This system of $2N$ equations, indexed by n, which runs from 1 to N, can be written in a compact form by introducing a new vector, $\mathbf{v} = (y_N, x_{N-1}, y_{N-1}....)$. In terms of this new vector, the Eq.(3.63) is given by

$$\frac{d\mathbf{v}}{d\tau} = g(\tau)\mathbf{A}.\mathbf{v} + \epsilon \mathbf{B}.\mathbf{v} + g(\tau)\mathbf{C} \tag{3.64}$$

where the matrices $\mathbf{A}, \mathbf{B}$, and $\mathbf{C}$ have the following structure:

$$\mathbf{A} = \frac{1}{\sqrt{N}} \begin{pmatrix} 0 & -\sqrt{N} & 0 & 0 & 0 & .... \\ 0 & 0 & \sqrt{N} & 0 & 0 & .... \\ 0 & 0 & 0 & -\sqrt{N-1} & 0 & .... \\ 0 & 0 & 0 & 0 & \sqrt{N-1} & .... \\ .... & & & & & \end{pmatrix} \tag{3.65}$$

$$\mathbf{B} = \begin{pmatrix} -1 & 0 & 0 & 0 & 0 & .... \\ 0 & -1/2 & 0 & 0 & 0 & .... \\ 0 & 0 & -1 & 0 & 0 & .... \\ 0 & 0 & 0 & -1 & 0 & .... \\ .... & & & & & \end{pmatrix} \tag{3.66}$$

$$\mathbf{C} = \frac{1}{\sqrt{N}} \begin{pmatrix} 0 \\ -\sqrt{N} \\ 0 \\ -\sqrt{N-1} \\ .... \end{pmatrix} \tag{3.67}$$

Although Eq.(3.63) is, certainly, much more complex than the corresponding coherent states equations, the steps that I used there are still applicable here. Introducing a

perturbative solution $\mathbf{v} = \mathbf{v^{(0)}} + \epsilon\mathbf{v^{(1)}} + ...$, which leaves us to 0^{th} order in ϵ

$$\frac{d\mathbf{v^{(0)}}}{d\tau} = g(\tau)\mathbf{A}.\mathbf{v^{(0)}} + g(\tau)\mathbf{C}, \tag{3.68}$$

and to 1^{st} order

$$\frac{d\mathbf{v^{(1)}}}{d\tau} = g(\tau)\mathbf{A}.\mathbf{v^{(1)}} + \mathbf{B}.\mathbf{v^{(0)}}. \tag{3.69}$$

Formal solutions to these equations, with $\theta = \int_0^\tau g(\tau')d\tau'$, are

$$\mathbf{v^{(0)}}(\theta) = \int_0^\theta e^{\mathbf{A}(\theta-\theta')}\mathbf{C}\, d\theta', \tag{3.70}$$

$$\mathbf{v^{(1)}}(\theta) = \int_0^\theta \frac{1}{g(\tau(\theta'))} e^{\mathbf{A}(\theta-\theta')}\mathbf{B}.\mathbf{v^{(0)}}(\theta')\, d\theta'. \tag{3.71}$$

It is then clear that, at the end, one needs to compute the matrix $e^{\mathbf{A}(\theta-\theta')}$. We can do this by noting that the power series expansion of this matrix exponential, due to the special structure of the matrix $\mathbf{A}$, terminates after a finite number of terms. For the N-photon case, since $\mathbf{A}^{2N} = 0$, the power series expansion can be used to obtain y_N. After a careful manipulation, the first row of the matrix exponential is

$$\left(1, -t, -\frac{t^2}{2}, \frac{\sqrt{N-1}t^3}{6\sqrt{N}}, \frac{(N-1)t^4}{24N}, ...\frac{(-1)^{N-1}(N-1)!}{(2N-1)!N^{(2N-3)/2}}t^{2N-1}\right). \tag{3.72}$$

Where the even and odd powers of t can be identified as

$$\begin{aligned} &\frac{(-1)^n N!}{(2n)!(N-n)!N^n}t^{2n}, && (0 \le n \le N-1) \\ &\frac{(-1)^n\sqrt{N}(N-1)!}{\sqrt{N-(n-1)}(2n-1)!(N-n)!N^{n-1}}t^{2n-1}, && (1 \le n \le N) \end{aligned} \tag{3.73}$$

At this stage, obtaining the 0^{th} order solution is slightly involved. The strategy is to write down $P_{e,N}$ for few photons, and from the pattern generalize the result to an

$(N-n)$-photon state. Using Eq.(3.67), Eq.(3.70), and Eq.(3.72), we get

$$
\begin{aligned}
y^{(0)}_{N-n}(\theta) &= \frac{(N-n)\theta^2}{2N} - \frac{(N-n)(N-n-1)\theta^4}{24N^2} + ... + \frac{(-1)^{(N-n-1)}(N-n)!\theta^{2(N-n)}}{(2(N-n))!N^{(N-n)}}, \\
y^{(0)}_{N-n}(\theta) &= \sum_{m=1}^{N-n}(-1)^{(m-1)}\frac{(N-n)!\,\theta^{2m}}{(2m)!\,(N-n-m)!\,N^m}.
\end{aligned}
\tag{3.74}
$$

Finally, one can express $y^{(0)}_{N-n}(\theta)$ in terms of the confluent hypergeometric function, ${}_1\mathbf{F_1}$, as

$$
y^{(0)}_{N-n}(\theta) = 1 - {}_1\mathbf{F_1}\left(-N+n, \frac{1}{2}, \frac{\theta^2}{4N}\right). \tag{3.75}
$$

As x_{N-n-1} and y_{N-n} are related by a simple differentiation, we have

$$
\begin{aligned}
x^{(0)}_{N-n-1}(\theta) &= -\sqrt{\frac{N}{N-n}}\frac{d}{d\theta}\left[1 - {}_1\mathbf{F_1}\left(-N+n, \frac{1}{2}, \frac{\theta^2}{4N}\right)\right], \\
x^{(0)}_{N-n-1}(\theta) &= -\theta\sqrt{\frac{N-n}{N}}\,{}_1\mathbf{F_1}\left(-N+n+1, \frac{3}{2}, \frac{\theta^2}{4N}\right), \\
x^{(0)}_{N-n}(\theta) &= -\theta\sqrt{\frac{N-(n-1)}{N}}\,{}_1\mathbf{F_1}\left(-N+n, \frac{3}{2}, \frac{\theta^2}{4N}\right).
\end{aligned}
\tag{3.76}
$$

We can compare these zeroth order results with the corresponding coherent state equations. For $n=0$, in the large N limit, we will then find [62]

$$
\begin{aligned}
{}_1\mathbf{F_1}\left(-N, \frac{1}{2}, \frac{\theta^2}{4N}\right) &\simeq 1 - e^{\theta^2/8N}\cos(\theta), \\
{}_1\mathbf{F_1}\left(-N, \frac{3}{2}, \frac{\theta^2}{4N}\right) &\simeq \frac{1}{\theta}e^{\theta^2/8N}\sin(\theta).
\end{aligned}
\tag{3.77}
$$

Strikingly, these equations are similar to that of coherent state results Eq.(3.47). Additionally, we can see that the excitation probability, $y_N/2$, will be maximum around $\theta \simeq \pi$. However, it is important to keep in mind that the zeroth order in ϵ is unphysical: ϵ, that includes the coupling, Γ_P, of atom to the field, can never be strictly zero. Therefore, it is natural to expect that the zeroth order prediction will be inaccurate. Since we want the

expression for $P_{e,N}$ that is correct upto a leading order in $1/N$, it is not right to ignore the exponential term completely at this stage. Therefore, to the lowest order in ϵ, the excitation probability is

$$\begin{aligned} P_{e,N} &= \frac{1}{2}\left((1 - e^{\theta^2/8N}\cos(\theta)\right), \\ P_{e,N} &\simeq 1 + \frac{\pi^2}{16N}. \end{aligned} \tag{3.78}$$

Obviously, an excitation probability greater than one is unphysical, and we will see below that the next order correction, $y_N^{(1)}$, will make sure that $P_{e,N}$ is less than 1.

Formally, with Eq.(3.66), Eq.(3.73), Eq.(3.75), and Eq.(3.76), we get the first order correction as

$$\begin{aligned} y_N^{(1)}(\theta) = -\int_0^\theta \frac{d\tau}{d\theta'}\Bigg(&\sum_{n=0}^{N-1}\frac{(-1)^n N!}{(2n)!(N-n)!N^n}(\theta-\theta')^{2n}\left[1 - {}_1\mathbf{F_1}\left(-N+n, \frac{1}{2}, \frac{\theta'^2}{4N}\right)\right] \\ &- \frac{1}{2}\sum_{n=1}^{N-1}\frac{(-1)^n (N-1)!}{(2n-1)!(N-n)!N^{n-1}}(\theta-\theta')^{2n-1}\left[\theta' {}_1\mathbf{F_1}\left(-N+n, \frac{3}{2}, \frac{\theta'^2}{4N}\right)\right]\Bigg), \end{aligned} \tag{3.79}$$

where, again, we can see the similarity with the corresponding coherent state result, Eq.(3.52). For a fixed θ (in particular, $\theta \simeq \pi$), it is possible to show, at least numerically, that the terms in the bracket of Eq.(3.79) approaches, in the large N limit ($N \to \infty$), $(1 - \cos(\theta'))\cos(\theta - \theta') + \frac{1}{2}\sin(\theta')\sin(\theta - \theta')$. Qualitatively, this result can be understood by noting that for large n, the prefactors of the hypergeometric function, in the expression Eq.(3.79), go to zero very rapidly. Therefore, it is safe to take the argument, $N - n$, of the hypergeometric function, approximately, equals to N. Finally, we can use Eq.(3.77) to establish the identity between Eq.(3.79) and the coherent state result Eq.(3.52). At the

end, we will have

$$1 - P_{e,N} \mid_{\theta=\pi} = -\frac{\pi^2}{16N} + \epsilon \int_0^{\pi} \frac{\sin^4(\theta'/2)}{g(\tau(\theta'))} d\theta'. \tag{3.80}$$

To get the optimized excitation probability, we can use the same procedure that we applied to the coherent state case. Since the second term on the right hand side of the Eq.(3.80) is exactly the same as for the coherent state case, the bandwidth optimization for various pulses will yield the same T_{opt} as given in Table 2.2; except, where the average number of photons ($\bar{n}$) in T_{opt} will be replaced by N. Furthermore, the maximum optimized Fock state excitation probability can be obtained by adding $\pi^2/16N$ to the corresponding coherent state excitation probability. Table 3.3 summarize (see Figure 3.4 for graphical summary) the optimum bandwidth and the maximum excitation probability for the Fock state case, where the contribution from the external loss term, Γ_B, is shown explicitly.

Table 3.3: The optimized Fock state excitation probability for various pulse profiles in terms of the number of photons (N) and the ratio of coupling rates (Γ_B/Γ_P).

Pulse	T_{opt}	$P_{e,N}$
Rising pulse	$\pi^2/(8N\Gamma_P)$	$1 - \frac{0.02397}{N} - \frac{0.64082\Gamma_B}{N\Gamma_P}$
Square pulse	$\pi^2/(4N\Gamma_P)$	$1 - \frac{\pi^2}{32N} - \frac{3\pi^2\Gamma_B}{32N\Gamma_P}$
Gaussian pulse	$1.45009/(N\Gamma_P)$	$1 - \frac{0.29912}{N} - \frac{0.91597\Gamma_B}{N\Gamma_P}$
Decaying pulse	$3.347/(N\Gamma_P)$	$1 - \frac{0.8621}{N} - \frac{1.47895\Gamma_B}{N\Gamma_P}$

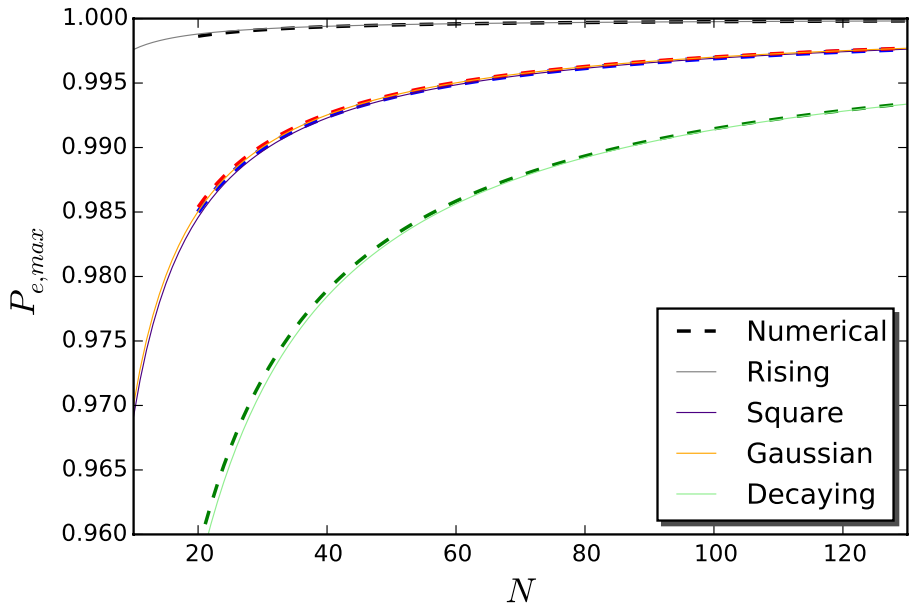

Figure 3.4: The optimized excitation probability for multiphoton Fock state, in the absence of external losses ($\Gamma_B = 0$), for various pulse shapes, as a function of the number of photons (N).

3.12 Conclusion

I have considered the maximum excitation probability of a two level system interacting with a quantum field in the presence of external losses. I have systematically analyzed this problem in two extreme limits: when the input field contains a single photon (or an average one photon in the case of coherent state), and in other limit where the field contains a large number of photons. It turns out that in both cases, the excitation probability critically depends on the temporal profile of the pulse. In particular, at the single photon level, the statistics of the field has a strong influence on the excitation probability: the behavior of optimized excitation probability of a single photon Fock state is strikingly different from its coherent state counter part (coherent state with an average number of one photon, $\bar{n} = 1$). Furthermore, I have given a simple proof to show that the only single photon pulse that

can give unit excitation is the rising exponential pulse; on the other hand, I have, also, showed that the maximum excitation due to a single photon coherent state can never reach one, and is bounded above by 0.632.

For multiphoton coherent state, I have used the perturbation theory to characterize the scaling of excitation probability with increasing number of photons. With optimum pulse duration T scales as $\alpha/\bar{n}\Gamma_P$, contrary to single photon case, T does not depend on external decay rate Γ_B, I find that $P_{e,\bar{n}}$ approaches 1 as $P_{e,\bar{n}} \simeq 1 - \beta/\bar{n}(1 + \Gamma_B/\Gamma_P)$, where α and β depend on the pulse shape.

For mutiphoton Fock state, it turns out that the optimum pulse bandwidth and the time at which the excitation peaks remain the same as for the corresponding coherent state with $\bar{n} = N$. However, the excitation probability is increased by $\pi^2/16N$, regardless of the pulse shape and the value of external decay.

Although the central theme of this chapter is on the excitation probability of a two level system, I have also showed how one can obtain the wavefunction of the scattered field from the Heisenberg-Langevin approach.

Chapter 4

Permanent population transfer in a Λ-system

The discussion from the earlier chapter, clearly, revealed that the transient excitation, and hence the scheme that relies on transient excitation probability for routing the target photon, depends on the control photon pulse shape. Here, I will consider an alternate scheme that uses permanent population transfer in an atomic system.

The scheme that uses permanent population transfer consists of a N-level system in a single-sided geometry. Where, the control field or multiple control fields act on the Λ transition levels of the N-level atomic system and the target acts on the other transition. Figure 4.1 gives a possible representation of the atomic level structure and the action of the fields on them.

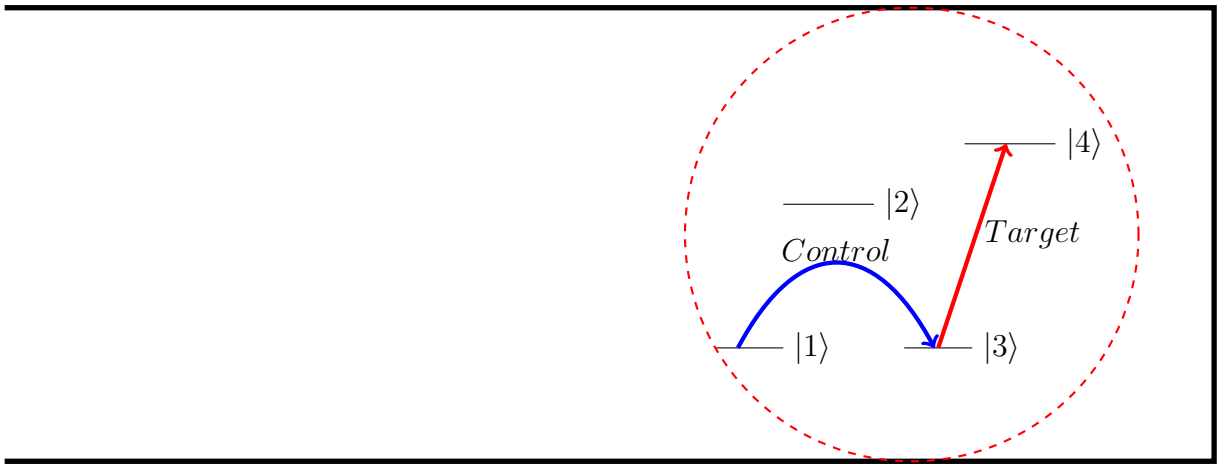

Figure 4.1: A depiction of the N-level structure. In this scheme, the control fields act on the Λ-system and the target field acts on the other transition.

As there are more atomic levels involved, the N-level scheme is, clearly, more flexible to control the target photon's phase. In the absence of control fields, the atom, which is initially in level 1, is transparent to the target photon. The target photon, however, gets a

phase of π, after the control field successfully transfer the population from level 1 to level 3, when it interacts adiabatically with the atomic system. Therefore, the phase of the target photon and the earlier discussed interferometric routing scheme that uses this phase for routing the photon depend on the efficiency of the control fields to transfer population from level 1 to level 3. Hence, I will ignore the target photon in the following discussion and devote this entire chapter to various schemes and their efficiency in transferring the population in a Λ-system.

There are many ways to transfer population from $|1\rangle \rightarrow |3\rangle$: the well-known technique STIRAP (Stimulated Raman Adiabatic Passage) [63], uses two different optical pulses, sent in a counter-intuitive way, acting on the two separate legs of the Λ-system, and efficiently transfers the population. On the other hand, SPRINT (Single-Photon Raman Interaction) [64, 65, 66] where a single photon acts between the initially populated level and the upper level in a single-sided geometry, can also effectively transfer population when both the legs of the Λ-system are coupled identically to the optical fields. Also, one could use a single photon in the $|1\rangle \rightarrow |2\rangle$ transition to efficiently excite the atom followed by a π-pulse in the other transition. However, we have seen that the complete inversion of the Λ-system with a single photon critically depends on the photon pulse profile, and may be practically difficult to implement. Therefore, I will limit the discussion to STIRAP and SPRINT.

I have organized this chapter in the following way. First I will consider the perfect case scenario: in the absence of external decay, I will study single-photon STIRAP (SSTIRAP), with a single pump and a single Stokes photon acting resonantly on the two separate legs of the Λ-system. I will use the techniques of chapter 1 to characterize the transfer probability. Later, I will focus on the corresponding SPRINT scenario and show that the

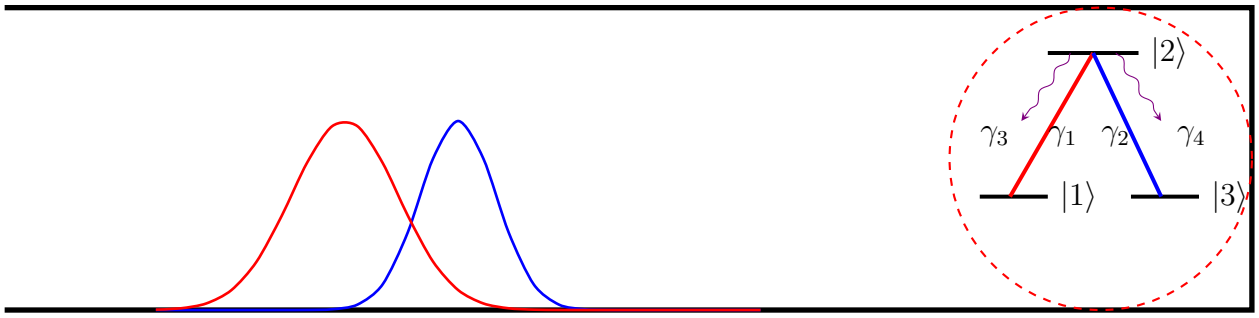

Figure 4.2: A diagram that depicts the SSTIRAP process in a single-sided geometry. Here, the pump (red) and the Stokes (blue) are acting on the separate legs of the Λ-system. The coupling rates γ_1 and γ_2 are the rates at which the pump and the Stokes photons couple to their respective transition. The other rates, γ_3 and γ_4, represent the external decay rates.

SPRINT is a limiting case of SSTIRAP. Finally, I will relax these perfect conditions and study the transfer probability: with more than one pump photon, and when the system has additional decay channels, I will explore the possibility of obtaining an optimized transfer with a minimum number of pump photons.

4.1 Single-photon STIRAP (SSTIRAP)

Figure 4.2, for instance, gives the details of this scheme. The γ_1 shown in the figure represents the strength of coupling between the modes that constitute the incoming pump photon (shown in red color) and the atomic transition $|1\rangle \leftrightarrow |2\rangle$. Similarly, γ_2 denotes the rate at which the other transition couples to the modes that make up the Stokes photon. Additionally, we have considered two extra decay channels: γ_3 denotes the rate at which the atom decays to the bath modes that act on the $|1\rangle \leftrightarrow |2\rangle$ transition, and γ_4 corresponds to the bath modes that act on $|3\rangle \leftrightarrow |2\rangle$ transition.

Here in this section, I will consider a two-photon multimode Fock state. For convenience, we will reserve the first place in the input Fock state for the pump photon and the second

place for the Stokes photon. Ignoring the external decays, we can study this system using the techniques developed in chapter 1. In this case, the Hamiltonian of the system, in terms of the multimode field operators ($A_{0j}(t) = \int d\omega_j a_{\omega_j}^{(j)} e^{-i\omega_j t}/\sqrt{2\pi}, j = 1, 2$), reads

$$H = -i\hbar\sqrt{2\gamma_1}\sigma_1^\dagger A_{01}(t) - i\hbar\sqrt{2\gamma_2}\sigma_2^\dagger A_{02}(t) + H.C. \tag{4.1}$$

Where, σ_1 and σ_2 are the atomic lowering operators acting on the levels $|1\rangle \leftrightarrow |2\rangle$ and $|2\rangle \leftrightarrow |3\rangle$, respectively. Further, the action of the multimode annihilation operator of the pump [Stokes] photon $A_{01}(t)$ [$A_{02}(t)$], which satisfies the commutation relation $\left[A_{0i}(t), A_{0i}^\dagger(t)\right] = \delta(t - t')$, on the input Fock state $|M, N\rangle$ gives

$$\begin{aligned} A_{01}(t)\,|M, N\rangle &= \sqrt{M} f_1(t)\,|M-1, N\rangle\,, \\ A_{02}(t)\,|M, N\rangle &= \sqrt{N} f_2(t)\,|M, N-1\rangle\,. \end{aligned} \tag{4.2}$$

Here, the $f_i(t)$ in Eq.(4.2) provides the temporal shape of the corresponding photon. At this stage, we can simply apply Schrodinger equation to the most general state of the atom-field combined system $|\psi\rangle = \sum_{j=1}^{3} |\psi_j\rangle\,|j\rangle$, which, after tracing over atomic states, leaves us

$$|\dot{\psi_1}\rangle = \sqrt{2\gamma_1} A_{01}^\dagger(t)\,|\psi_2\rangle\,, \tag{4.3}$$

$$|\dot{\psi_3}\rangle = \sqrt{2\gamma_2} A_{02}^\dagger(t)\,|\psi_2\rangle\,, \tag{4.4}$$

$$|\dot{\psi_2}\rangle = -\sqrt{2\gamma_1} A_{01}(t)\,|\psi_1\rangle - \sqrt{2\gamma_2} A_{02}(t)\,|\psi_3\rangle\,. \tag{4.5}$$

To get the transfer probability, we need to solve for $|\psi_3\rangle$; this may be practically difficult for an arbitrary number of input photons. However, this is certainly doable in this case. The idea here is to formally integrate Eq.(4.3) and Eq.(4.4) and substitute the

resulting expression in Eq.(4.5). For the initial field state $|\psi_1(0)\rangle = |1,1\rangle$, we get

$$\frac{d}{dt}|\psi_2(t)\rangle + (\gamma_1+\gamma_2)|\psi_2\rangle = -\sqrt{2\gamma_1}A_{01}(t)|1,1\rangle - 2\gamma_1\int_{-\infty}^{t} dt_1 A_{01}^{\dagger}(t_1)A_{01}(t)|\psi_2(t_1)\rangle \\ -2\gamma_2\int_{-\infty}^{t} dt_1 A_{02}^{\dagger}(t_1)A_{02}(t)|\psi_2(t_1)\rangle\,. \tag{4.6}$$

Letting $\gamma_1+\gamma_2=\Gamma$, we can formally integrate this equation:

$$|\psi_2(t)\rangle = -\sqrt{2\gamma_1}\int_{-\infty}^{t} e^{-\Gamma(t-t_1)}f_1(t_1)|0,1\rangle - \int_{-\infty}^{t} dt_1\left(2\gamma_1\int_{-\infty}^{t_1} dt_2 e^{-\Gamma(t-t_1)}\right. \\ \left. A_{01}^{\dagger}(t_2)A_{01}(t_1)|\psi_2(t_2)\rangle + 2\gamma_2\int_{-\infty}^{t_1} dt_2 e^{-\Gamma(t-t_1)}A_{02}^{\dagger}(t_2)A_{02}(t_1)|\psi_2(t_2)\rangle\right) \tag{4.7}$$

The form of $|\psi_2\rangle$ in Eq.(4.7) immediately calls for a recursive solution. In each iteration, we could normally order the operators and use Eq.(4.2) to simplify the expression. If the number of input photons are finite, the iterative series will eventually converge to a finite expression. In this case, it is evident from Eq.(4.2) that we only need a single iteration to get $|\psi_2\rangle$. Finally, $|\psi_2\rangle$ can be written, in terms of a new function $G_i(t) = \int_{-\infty}^{t} dt_1 e^{-\Gamma(t-t_1)}f_i(t_1)$ as

$$|\psi_2(t)\rangle = -\sqrt{2\gamma_1}G_1(t)|0,1\rangle + 2\gamma_2\sqrt{2\gamma_1}\int_{-\infty}^{t} dt_1\int_{-\infty}^{t_1} dt_2 e^{-\Gamma(t-t_1)}A_{02}^{\dagger}(t_2)G_1(t_2)f_2(t_1)|0,0\rangle\,. \tag{4.8}$$

Here we can go a step further by integrating the second term by parts, which leads to

$$|\psi_2(t)\rangle = -\sqrt{2\gamma_1}G_1(t)|0,1\rangle + 2\gamma_2\sqrt{2\gamma_1}\int_{-\infty}^{t} dt_2 A_{02}^{\dagger}(t_2)\left(G_2(t)G_1(t_2) - e^{-\Gamma(t-t_2)}G_1(t_2)G_2(t_2)\right). \tag{4.9}$$

Now, it is relatively straightforward to get $|\psi_3\rangle$ by substituting Eq.(4.9) for $|\psi_2\rangle$ in the

formal solution of Eq.(4):

$$
\begin{aligned}
|\psi_3(t)\rangle = & -2\sqrt{\gamma_1\gamma_2}\int_{-\infty}^{t} dt_1 \int_{-\infty}^{\infty} dt_2 A_{02}^{\dagger}(t_1)A_{02}^{\dagger}(t_2)G_1(t_1)f_2(t_2)\,|0,0\rangle \\
& + 4\sqrt{\gamma_1\gamma_2^3}\int_{-\infty}^{t} dt_1 \left[\int_{-\infty}^{t} dt_2 A_{02}^{\dagger}(t_1)A_{02}^{\dagger}(t_2)\Theta(t_1-t_2)\right. \\
& \left. \times \left(G_2(t_1)G_1(t_2) - e^{-\Gamma(t_1-t_2)}G_1(t_2)G_2(t_2)\right)|0,0\rangle\right]
\end{aligned}
\tag{4.10}
$$

Where the Θ represents the usual Heaviside step function. Since we are interested in getting the form of asymptotic transfer probability $\langle\psi_3(\infty)|\psi_3(\infty)\rangle$, which, in fact, can be obtained from Eq.(4.10) by simply extending the limit of the integration to infinity. The resulting form of the asymptotic transfer probability will be a complicated expression involving many operators, which can be simplified further by normally ordering the operators. For instance, one can easily verify that the terms that survive the normal ordering in the transfer probability, which contained operators of the form

$$
\int_{-\infty}^{\infty} dt_1 \int_{-\infty}^{\infty} dt_2 \int_{-\infty}^{\infty} dt_3 \int_{-\infty}^{\infty} dt_4 A_{02}(t_1)A_{02}(t_2)A_{02}^{\dagger}(t_3)A_{02}^{\dagger}(t_4),
$$

are those which respect the constrain $\delta(t_1-t_3)\delta(t_2-t_4)+\delta(t_1-t_4)\delta(t_2-t_3)$. The delta function brings down the evaluation of integrals to two. Finally, using the adiabatic condition by replacing $G_i(t)$ with $f_i(t)/\Gamma$ (see chapter 1), we can express the transfer probability (P_T) as a function of the ratio of the coupling rates ($X=\gamma_1/\gamma_2$):

$$
P_T = \frac{4X}{(1+X)^2} - \frac{16X^2}{(1+X)^4}\int_{-\infty}^{\infty} f_2(t)^2\,dt \int_{-\infty}^{t} f_1(y)^2\,dy + \frac{4X}{(1+X)^3}(X-1)\left(\int_{-\infty}^{\infty} f_2(t)f_1(t)\,dt\right)^2
\tag{4.11}
$$

This expression is quite general as it includes the Stokes and the pump photons of arbitrary pulse shapes. However, following the semiclassical STIRAP procedure, we assume

both the Stokes and the pump photons have identical pulse shape; but they are shifted apart. In the subsequent sections, we will assume that $f_2(t) = f_1(t + \tau)$, and appropriately shifting the pulse, we can imitate the intuitive and the counter intuitive pulse sequence of the semiclassical STIRAP.

In the intuitive pulse sequence ($\tau < 0$), the pump photon pulse will act first followed by the Stokes photon in a way that both these pulses have some overlap. In the counter-intuitive sequence, the Stokes photon, which has no direct link to the initially populated level $|1\rangle$, will act first; the pump photon which acts on the initially populated level will follow the Stokes photon. In the semiclassical STIRAP process, both these pulse sequences, where there is sufficient overlap between the pump and the Stokes photon pulses, are effective in transferring population from $|1\rangle \rightarrow |3\rangle$ [67]. However, the intuitive sequence scheme, before transferring the population to the level $|3\rangle$, will cause significant transient excitation to the level $|2\rangle$, and therefore the speed at which the transfer happens in the intuitive scheme is slower compare to the counter-intuitive scheme. Also, additional decay rates that arise from the coupling of the upper level to the external degrees of freedom can affect the performance of this scheme. On the other hand, in the counter-intuitive scheme, it is possible to transfer the population adiabatically without populating the upper level. Therefore, from the performance standpoint, the counter-intuitive pulse sequence is more effective in transferring the population among the lower levels of the Λ-system.

A quick remark will be useful here. It is important to note that most of the semiclassical works on STIRAP have not considered the spontaneous decay from the excited state ($|2\rangle$) state. However, a recent work [68] that considered the effect of spontaneous emission in STIRAP revealed that the counter-intuitive scheme is ideal in the

presence of spontaneous emission. We will see shortly that this is, indeed, true here as spontaneous emission is part of this fully quantized treatment of STIRAP.

The SPRINT limit of SSTIRAP is the other noteworthy point that I want to emphasize here. There are two ways to realize SPRINT in the SSTIRAP setup: the SSTIRAP in the absence of the Stokes photon ($f_2(t) = 0$) is the SPRINT. Therefore, one immediately finds the SPRINT transfer probability,

$$P_{T,sprint} = \frac{4X}{(1+X)^2}, \tag{4.12}$$

by just equating $f_2(t)$ in the Eq.(4.11) to zero. The other possible way would be by sending both the pump and the Stokes in the counter-intuitive sequence such that both the pulses have no overlap with each other. It is clear that under this limit ($\tau \to \infty$) when the pulses are separated far apart, the last term in the right-hand side of the Eq.(4.11) is zero. Also, for reasons that will become clear when we compute the transfer probability for a specific pulse, the second term in the right-hand side of Eq.(4.11) vanishes in the large τ limit.

A remarkable point to note here is that the SPRINT transfer probability does not depend on the shape of the pump photon. The transfer probability can even reach unity provided that the legs of the Λ-system have identical coupling strength; that is when $X = 1$. This important result, which is in agreement with the earlier study[64], points out that SPRINT, which uses fewer resources (one photon less compared to the SSTIRAP), performs far more effectively at $X = 1$. On the other hand, a simple inspection of Eq.(4.11) reveals that the STIRAP transfer probability is strictly less than 1 when $X = 1$. For values other than $X = 1$, a comparative study of the performance of these two methods (SSTIRAP and SPRINT) will have a greater practical significance: it helps us to identify

the values of X for which we can effectively transfer the population with fewer resources (SPRINT) or with more resources (SSTIRAP).

Another result that is immediately evident from Eq.(4.11) is that the performance of SPRINT is superior to STIRAP for values of X that are smaller than 1; this corresponds to the case in which $\gamma_2 > \gamma_1$. However, for other values of X, a straightforward comparison of the SPRINT and the SSTIRAP is not possible. Therefore, I will compute Eq.(4.11) for various pulse profiles and optimize the transfer probability with respect to the pulse separation. The reason for just considering the pulse separation in the optimization part is that in the adiabatic limit the duration of the pulse (T) is not an important parameter: we can safely equate $T = 1$ and express every other parameter relative to T. Finally, once we have the optimized result for a given pulse, a straightforward comparison with the SPRINT result will reveal whether the SPRINT or the STIRAP is more effective for a specific value of $X > 1$.

Gaussian pulse

I will assume both the pump and the Stokes photon pulses have identical shape; but one is shifted relative to the other. For the pump photon of the form $f_1(t) = e^{-t^2/2T^2}/\sqrt{T\sqrt{\pi}}$, the shape of the Stokes photon is then $f_2(t) = f_1(t + \tau)$. Observe that by changing the sign of the shift parameter τ we can get both the intuitive and counter intuitive pulse sequence in this method. As mentioned before, we will consider the duration of the pulse to be unity ($T = 1$), and compute various integrals that are in the Eq.(4.11). For Gaussian pulses of

identical shape, the overlap integral integral is straightforward:

$$\left(\int_{-\infty}^{\infty} f_2(t) f_1(t)\, dt\right)^2 = e^{-\tau^2/2} \tag{4.13}$$

However, the other integral in Eq.(4.11), compared to the overlap integral, is slightly involved. The double integral appearing in the expression, after computing the innermost integral, will reduce to a single integral:

$$\int_{-\infty}^{\infty} f_2(t)^2\, dt \int_{-\infty}^{t} f_1(y)^2\, dy = \int_{-\infty}^{\infty} \frac{e^{-(t+\tau)^2}}{2\sqrt{\pi}} \left(1 + Erf(t)\right) dt. \tag{4.14}$$

Where the Erf represents the error function. By an appropriate change of variable, it is relatively easy to show that Eq.(4.14) is identical to

$$\int_{-\infty}^{\infty} \frac{e^{-t^2}}{2\sqrt{\pi}} \left(1 + Erf(t-\tau)\right) dt = \int_{-\infty}^{\infty} \frac{e^{-t^2}}{2\sqrt{\pi}}\, Erfc(\tau - t)\, dt. \tag{4.15}$$

Finally, using the complementary error function ($Erfc(x) = 1 - Erf(x)$) identity $\int_{-\infty}^{\infty} e^{-x^2} Erfc(a+bx)dx = \sqrt{\pi} Erfc(a/\sqrt{1+b^2})$, we get the transfer probability as

$$P_T = \frac{4X}{(1+X)^2} - \frac{8X^2}{(1+X)^4} Erfc(\tau/\sqrt{2}) + \frac{4X}{(1+X)^3}(X-1)e^{-\tau^2/2}. \tag{4.16}$$

Clearly, in the large τ limit Eq.(4.16) approaches the SPRINT result. For other intermediate τ values, we can get the optimum pulse shift (τ_{opt}) that maximizes the transfer probability by a straightforward differentiation of Eq.(4.16). The corresponding optimized pulse shift, as a function of X, is $\tau_{opt} = 2\sqrt{2/\pi}X/(X^2-1)$. Since we are interested in the region where $X > 1$, we can safely ignore the singular nature of τ_{opt} at $X = 1$. Now that we have the optimized pulse separation, we can compute the optimized STIRAP transfer probability and compare the result with the SPRINT in the region $X > 1$.

Hypebolic secant pulse

For a normalized hyperbolic secant pulse, $f_1(t) = \mathrm{sech}(t/T)/\sqrt{2T}$, of unit pulse width ($T = 1$), the overlap integral is $\tau^2\,\mathrm{csch}^2(\tau)$. Similarly, the expression which contains double integrals can be integrated without much difficulty. We immediately obtain

$$\begin{aligned}\int_{-\infty}^{\infty} f_2(t)^2\,dt \int_{-\infty}^{t} f_1(y)^2\,dy &= \int_{-\infty}^{\infty} \frac{\mathrm{sech}(t+\tau)}{2\sqrt{2}}\,(1+\tanh(t))\,dt, \\ &= \frac{1}{2}\left(1 - \coth(\tau) + \tau\,\mathrm{csch}^2(\tau)\right).\end{aligned} \tag{4.17}$$

In this case, the optimized pulse separation that maximizes the resulting transfer probability

$$P_{T,sech} = \frac{4X}{(1+X)^2} - \frac{8X^2}{(1+X)^4}\left(1 - \coth(\tau) + \tau\,\mathrm{csch}^2(\tau)\right) + \frac{4X}{(1+X)^3}(X-1)\tau^2\,\mathrm{csch}^2(\tau), \tag{4.18}$$

has turned out to be $\tau_{opt} = 2X/(X^2-1)$. Again, note the similarity with the corresponding Gaussian case: in both of these cases the optimum pulse separation is singular at $X = 1$, and the optimized transfer probability approaches the SPRINT result in the large τ limit.

Square pulse

For the Gaussian and the secant pulses, as a consequence of their symmetric form, the final expression obtained for the transfer probability is valid for both positive ($\tau > 0$) and negative ($\tau < 0$) pulse shift; but for square, rising, and decaying pulse we need to compute the integrals separately for positive shift and negative shift. For the square pulse case, we will use the pump photon of the form $f_1(t) = \Theta(t-\tau)\Theta(1+\tau-t)/\sqrt{T}$ and the Stokes photon of the form $f_2(t) = \Theta(t)\Theta(1-t)/\sqrt{T}$ to compute the integrals. The first overlap

integral will give

$$\left(\int_{-\infty}^{\infty} f_2(t) f_1(t)\, dt\right)^2 = \begin{cases} (T-\tau)^2 & \tau > 0 \\ (T+\tau)^2 & \tau < 0 \end{cases} \tag{4.19}$$

In a similar, way we find

$$\int_{-\infty}^{\infty} f_2(t)^2\, dt \int_{-\infty}^{t} f_1(y)^2\, dy = \begin{cases} \frac{1}{2}(T-\tau)^2 & \tau > 0 \\ T^2 - \frac{(T+\tau)^2}{2} & \tau < 0 \end{cases} \tag{4.20}$$

Although I have kept the pulse duration explicitly in my calculation, I will take it to be 1 in what follows.

Rising and decaying exponential pulses

Fortunately, in the case of pulses with rising and decaying exponential profiles, the calculation yields the exact same result. For rising pulse of the form $f_1(t) = \Theta(-t)\sqrt{2/T}e^{t/T}$, and decaying pulse with the temporal shape $f_1(t) = \Theta(t)\sqrt{2/T}e^{-t/T}$, the overlap integral, assuming a unit pulse width, gives

$$\left(\int_{-\infty}^{\infty} f_2(t) f_1(t)\, dt\right)^2 = \begin{cases} e^{-2\tau} & \tau > 0 \\ e^{2\tau} & \tau < 0 \end{cases} \tag{4.21}$$

Similarly, the other integral yields

$$\int_{-\infty}^{\infty} f_2(t)^2\, dt \int_{-\infty}^{t} f_1(y)^2\, dy = \begin{cases} \frac{1}{2}e^{-2\tau} & \tau > 0 \\ 1 - \frac{1}{2}e^{2\tau} & \tau < 0 \end{cases} \tag{4.22}$$

At this point, we can optimize the transfer probability with respect to the pulse separation. Numerically, it is easy to verify that maximum transfer happens when the pulse shift is positive: the scheme that uses the counter-intuitive pulse sequence. This result is in agreement with [68] where they have reported that in the presence of spontaneous emission

it is the counter-intuitive scheme that optimizes the transfer. Since the spontaneous emission is part of this framework, the result is different from the corresponding semiclassical STIRAP with no spontaneous decay, where both the intuitive and counter-intuitive schemes can effectively transfer the population[67].

In Figure 4.3, the optimized transfer probability, corresponding to the SSTIRAP scenario, is plotted as a function of the ratio of coupling rates $X = \gamma_1/\gamma_2$. Evidently, for small X ($\gamma_2 \gg \gamma_1$ and may be a little beyond that), the SPRINT is very effective compared to the SSTIRAP. On the other hand, in the exact opposite case, where $\gamma_1 \gg \gamma_2$, the SSTIRAP maximizes the transfer, and numerically one can verify that the optimized pulse separation, corresponding to this case, approaches zero. In these two limits, the pulse shape has no effect on the transfer probability. However, in the intermediate region where γ_1 slightly bigger than γ_2, we can see that the transfer probability does depend on the pulse shape. The values of X for which the pulse shape influences the transfer probability is where the SPRINT-SSTIRAP trade-off happens.

Here, we have seen that a single photon is sufficient to transfer the population with unit probability in a Λ-system. The only caveat is that for the successful implementation of this low-resource scheme (SPRINT), both the legs of the Λ-system have to have the same coupling strength ($\gamma_1 = \gamma_2$); in literature, this is known as the quantum impedance-matching in the Λ-system. However, in the absence of quantum impedance-matching, SPRINT can't transfer the population with unit probability. Also, adding an extra Stokes photon to facilitate this transfer by mimicking the semi-classical STIRAP does give any better result than SPRINT when $X > 1$,but no improvement when $X < 1$. Therefore, it is intuitive that we need to consider the quantum fields with greater

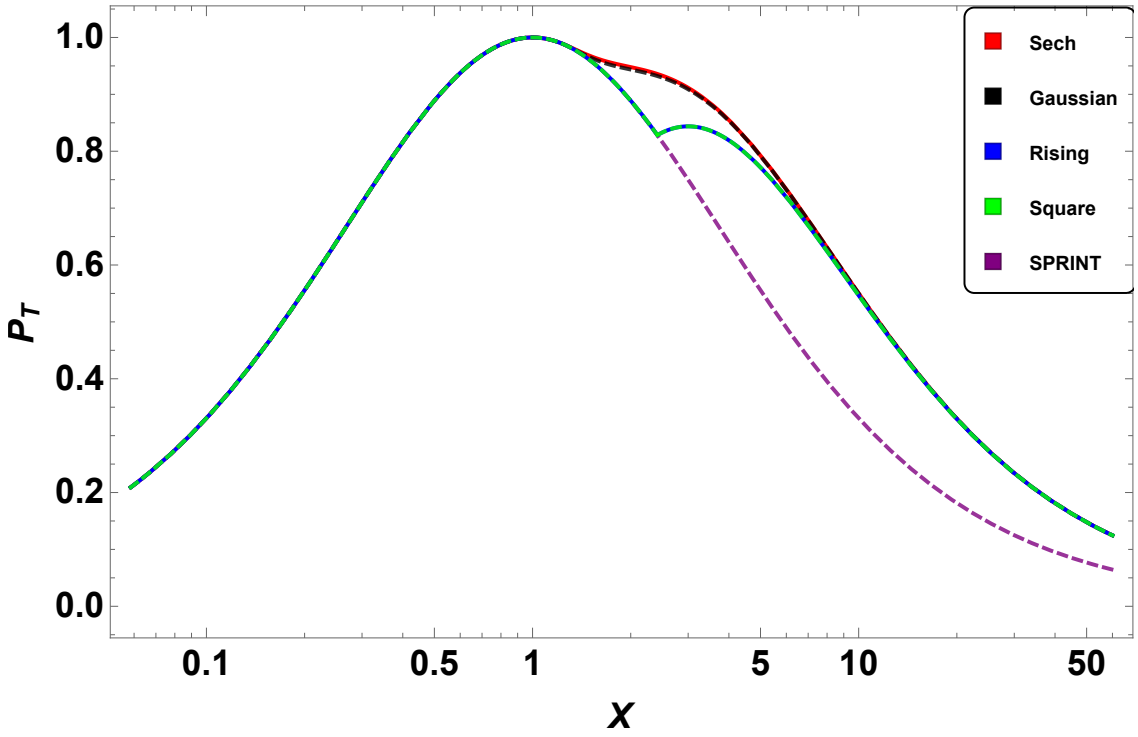

Figure 4.3: The optimized SSTIRAP transfer probability as a function of the ratio of the coupling rates ($X = \gamma_1/\gamma_2$).

number of photons, just as in the case of semiclassical STIRAP, to increase the efficiency of the transfer in the absence of quantum impedance-matching. Furthermore, since it is desirable to have an efficient transfer with a minimum number of resources, my object in the following sections will focus on the characterization of this transfer probability as a function of the number of photons and the additional parameters that are involved in the process.

4.2 Heisenberg-Langevin Approach

As we have seen from chapter 2, it is practically difficult to study the effect of external dissipation in the framework of pure-state analysis. Also, I want to characterize the transfer probability with an increasing number of photons. Therefore, I will resort to

Heisenberg-Langevin formalism in this section.

Abbreviating the Hermitian conjugate as H.C, the Hamiltonian of the system, including external decays, under the rotating wave approximation is

$$H = -i\hbar \left(\sum_{j=1}^{2} g_{2j-1} \int d\omega_{2j-1} \sigma_1^\dagger a_{\omega_{2j-1}}^{(2j-1)} e^{-i\omega_{2j-1}t} + g_{2j} \int d\omega_{2j} \sigma_2^\dagger a_{\omega_{2j}}^{(2j)} e^{-i\omega_{2j}t} \right) + H.C. \quad (4.23)$$

Here, g_1 and g_2 correspond to the strength at which the pump and the Stokes photons couple to their respective transitions. Whereas, g_3 denotes the coupling strength of the bath that acts on the pump photon's transition and g_4 represents the strength at which the bath couples to the other transition. As earlier, I will use the Heisenberg equation, $\dot{a}_\omega = i/\hbar\,[H, a_\omega]$, to get the equations of motion of the field operators, and their formal solutions have the following form:

$$a_{\omega_{2j-1}}^{(2j-1)}(t) = a_{\omega_{2j-1}}^{(2j-1)}(0) + g_{2j-1} \int_{-\infty}^{t} \sigma_1(t') e^{-i\omega_{2j-1}t'} dt', \quad (4.24)$$

$$a_{\omega_{2j}}^{(2j)}(t) = a_{\omega_{2j}}^{(2j)}(0) + g_{2j} \int_{-\infty}^{t} \sigma_2(t') e^{-i\omega_{2j}t'} dt'. \quad (4.25)$$

We can use these equations to eliminate the field part that we will encounter in the equation of an atomic operator. The equations for the following operators are relevant to compute the transfer probability: the operator $\sigma_{z1} = |2\rangle\langle 2| - |1\rangle\langle 1|$ gives the population inversion of the levels where the pump is acting, and $\sigma_{z2} = |2\rangle\langle 2| - |3\rangle\langle 3|$, similarly, gives the population inversion of the levels on which the Stokes field acts. Additionally, apart from the coherence operator σ_i ($|i\rangle\langle 2|\,; i = 1, 3$), we also need an equation for the operator ($J = |1\rangle\langle 3|$) that gives the coherence between the levels $|1\rangle$ and $|3\rangle$. Once we have the solutions of these atomic operators, the population in the level $|3\rangle$, or in other words the transfer probability, is given by $P_T = \langle \sigma_{z1} - 2\sigma_{z2} + \mathbf{I} \rangle / 3$. Where the identity operator $\mathbf{I}$ is

$|1\rangle\langle 1| + |2\rangle\langle 2| + |3\rangle\langle 3|$, and the angular bracket represents the expectation value which is taken over the initial state.

To illustrate this method, I will take the operator σ_{z1} as an example and demonstrate how to get its equation. From the Heisenberg equation, it immediately follows

$$\dot{\sigma}_z = -2g_1 \int d\omega_1 \sigma_1^\dagger a_{\omega_1}^{(1)}\, e^{-i\omega_1 t} - g_2 \int d\omega_2 \sigma_2^\dagger a_{\omega_2}^{(2)} e^{-i\omega_2 t} \\ - 2g_3 \int d\omega_3 \sigma_1^\dagger a_{\omega_3}^{(3)}\, e^{-i\omega_3 t} - g_4 \int d\omega_4 \sigma_2^\dagger a_{\omega_4}^{(4)} e^{-i\omega_4 t} + H.C. \tag{4.26}$$

Now we can use Eqs.(4.24) and (4.25) to eliminate the field part of Eq.(4.26), and express

$$\dot{\sigma}_{z1} = -2\pi g_1^2 \sigma_1^\dagger(t)\sigma_1(t) - \pi g_2^2 \sigma_2^\dagger(t)\sigma_2(t) - 2g_1 \int d\omega_1 \sigma_1^\dagger a_{\omega_1}^{(1)}(0) e^{-i\omega_1 t} - g_2 \int d\omega_2 \sigma_2^\dagger a_{\omega_2}^{(2)}(0) e^{-i\omega_2 t} \\ - 2g_3 \int d\omega_3 \sigma_1^\dagger a_{\omega_3}^{(3)}(0) e^{-i\omega_3 t} - g_4 \int d\omega_4 \sigma_2^\dagger a_{\omega_4}^{(4)}(0) e^{-i\omega_4 t} + H.C, \tag{4.27}$$

in terms of the multimode field operators (A_{0i}) as

$$\dot{\sigma}_{z1} = -(2\gamma_1 + 2\gamma_3 + \gamma_2 + \gamma_4)\frac{\sigma_{z1} + \sigma_{z2} + \mathbf{I}}{3} - 2\sqrt{\gamma_1}\sigma_1^\dagger A_{01}(t) - 2\sqrt{\gamma_2} A_{02}^\dagger(t)\sigma_1 - \sqrt{\gamma_2}\sigma_2^\dagger A_{02}(t) \\ - \sqrt{\gamma_2} A_{02}^\dagger(t)\sigma_2 - 2\sqrt{\gamma_3}\sigma_1^\dagger A_{03}(t) - 2\sqrt{\gamma_3} A_{03}^\dagger(t)\sigma_1 - \sqrt{\gamma_4}\sigma_2^\dagger A_{04}(t) - \sqrt{\gamma_4} A_{04}^\dagger(t)\sigma_2. \tag{4.28}$$

Where I have taken $2\pi g_i^2 = \gamma_i$ in the final expression, and it corresponds to the rate at which the field mode (A_{0i}) couples to the respective atomic transition. In this fashion, getting the equations of the other atomic operators is also relatively straightforward. However, instead of deriving the equation by going through each step, we can use the

symmetry of the problem to get the σ_{z2} expression:

$$\dot{\sigma}_{z2} = -\left(\gamma_1+\gamma_3+2\gamma_2+2\gamma_4\right)\frac{\sigma_{z1}+\sigma_{z2}+\mathbf{I}}{3} - \sqrt{\gamma_1}\sigma_1^\dagger A_{01}(t) - \sqrt{\gamma_2}A_{02}^\dagger(t)\sigma_1 - 2\sqrt{\gamma_2}\sigma_2^\dagger A_{02}(t)$$
$$- 2\sqrt{\gamma_2}A_{02}^\dagger(t)\sigma_2 - \sqrt{\gamma_3}\sigma_1^\dagger A_{03}(t) - \sqrt{\gamma_3}A_{03}^\dagger(t)\sigma_1 - 2\sqrt{\gamma_4}\sigma_2^\dagger A_{04}(t) - 2\sqrt{\gamma_4}A_{04}^\dagger(t)\sigma_2. \tag{4.29}$$

The other relevant equations that are important in this context are

$$\dot{\sigma_1} = -\frac{\gamma_1+\gamma_2+\gamma_3+\gamma_4}{2}\sigma_1 + \sqrt{\gamma_1}\sigma_{z1}A_{01}(t) + \sqrt{\gamma_3}\sigma_{z1}A_{03}(t) - \sqrt{\gamma_2}JA_{02}(t) - \sqrt{\gamma_4}JA_{04}(t), \tag{4.30}$$

$$\dot{\sigma_2} = -\frac{\gamma_1+\gamma_2+\gamma_3+\gamma_4}{2}\sigma_2 + \sqrt{\gamma_2}\sigma_{z2}A_{02}(t) + \sqrt{\gamma_4}\sigma_{z2}A_{04}(t) - \sqrt{\gamma_1}J^\dagger A_{01}(t) - \sqrt{\gamma_3}J^\dagger A_{03}(t), \tag{4.31}$$

$$\dot{J} = \sqrt{\gamma_1}\sigma_2^\dagger A_{01}(t) + \sqrt{\gamma_2}A_{02}^\dagger(t)\sigma_1 + \sqrt{\gamma_3}\sigma_2^\dagger A_{03}(t) + \sqrt{\gamma_4}A_{04}^\dagger(t)\sigma_1. \tag{4.32}$$

Although these equations contain additional operators like $J^\dagger, \sigma_1^\dagger$, and $\sigma_2^\dagger$, we do not need to get their equations separately: in a resonant interaction, the expectation values of these operators are identical to their Hermitian conjugates. Therefore, in order to get the transfer probability, one needs to solve for the expectation value of these operator equations.

For an initial input Fock state, getting an analytical result for the transfer probability is difficult in this formalism: one needs to integrate a massive number of equations; even for the simple case that I considered in the previous section, where a single Stokes and pump photon act on the Λ-system, the number of equations need to be solved are 16. Also, the expectation value equations grow very rapidly with increasing number of Fock state photons, obtaining the transfer probability is also harder numerically. Further, the

practical realization of multiphoton Fock state is even more challenging. When it comes to multiphoton process, it makes more sense to describe it in terms of coherent states. Therefore, in what follows, I will consider the case in which two multimode coherent states act on the separate legs of the Λ-system, and characterize the transfer probability as a function of the average number of photons in the field.

4.3 Coherent state STIRAP

Here I will consider the case in which the atom is initially in the state $|1\rangle$, and the fields, both the Stokes and the pump, that induce the transition in the Λ-system, are in the multimode coherent state. I will denote the initial state of the fields by $|\alpha_T, \alpha_C, 0, 0\rangle$, where the multimode field operator A_{0i} will act only on the i^{th} position of this state. For instance, the action of A_{01} and A_{02} on this state give

$$\begin{aligned} A_{01} |\alpha_T, \alpha_C, 0, 0\rangle &= \sqrt{\bar{n}} f_1(t) |\alpha_T, \alpha_C, 0, 0\rangle , \\ A_{02} |\alpha_T, \alpha_C, 0, 0\rangle &= \sqrt{\bar{m}} f_2(t) |\alpha_T, \alpha_C, 0, 0\rangle . \end{aligned} \tag{4.33}$$

Where, $\bar{n}$ ($\bar{m}$) represents the average number of photons in the pump (Stokes) field, and f_i corresponds to their pulse shape. Using Eq(4.33) we get

$$\langle \dot{\sigma}_{z1} \rangle = -\frac{2(\gamma_1+\gamma_3)+\gamma_2+\gamma_4}{3} \left(\langle \sigma_{z1} + \sigma_{z2} + I \rangle \right) - 4\sqrt{\gamma_1 \bar{n}} f_1(t) \langle \sigma_1 \rangle - 2\sqrt{\gamma_2 \bar{m}} f_2(t) \langle \sigma_2 \rangle , \tag{4.34}$$

$$\langle \dot{\sigma}_{z2} \rangle = -\frac{2(\gamma_2+\gamma_4)+\gamma_1+\gamma_3}{3} \left(\langle \sigma_{z1} + \sigma_{z2} + I \rangle \right) - 2\sqrt{\gamma_1 \bar{n}} f_1(t) \langle \sigma_1 \rangle - 4\sqrt{\gamma_2 \bar{m}} f_2(t) \langle \sigma_2 \rangle , \tag{4.35}$$

$$\langle \dot{\sigma}_1 \rangle = -\frac{\gamma_1+\gamma_3+\gamma_2+\gamma_4}{2} \langle \sigma_1 \rangle + \sqrt{\gamma_1 \bar{n}} f_1(t) \langle \sigma_{z1} \rangle - \sqrt{\gamma_2 \bar{m}} f_2(t) \langle J \rangle , \tag{4.36}$$

$$\langle \dot{\sigma}_2 \rangle = -\frac{\gamma_1+\gamma_3+\gamma_2+\gamma_4}{2} \langle \sigma_2 \rangle + \sqrt{\gamma_2 \bar{m}} f_2(t) \langle \sigma_{z2} \rangle - \sqrt{\gamma_1 \bar{n}} f_1(t) \langle J \rangle , \tag{4.37}$$

$$\left\langle \dot{J} \right\rangle = \sqrt{\gamma_1 \bar{n}} f_1(t) \langle \sigma_2 \rangle + \sqrt{\gamma_2 \bar{m}} f_2(t) \langle \sigma_1 \rangle . \tag{4.38}$$

While writing these equations, I have used the fact that the expectation value of the coherence operator is equal to its Hermitian conjugate; which is a valid assumption as long as the functions f_is are real and the detunings are zero. All that we need to compute the transfer probability, $P_T = \langle \sigma_{z1} - 2\sigma_{z2} + \mathbf{I} \rangle / 3$, are $\langle \sigma_{z1} \rangle$, and $\langle \sigma_{z2} \rangle$, which is certainly difficult as it involves the integration of a set of coupled differential equations with time-dependent coefficients. Certainly, we can solve them numerically: the numerical solutions are useful for making a suitable approximation to get an approximate analytical expression of the transfer probability.

Earlier works on STIRAP revealed that the counter-intuitive pulse sequence in the adiabatic regime is very effective in transferring the population among the lower levels of the Λ-system. The reason for this is that in the adiabatic regime, this pulse sequence will not contribute much to the population of the upper level. Therefore in the adiabatic

interaction (in this context, it simply means that $\gamma_i T \gg 1$), it is sensible to assume the expectation value of $|2\rangle\langle 2| \approx 0$, and the form of the transfer probability as a consequence of this reasonable assumption is:

$$P_T \approx 1 + \langle \sigma_{z1} \rangle. \tag{4.39}$$

Note that the system that I study here is slightly different from its semiclassical STIRAP with no spontaneous emission. In the semiclassical case, the adiabatic regime means that the product of Rabi frequency and the pulse duration should be much greater than 1 ($\Omega T \gg 1$). However, in this fully quantized version, $\gamma_i T \gg 1$ in the adiabatic regime.

Before proceeding further with the analysis of the fully quantized version of STIRAP, we want to examine the coherent state analog of the SPRINT process: CRINT (Coherent state Raman Interaction– a single coherent field is acting on the initially populated level and the upper level of the Λ-system). At the single photon level, we have seen that the SPRINT (a low-resource scheme) is very efficient under ideal conditions. Therefore, in the absence of these perfect SPRINT conditions, it is imperative that we identify how to transfer the population in a Λ-system with minimum resources. Hence, the CRINT, which uses fewer resources compared to the STIRAP, is certainly a simple scheme that is worth considering.

4.3.1 CRINT

The CRINT equations immediately follow from the corresponding STIRAP equations: the STIRAP equations with $f_2 = 0$ are the CRINT equations. The required equations that we

need to solve for getting the transfer probability are

$$\langle \dot{\sigma}_{z1} \rangle = -\frac{2(\gamma_1+\gamma_3)+\gamma_2+\gamma_4}{3} \left(\langle \sigma_{z1} + \sigma_{z2} + I \rangle \right) - 4\sqrt{\gamma_1 \bar{n}} f_1(t) \langle \sigma_1 \rangle , \tag{4.40}$$

$$\langle \dot{\sigma}_{z2} \rangle = -\frac{2(\gamma_2+\gamma_4)+\gamma_1+\gamma_3}{3} \left(\langle \sigma_{z1} + \sigma_{z2} + I \rangle \right) - 2\sqrt{\gamma_1 \bar{n}} f_1(t) \langle \sigma_1 \rangle , \tag{4.41}$$

$$\langle \dot{\sigma_1} \rangle = -\frac{\gamma_1+\gamma_3+\gamma_2+\gamma_4}{2} \langle \sigma_1 \rangle + \sqrt{\gamma_1 \bar{n}} f_1(t) \langle \sigma_{z1} \rangle . \tag{4.42}$$

Although it is easy to handle these equations numerically, analytical integration of these equations is hard for arbitrary f_1. Nevertheless, with suitable approximations based on the numerical solution, we can solve them in the following way. It turns out that under adiabatic conditions ($\gamma_i T \gg 1$), we can equate the derivative term of the coherence operator ($\langle \dot{\sigma_1} \rangle$=0). We then get

$$\langle \sigma_1 \rangle = \frac{2\sqrt{\gamma_1 \bar{n}} f_1(t)}{\gamma_1+\gamma_3+\gamma_2+\gamma_4} \langle \sigma_{z1} \rangle . \tag{4.43}$$

Similarly, the resulting expression obtained by adding Eqs.(4.40) and (4.41) also respects the adiabatic approximation:

$$\langle \sigma_{z1} + \sigma_{z2} + I \rangle = -\frac{12\gamma_1 \bar{n} \left(f_1(t) \right)^2}{\left(\gamma_1+\gamma_3+\gamma_2+\gamma_4 \right)^2} \langle \sigma_{z1} \rangle . \tag{4.44}$$

On the other hand, one shouldn't apply the adiabatic approximation blindly by equating the derivative part of the remaining equations to zero; one needs to verify the validity of such approximations numerically. Finally, a straightforward substitution of Eq.(4.44) and Eq.(4.43) in Eq.(4.40) will lead to a first order differential equation,

$$\langle \dot{\sigma_z} \rangle = -\frac{4\gamma_1 \bar{n} f_1(t)^2}{\left(\gamma_1+\gamma_3+\gamma_2+\gamma_4 \right)^2} \left(\gamma_2+\gamma_4 \right) \langle \sigma_{z1} \rangle \tag{4.45}$$

which has a simple solution:

$$\langle \sigma_{z1}(t) \rangle = \langle \sigma_{z1}(0) \rangle \; exp\left(-\frac{4\gamma_1 \left(\gamma_2 + \gamma_4\right) \bar{n} \int_{-\infty}^{t} dt' f_1(t')^2}{\left(\gamma_1 + \gamma_3 + \gamma_2 + \gamma_4\right)^2} \right). \tag{4.46}$$

Therefore, since $\langle \sigma_{z1}(0) \rangle = -1$, the asymptotic transfer probability is

$$\begin{aligned} P_T(t) &= 1 - exp\left(-\frac{4\gamma_1 \left(\gamma_2 + \gamma_4\right) \bar{n} \int_{-\infty}^{t} dt' f_1(t')^2}{\left(\gamma_1 + \gamma_3 + \gamma_2 + \gamma_4\right)^2} \right), \\ P_T(\infty) &= 1 - exp\left(-\frac{4X\left(1 + Z\right)\bar{n}}{\left(1 + X + Y + Z\right)^2} \right). \end{aligned} \tag{4.47}$$

Where I denoted γ_1/γ_2 by X, γ_3/γ_2 by Y, and γ_4/γ_2 by Z. Note that the CRINT transfer probability is very promising as it approaches one exponentially fast as $\bar{n}$ increases. This exponential scaling of the transfer probability is much better than the scaling that we encountered in the transient excitation probability: in the transient case, the excitation probability approaches one inversely proportional to the number of photons in the field. Also, it is worth noting that the asymptotic transfer probability, in the CRINT case, does not depend on the pulse shape. However, in the transient excitation, we have seen that the transient excitation probability critically depends on the temporal profile of the pulse.

In the absence of any external dissipation, both the CRINT and the SPRINT show some strikingly similar behavior: these two processes are very efficient when the atomic system satisfies the quantum impedance matching condition ($X = 1$). But, unlike SPRINT, the CRINT can still transfer the population even in the absence of the quantum impedance matching condition; the only caveat is that the number of photons required under this condition could be potentially large to make the transfer probability close to one.

4.3.2 STIRAP

Getting an anlytical result for the STIRAP process is very hard: it involves solving five coupled differential equations (Eq.(4.34)–Eq.(4.38)). However, using adiabatic approximation appropriately, we can reduce them to two. In terms of the dimensionless coupling rates, the relevant STIRAP equations are

$$\left\langle \dot{J} \right\rangle = -2\frac{\left((X\bar{n} f_1(t)^2 + \bar{m} f_2(t)^2)\, J + \sqrt{X\bar{m}\bar{n}} f_1(t) f_2(t) \right)}{1 + X + Y + Z}, \tag{4.48}$$

$$\begin{aligned} \langle \dot{\sigma_{z1}} \rangle = -\frac{4(X+Y)\bar{m} f_2(t)^2}{(1+X+Y+Z)^2} + 4\langle J \rangle \frac{f_1(t) f_2(t) \sqrt{X\bar{m}\bar{n}}\,(1+Z-X-Y)}{(1+X+Y+Z)^2} \\ - 4\langle \sigma_{z1} \rangle \frac{(X+Y)\bar{m} f_2(t)^2 + X(1+Z)\bar{n} f_1(t)^2}{(1+X+Y+Z)^2}. \end{aligned} \tag{4.49}$$

Although I was able to bring down the number of equations, it is still hard to integrate remaining equations; except when both the Stokes and the pump photons have the square pulse profile or when the net coupling rate of the first leg is equal to the net coupling rate of the second leg ($\gamma_1 + \gamma_3 = \gamma_2 + \gamma_4$). Ignoring the external decays ($Y = Z = 0$) for simplicity I will consider the first case, where both the Stokes and the pump are identical square pulses.

Let $f_1(t) = \Theta(t)\Theta(1-t)$, and $f_2(t) = \Theta(t+\tau)\Theta(1-\tau-t)$; where τ denotes the pulse separation.The formal solution of Eq.(4.49), with initial condition $\langle \sigma_{z1}(0) \rangle = -1$, can be written as

$$\begin{aligned} \sigma_z(\infty) = -e^{-4X(\bar{m}+\bar{n})/(1+X)^2} \Bigg[1 + \frac{4X\bar{m}}{(1+X)^2} \int_{-\infty}^{\infty} dt' f_2(t')^2 e^{4X\left(\int_{-\infty}^{t'} \bar{m} f_2(y)^2 dy + \bar{n} f_1(y)^2 dy\right)/(1+X)^2} \\ - 4\frac{\sqrt{X\bar{m}\bar{n}}\,(1-X)}{(1+X)^2} \int_{-\infty}^{\infty} dt' e^{4X\left(\int_{-\infty}^{t'} \bar{m} f_2(y)^2 dy + \bar{n} f_1(y)^2 dy\right)/(1+X)^2} \langle J(t') \rangle\, f_1(t') f_2(t') \Bigg] \end{aligned} \tag{4.50}$$

Case 1: $0 < \tau < 1$

This is the genuine STIRAP situation. All that we required at this stage is the expectation value $\langle J(t)\rangle$, which in this case is

$$\langle J(t)\rangle = -\frac{\sqrt{X\bar{m}\bar{n}}}{\bar{m}+\bar{n}X}\left(1-e^{-2(\bar{m}t+\bar{n}Xt)/(1+X)}\right). \tag{4.51}$$

Now that we have an expression for the expectation value of the coherence operator J, the integrals in Eq.(4.50) can be easily carried out, and the Final form of the transfer probability is

$$\begin{aligned} P_T =& 1-\frac{1}{\bar{m}+\bar{n}}\left(\bar{n}e^{-4X(\bar{m}+\bar{n}-\bar{m}\tau)/(1+X)^2}+\bar{m}e^{-4X\bar{n}\tau/(1+X)^2}\right) \\ &+\frac{\bar{m}\bar{n}\,e^{-4X(\bar{m}+\bar{n}-\bar{m}\tau)/(1+X)^2}}{(\bar{m}+\bar{n})(\bar{m}^2-\bar{n}^2X^2)}\times\left[(1+X)(\bar{m}+\bar{n}X)\right] \\ &-\frac{\bar{m}\bar{n}\,e^{-4X(\bar{m}+\bar{n}-\bar{m}\tau)/(1+X)^2}}{(\bar{m}+\bar{n})(\bar{m}^2-\bar{n}^2X^2)}\times\left[(1-X)(\bar{m}-\bar{n}X)e^{4X(\bar{m}+\bar{n})(1-\tau)/(1+X)^2}\right] \\ &-\frac{\bar{m}\bar{n}\,e^{-4X(\bar{m}+\bar{n}-\bar{m}\tau)/(1+X)^2}}{(\bar{m}+\bar{n})(\bar{m}^2-\bar{n}^2X^2)}\times\left[2X(\bar{m}+\bar{n})e^{-2(1-\tau)(1-X)(\bar{m}-\bar{n}X)/(1+X)^2}\right] \end{aligned} \tag{4.52}$$

Case 1: $\tau > 1$

This is the CRINT limit of STIRAP, which can be immediately obtained from Eq.(4.52) by taking the limit of the transfer probability at $\tau = 1$. With a little bit algebra one can show that

$$\lim_{\tau\to 1} P_T = 1-e^{-4\bar{n}X/(1+X)^2}. \tag{4.53}$$

This result is in agreement with the result that we obtained earlier in the CRINT case with no external decays (see Eq.(4.47)).

Similar to the semiclassical STIRAP, we expect that the optimized transfer probability

in the fully quantized version of the STIRAP should not depend on the pulse shapes. Hence, the analytical result that we obtained for the square pulse-STIRAP is sufficient to understand the behavior of optimized transfer probability of various other pulses. Finally, to get the optimized STIRAP transfer probability for the square pulse, we need to optimize the Eq.(4.52) numerically. However, for the rest of the pulses, one needs to integrate Eqs(4.48) and (4.49) and optimize the transfer probability numerically. Although we have restricted our discussion to the case where there are no external decays and the average number of photons in the fields are also small, it is possible to get the optimized results for other values by numerical integration of Eqs.(4.48) and (4.49). I will illustrate a special case of the STIRAP with external decay in the following section.

4.4 Bidirectional setup

A special case of the STIRAP with external decays is where $\gamma_1 = \gamma_3$ and $\gamma_2 = \gamma_4$. This situation is identical to a bidirectional STIRAP: we can relate the bath modes to those modes, which carry no excitation initially and are counter-propagating to the modes that constitute the initial photon wavepackets. Also, the rate at which these counter-propagating modes couple to the particular transition of the Λ-system is identical to the modes that form the initial wavepacket acting on that transition.

Although getting an analytical result is hard for this STIRAP case, it is possible to get a closed form solution when $\gamma_1 + \gamma_3 = \gamma_2 + \gamma_4$. Under this condition, it is easy to see from Eq.(4.48) that the coherence operator has no influence on the transfer probability, and with

a little bit algebra, one can show

$$\sigma_{z1}(\infty) = \frac{2X}{(1+X)^2} 2e^{2X/(1+X)^2(\bar{n}+\bar{m})} \int_{-\infty}^{\infty} f_1(t')^2 e^{2X/(1+X)^2 \int_{-\infty}^{t'} (\bar{n} f_1(t'')^2 + \bar{m} f_2(t''+\tau)^2)}. \quad (4.54)$$

It easy to verify from this expression that $\tau \to \infty$ maximizes the transfer probability $1 + \sigma_{z1}(\infty)$, and the resulting transfer probability is

$$P_T = 1 - e^{-2\bar{n}X/(1+X)^2}. \quad (4.55)$$

This CRINT result is not surprising: when the Λ-system satisfies the quantum impedance

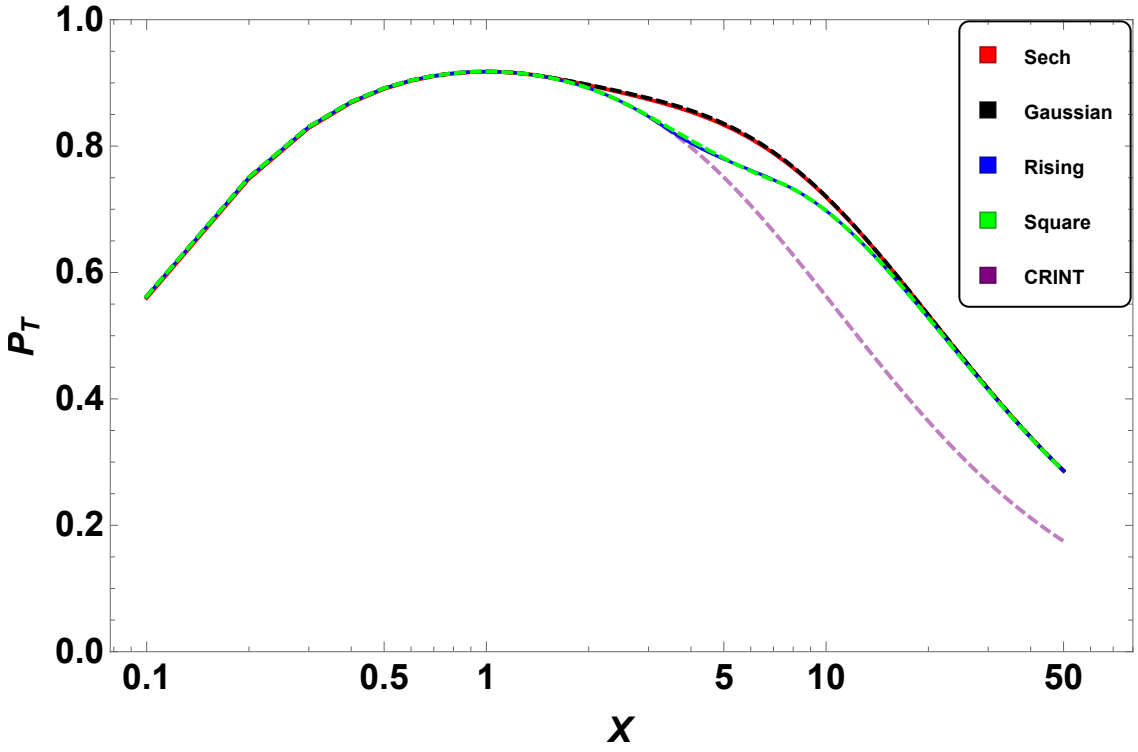

Figure 4.4: The optimized coherent SSTIRAP transfer probability, when the average number of photons in the pump and the Stokes field is 5, and the rate of external decay on a particular transition matches with the pulse mode coupling of that transition, as a function of the ratio of the coupling rates ($X = \gamma_1/\gamma_2$).

matching condition, the CRINT is very efficient and outperform the STIRAP. However, the CRINT in this bidirectional scenario requires twice the number photons to achieve the

efficiency of the CRINT in a single-sided setup with no external decay.To make a direct comparison with the SSTIRAP case, I have shown the transfer probability for this particular STIRAP case ($\gamma_1 = \gamma_3$ and $\gamma_2 = \gamma_4$), when both the Stokes and the pump fields have an average number of 5 photons in it ($\bar{n} = \bar{m} = 5$), as a function of $\gamma_1/\gamma_2 = X$ in FIG.3. Notice that the coherent STIRAP and the coressponding SSTIRAP have a lot in common: similar to the SSTIRAP case, the pulse shape has very little effect on the coherent STIRAP transfer probability. The values of X for which the pulse shape influences the transfer probability is the CRINT-STIRAP trade-off region. An additional point that is worth noting is that the behavior of coherent STIRAP, unlike to the SSTIRAP, is smooth for all pulses in the trade-off region.

Remarkably, for a fixed number of pump photons, one can boost the transfer probability to some extent in the purely STIRAP region ($X \gg 1$) by increasing the number of Stokes photons. As shown in Figure 4.5 (a), the STIRAP transfer probability, for a fixed number of pump photons ($\bar{n} = 5$), increases initially. However, it is evident from Figure 4.5 (b) that if we keep increasing the number of photons in the Stokes fields, the transfer probability starts decreasing after reaching a maximum value. In any case, the maximum boost that we can give to the transfer probability in the STIRAP region is still lower than the maximum that we can achieve with CRINT for the same total number of photons. Therefore, adding more photons to the pump field is more effective compared to adding more to the Stokes field in this case. For the case where the rates of coupling is different from the pulse mode coupling rates, it is difficult to get any analytical result, and I will not be discussing this topic in this thesis.

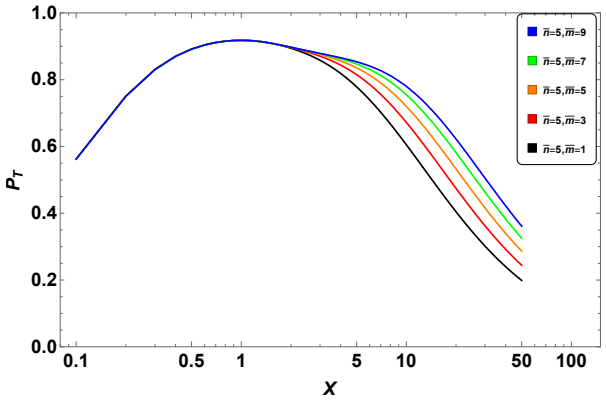

(a) Optimized bidirectional STIRAP transfer probability for a Gaussian pulse as a function of the ratio of coupling rates.

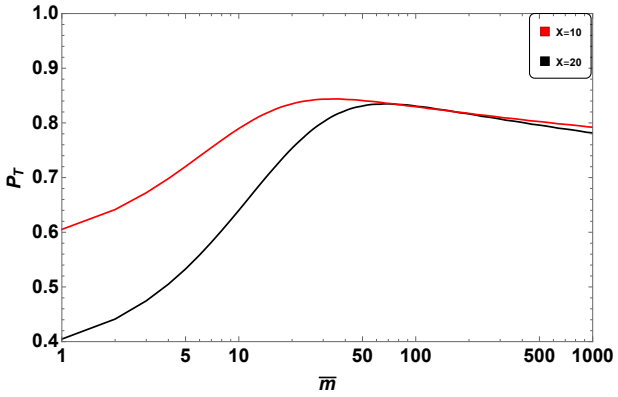

(b) Optimized bidirectional STIRAP transfer probability, as a function of the number of photons in the Stokes field.

Figure 4.5: The behavior of the optimized STIRAP transfer probability for a fixed number of pump photons ($\bar{n} = 5$) with an increasing number of photons in the Stokes field. In both these cases $\gamma_1 = \gamma_3$ and $\gamma_2 = \gamma_4$.

4.5 Conclusion

In conclusion, we have considered the effectiveness of a single photon in a single-sided geometry to transfer the population among the lower levels of the Λ-system using two process: the SPRINT, and SSTIRAP. With a fully quantized treatment, we have shown that the SPRINT, which is a limiting case of SSTIRAP, performs better than the SSTIRAP under ideal conditions. The SSTIRAP, which mimics the semiclassical STIRAP by sending two single photons of identical shape, can perform better than the SPRINT only in the region where the coupling rate of the first leg is much bigger than the coupling rate of the second leg ($\gamma_1 \gg \gamma_2$). However in the opposite limit, it is the SPRINT that optimizes the transfer. Furthermore, we have also obtained the earlier reported result of unit transfer probability [64] with the SPRINT when the coupling rates of both legs of the Λ-system are equal. As expected, the pulse shape has very little effect on the transfer

probability; except in the region where γ_1 is slightly bigger than γ_2. The range of values of γ_1/γ_2 for which the transfer probability does depend on the smoothness of the pulse, is where the SPRINT–STIRAP trade-off region.

Remarkably, the behavior of the transfer probability of the coherent state STIRAP is qualitatively identical to its single-photon counterpart: the SSTIRAP. Although, the CRINT, the coherent state version of the SPRINT, is not that effective when the average number of photons in the field is one (It is not a surprising result; since, for most of the time the number of photon in the field is zero), surprisingly, it transfers the population exponentially fast with increasing number of photons. Moreover, identical to the SPRINT, the performance of CRINT peaks when the coupling rates of both legs are the same. Another point that is worth mentioning is that the CRINT, unlike the SPRINT, can still transfer the population with near unit probability even in the absence of quantum impedance matching condition; the only catch is that it requires more number of photons.

The coherent STIRAP transfer probability in the pure STIRAP region ($X \gg 1$) is the other point that I want to emphasize. We have seen that it is possible to boost the probability in that region by increasing the number of Stokes photons. However, the maximum transfer probability corresponding to the optimum number of Stokes photons, for a specific value of $X \gg 1$ and pump photon ($\bar{n}$), is still less than the maximum we can obtain using the CRINT if we add all the Stokes photons to the pump pulse instead.

Chapter 5

Summary

In an optical quantum network, a confined atom could be used as a mediator to implement photon routing or a logic gate. It is known that, in interaction with a two-level system in a single-sided waveguide or optical cavity, a photon gets a π phase shift. I have explored the possibility of using a single control photon to switch this interaction on and off. The transient scheme that I considered in chapter 2 showed that the coherent control of the target photon's phase is possible, provided the control photon has the right pulse shape: the rising exponential pulse profile. At the single photon level, the rising exponential pulse is the only pulse that can invert an atom with unit probability. Therefore by timing both the target and the control with the right shape and pulse duration, we should be able to control the target photon's phase.

Furthermore, I have discussed, how one could use this transient excitation in an interferometric arrangement for routing the target photon. Although the interferometer setup that I discussed for routing a photon looks deceptively simple, it may require additional components, such as optical circulators for ensuring the unidirectionality of the modes. On the other hand, in the absence of a single control photon with the right shape, it is possible to achieve near unit excitation, within a time scale shorter than the characteristic decay rate of the upper level, by using larger numbers of photons. Surprisingly, the multiphoton excitation, analogous to the single photon result, is found to be dependent on the pulse shape as well as the statistics of the field. Therefore the routing probability, which in turn depends on the transient excitation probability in this routing

scheme, will critically depend on the shape of the pulse and the nature of the field. However, the nature of the field is not that important as it is hard to realize a multiphoton Fock state; it makes more sense to use a coherent state for describing a multiphoton process. Moreover, apart from a small term ($\pi^2/16N$, where N is the number of photons in the Fock state), which slightly improves the multiphoton Fock state excitation probability compared to the corresponding coherent-state, the behavior of the Fock state excitation probability is identical to the coherent state excitation probability. For all optimized pulses where the duration of the pulse is optimized, the way the transient excitation probability approaches one is inversely proportional to the number of photons (Fock state)/the average number of photons (coherent state) in the field. However, when the duration of the pulse is not optimized, the excitation probability still approaches 1, but the scaling, in this case, is less favorable.

Alternately, I discussed a scheme that involves an N-level system inside a single-sided geometry. In this scheme, the control field or multiple control fields act on the Λ-system and the target photon, whose phase we want to control, acts on the other transition. From the discussion, it was clear that the effectiveness of this system to act as a router depends critically on the ability of control field/fields to transfer the population among the lower levels of Λ-system. I have considered two schemes which mimics the semiclassical STIRAP for an effective population transfer.

The first scheme that I considered, SSTIRAP, which uses two single-photon pulses to imitate the semiclassical STIRAP, revealed some interesting results. A fully quantized version of the problem, where spontaneous emission is part of the framework, revealed that the counter-intuitive pulse sequence is effective in achieving the optimized transfer. This

result is strikingly different from the semiclassical STIRAP with no spontaneous emission; where both the intuitive and counter-intuitive schemes can successfully transfer the population. Another point that is worth noting is that at the single photon level it is the SPRINT, a single-photon scheme (which can be considered a limiting case of the single photon STIRAP) that transfers the population with unit probability. The only catch is that the SPRINT, where the Stokes photon has no role to play, requires both legs of the Λ-system to have the same coupling. Also, SPRINT is more efficient when the coupling strength of the first transition is smaller than the second one ($\gamma_2 \gg \gamma_1$). However, in the other limit when the coupling strength of the Stokes photon's transition is smaller than the other transition($\gamma_1 \gg \gamma_2$), it is the SSTIRAP that optimizes the transfer . Finally, apart from these two cases, there is an intermediate region where the pulse shape does influence the transfer probability: this is the SPRINT–SSTIRAP trade-off region. Another point that I want to emphasize is that adding more Stokes photons, in the absence of equal coupling and when we have a single pump photon, will not improve the optimized transfer substantially.

Additionally, I have also studied the transfer probability when the STIRAP is carried out with multiphoton coherent states. Remarkably, the coherent STIRAP behavior is qualitatively identical to that of SSTIRAP. In particular, we could see that the coherent state analog of SPRINT optimizes the transfer in the region where the SPRINT performance is superior to the SSTIRAP. However, in the opposite region, it is the coherent STIRAP with the counter-intuitive scheme that optimizes the transfer.

Finally, we have seen that under perfect conditions, neglecting the roles of optical elements that are needed to ensure the unidirectionality, both the schemes can succeed in

routing the target photon using a single control photon. However, the price that we need to pay in the transient scheme is that the control photon needs to have the right pulse shape; whereas, in the N-level scheme it is required that the legs of the Λ-system have the same coupling strengths. From the practical side, shaping a single photon pulse into a rising exponential shape is far more challenging compared to getting the identical coupling strengths required in an N-level scheme. With the recent advancements in the field of artificially engineered quantum systems, the latter is certainly possible. Moreover, if more than one photon is needed, the exponential scaling that we have seen with the permanent population transfer is much more favorable compared to the $1/N$ scaling obtained in the case of transient excitation.

Bibliography

[1] R. J. Thompson, G. Rempe, and H. J. Kimble. Observation of normal-mode splitting for an atom in an optical cavity. *Phys. Rev. Lett.*, 68:1132–1135, Feb 1992.

[2] H Mabuchi and AC Doherty. Cavity quantum electrodynamics: coherence in context. *Science*, 298(5597):1372–1377, 2002.

[3] Kevin M Birnbaum, Andreea Boca, Russell Miller, Allen D Boozer, Tracy E Northup, and H Jeff Kimble. Photon blockade in an optical cavity with one trapped atom. *Nature*, 436(7047):87, 2005.

[4] G Nogues, A Rauschenbeutel, S Osnaghi, M Brune, JM Raimond, and S Haroche. Seeing a single photon without destroying it. *Nature*, 400(6741):239, 1999.

[5] Christine Guerlin, Julien Bernu, Samuel Deleglise, Clement Sayrin, Sebastien Gleyzes, Stefan Kuhr, Michel Brune, Jean-Michel Raimond, and Serge Haroche. Progressive field-state collapse and quantum non-demolition photon counting. *Nature*, 448(7156):889, 2007.

[6] Alexandre Blais, Ren-Shou Huang, Andreas Wallraff, S. M. Girvin, and R. J. Schoelkopf. Cavity quantum electrodynamics for superconducting electrical circuits: An architecture for quantum computation. *Phys. Rev. A*, 69:062320, Jun 2004.

[7] Andreas Wallraff, David I Schuster, Alexandre Blais, Luigi Frunzio, R-S Huang, Johannes Majer, Sameer Kumar, Steven M Girvin, and Robert J Schoelkopf. Strong coupling of a single photon to a superconducting qubit using circuit quantum electrodynamics. *Nature*, 431(7005):162, 2004.

[8] SM Girvin, MH Devoret, and RJ Schoelkopf. Circuit qed and engineering charge-based superconducting qubits. *Physica Scripta*, 2009(T137):014012, 2009.

[9] Thomas Niemczyk, F Deppe, H Huebl, EP Menzel, F Hocke, MJ Schwarz, JJ Garcia-Ripoll, D Zueco, T Hümmer, E Solano, et al. Circuit quantum electrodynamics in the ultrastrong-coupling regime. *Nature Physics*, 6(10):772, 2010.

[10] Io-Chun Hoi, Tauno Palomaki, Joel Lindkvist, Göran Johansson, Per Delsing, and C. M. Wilson. Generation of nonclassical microwave states using an artificial atom in 1d open space. *Phys. Rev. Lett.*, 108:263601, Jun 2012.

[11] Dibyendu Roy, C. M. Wilson, and Ofer Firstenberg. Colloquium: Strongly interacting photons in one-dimensional continuum. *Rev. Mod. Phys.*, 89:021001, May 2017.

[12] Jung-tsung Shen and Shanhui Fan. Coherent photon transport from spontaneous emission in one-dimensional waveguides. *Optics letters*, 30(15):2001–2003, 2005.

[13] Marta Arcari, Immo Söllner, Alisa Javadi, S Lindskov Hansen, Sahand Mahmoodian, Jin Liu, Henri Thyrrestrup, Eun Hye Lee, Jin Dong Song, Søren Stobbe, et al. Near-unity coupling efficiency of a quantum emitter to a photonic crystal waveguide. *Physical review letters*, 113(9):093603, 2014.

[14] Alisa Javadi, I Söllner, Marta Arcari, S Lindskov Hansen, Leonardo Midolo, Sahand Mahmoodian, G Kiršanskė, Tommaso Pregnolato, EH Lee, JD Song, et al. Single-photon non-linear optics with a quantum dot in a waveguide. *Nature communications*, 6:8655, 2015.

[15] A. Laucht, S. Pütz, T. Günthner, N. Hauke, R. Saive, S. Frédérick, M. Bichler, M.-C. Amann, A. W. Holleitner, M. Kaniber, and J. J. Finley. A waveguide-coupled on-chip single-photon source. *Phys. Rev. X*, 2:011014, Mar 2012.

[16] M. Bajcsy, S. Hofferberth, V. Balic, T. Peyronel, M. Hafezi, A. S. Zibrov, V. Vuletic, and M. D. Lukin. Efficient all-optical switching using slow light within a hollow fiber. *Phys. Rev. Lett.*, 102:203902, May 2009.

[17] Julien Claudon, Joël Bleuse, Nitin Singh Malik, Maela Bazin, Périne Jaffrennou, Niels Gregersen, Christophe Sauvan, Philippe Lalanne, and Jean-Michel Gérard. A highly efficient single-photon source based on a quantum dot in a photonic nanowire. *Nature Photonics*, 4(3):174, 2010.

[18] A. Goban, K. S. Choi, D. J. Alton, D. Ding, C. Lacroûte, M. Pototschnig, T. Thiele, N. P. Stern, and H. J. Kimble. Demonstration of a state-insensitive, compensated nanofiber trap. *Phys. Rev. Lett.*, 109:033603, Jul 2012.

[19] Takao Aoki, AS Parkins, DJ Alton, CA Regal, Barak Dayan, E Ostby, Kerry J Vahala, and HJ Kimble. Efficient routing of single photons by one atom and a microtoroidal cavity. *Physical review letters*, 102(8):083601, 2009.

[20] Io-Chun Hoi, C. M. Wilson, Göran Johansson, Tauno Palomaki, Borja Peropadre, and Per Delsing. Demonstration of a single-photon router in the microwave regime. *Phys. Rev. Lett.*, 107:073601, Aug 2011.

[21] GS Agarwal and Sumei Huang. Optomechanical systems as single-photon routers. *Physical Review A*, 85(2):021801, 2012.

[22] Jing Lu, Lan Zhou, Le-Man Kuang, Franco Nori, et al. Single-photon router: Coherent control of multichannel scattering for single photons with quantum interferences. *Physical Review A*, 89(1):013805, 2014.

[23] Wei-Bin Yan and Heng Fan. Single-photon quantum router with multiple output ports. *Scientific reports*, 4:4820, 2014.

[24] GJ Milburn. Coherent control of single photon states. *The European Physical Journal Special Topics*, 159(1):113–117, 2008.

[25] KJ Blow, Rodney Loudon, Simon JD Phoenix, and TJ Shepherd. Continuum fields in quantum optics. *Physical Review A*, 42(7):4102, 1990.

[26] C. W. Gardiner and P. Zoller. *Quantum Noise*. Springer, second edition, 2000.

[27] Julio Gea-Banacloche. Atom in waveguide interacting with multiphoton pulse. *Unpublished*, 2014.

[28] Peter Domokos, Peter Horak, and Helmut Ritsch. Quantum description of light-pulse scattering on a single atom in waveguides. *Phys. Rev. A*, 65:033832, Mar 2002.

[29] Alexandre Roulet and Valerio Scarani. Solving the scattering of n photons on a two-level atom without computation. *New Journal of Physics*, 18(9):093035, 2016.

[30] J. T. Shen and Shanhui Fan. Coherent photon transport from spontaneous emission in one-dimensional waveguides. *Opt. Lett.*, 30(15):2001–2003, Aug 2005.

[31] Jung-Tsung Shen and Shanhui Fan. Coherent single photon transport in a one-dimensional waveguide coupled with superconducting quantum bits. *Phys. Rev. Lett.*, 95:213001, Nov 2005.

[32] Zeyang Liao, Xiaodong Zeng, Hyunchul Nha, and M Suhail Zubairy. Photon transport in a one-dimensional nanophotonic waveguide qed system. *Physica Scripta*, 91(6):063004, 2016.

[33] Dibyendu Roy, Christopher M Wilson, and Ofer Firstenberg. Colloquium: Strongly interacting photons in one-dimensional continuum. *Reviews of Modern Physics*, 89(2):021001, 2017.

[34] Mikhail Pletyukhov and Vladimir Gritsev. Quantum theory of light scattering in a one-dimensional channel: Interaction effect on photon statistics and entanglement entropy. *Physical Review A*, 91(6):063841, 2015.

[35] Mikhail Pletyukhov and Vladimir Gritsev. Scattering of massless particles in one-dimensional chiral channel. *New Journal of Physics*, 14(9):095028, 2012.

[36] Yue Chang, Alejandro González-Tudela, Carlos Sánchez Muñoz, Carlos Navarrete-Benlloch, and Tao Shi. Deterministic down-converter and continuous photon-pair source within the bad-cavity limit. *Physical review letters*, 117(20):203602, 2016.

[37] T Shi and CP Sun. Lehmann-symanzik-zimmermann reduction approach to multiphoton scattering in coupled-resonator arrays. *Physical Review B*, 79(20):205111, 2009.

[38] Tian Feng See, Changsuk Noh, and Dimitris G Angelakis. Diagrammatic approach to multiphoton scattering. *Physical Review A*, 95(5):053845, 2017.

[39] Huaixiu Zheng, Daniel J Gauthier, and Harold U Baranger. Waveguide qed: Many-body bound-state effects in coherent and fock-state scattering from a two-level system. *Physical Review A*, 82(6):063816, 2010.

[40] Shanshan Xu and Shanhui Fan. Input-output formalism for few-photon transport: A systematic treatment beyond two photons. *Physical Review A*, 91(4):043845, 2015.

[41] Shanhui Fan, Şükrü Ekin Kocabaş, and Jung-Tsung Shen. Input-output formalism for few-photon transport in one-dimensional nanophotonic waveguides coupled to a qubit. *Physical Review A*, 82(6):063821, 2010.

[42] Michael P Schneider, Tobias Sproll, Christina Stawiarski, Peter Schmitteckert, and Kurt Busch. Green's-function formalism for waveguide qed applications. *Physical Review A*, 93(1):013828, 2016.

[43] Tommaso Caneva, Marco T Manzoni, Tao Shi, James S Douglas, J Ignacio Cirac, and Darrick E Chang. Quantum dynamics of propagating photons with strong interactions: a generalized input–output formalism. *New Journal of Physics*, 17(11):113001, 2015.

[44] Yu Pan, Daoyi Dong, and Guofeng Zhang. Exact analysis of the response of quantum systems to two-photons using a qsde approach. *New Journal of Physics*, 18(3):033004, 2016.

[45] Tao Shi, Darrick E Chang, and J Ignacio Cirac. Multiphoton-scattering theory and generalized master equations. *Physical Review A*, 92(5):053834, 2015.

[46] Ben Q Baragiola, Robert L Cook, Agata M Brańczyk, and Joshua Combes. N-photon wave packets interacting with an arbitrary quantum system. *Physical Review A*, 86(1):013811, 2012.

[47] William Konyk and Julio Gea-Banacloche. Quantum multimode treatment of light scattering by an atom in a waveguide. *Physical Review A*, 93(6):063807, 2016.

[48] Anders Nysteen, Philip Trøst Kristensen, Dara PS McCutcheon, Per Kaer, and Jesper Mørk. Scattering of two photons on a quantum emitter in a one-dimensional waveguide: exact dynamics and induced correlations. *New Journal of Physics*, 17(2):023030, 2015.

[49] Julio Gea-Banacloche. Space-time descriptions of quantum fields interacting with optical cavities. *Phys. Rev. A*, 87:023832, Feb 2013.

[50] Gerd Leuchs and Markus Sondermann. Time-reversal symmetry in optics. *Physica Scripta*, 85(5):058101, 2012.

[51] Juan Ignacio Cirac, Peter Zoller, H Jeff Kimble, and Hideo Mabuchi. Quantum state transfer and entanglement distribution among distant nodes in a quantum network. *Physical Review Letters*, 78(16):3221, 1997.

[52] Magdalena Stobińska, Gernot Alber, and Gerd Leuchs. Perfect excitation of a matter qubit by a single photon in free space. *EPL (Europhysics Letters)*, 86(1):14007, 2009.

[53] Simon Heugel, Alessandro S Villar, Markus Sondermann, Ulf Peschel, and Gerd Leuchs. On the analogy between a single atom and an optical resonator. *Laser Physics*, 20(1):100–106, 2010.

[54] Shanchao Zhang, Chang Liu, Shuyu Zhou, Chih-Sung Chuu, Michael MT Loy, and Shengwang Du. Coherent control of single-photon absorption and reemission in a two-level atomic ensemble. *Physical review letters*, 109(26):263601, 2012.

[55] Marianne Bader, Simon Heugel, Alexander L Chekhov, Markus Sondermann, and Gerd Leuchs. Efficient coupling to an optical resonator by exploiting time-reversal symmetry. *New Journal of Physics*, 15(12):123008, 2013.

[56] Syed Abdullah Aljunid, Gleb Maslennikov, Yimin Wang, Hoang Lan Dao, Valerio Scarani, and Christian Kurtsiefer. Excitation of a single atom with exponentially rising light pulses. *Physical review letters*, 111(10):103001, 2013.

[57] J. Wenner, Yi Yin, Yu Chen, R. Barends, B. Chiaro, E. Jeffrey, J. Kelly, A. Megrant, J. Y. Mutus, C. Neill, P. J. J. O'Malley, P. Roushan, D. Sank, A. Vainsencher, T. C. White, Alexander N. Korotkov, A. N. Cleland, and John M. Martinis. Catching time-reversed microwave coherent state photons with 99.4absorption efficiency. *Phys. Rev. Lett.*, 112:210501, May 2014.

[58] Chang Liu, Yuan Sun, Luwei Zhao, Shanchao Zhang, MMT Loy, and Shengwang Du. Efficiently loading a single photon into a single-sided fabry-perot cavity. *Physical review letters*, 113(13):133601, 2014.

[59] Victor Leong, Mathias Alexander Seidler, Matthias Steiner, Alessandro Cere, and Christian Kurtsiefer. Time-resolved scattering of a single photon by a single atom. *Nature communications*, 7:13716, 2016.

[60] Yimin Wang, Ji ří Minář, Lana Sheridan, and Valerio Scarani. Efficient excitation of a two-level atom by a single photon in a propagating mode. *Phys. Rev. A*, 83:063842, Jun 2011.

[61] Hemlin Swaran Rag and Julio Gea-Banacloche. Two-level-atom excitation probability for single- and n-photon wave packets. *Phys. Rev. A*, 96:033817, Sep 2017.

[62] Milton Abramowitz and Irene A Stegun. *Handbook of mathematical functions: with formulas, graphs, and mathematical tables*, volume 55. Courier Corporation, 1965.

[63] U Gaubatz, P Rudecki, S Schiemann, and K Bergmann. Population transfer between molecular vibrational levels by stimulated raman scattering with partially overlapping laser fields. a new concept and experimental results. *The Journal of Chemical Physics*, 92(9):5363–5376, 1990.

[64] Dorothea Pinotsi and Atac Imamoglu. Single photon absorption by a single quantum emitter. *Physical review letters*, 100(9):093603, 2008.

[65] Kazuki Koshino, Satoshi Ishizaka, and Yasunobu Nakamura. Deterministic photon-photon swap gate using a λ system. *Physical Review A*, 82(1):010301, 2010.

[66] Serge Rosenblum, Adrien Borne, and Barak Dayan. Analysis of deterministic swapping of photonic and atomic states through single-photon raman interaction. *Phys. Rev. A*, 95:033814, Mar 2017.

[67] Bruce W. Shore. Picturing stimulated raman adiabatic passage: a stirap tutorial. *Adv. Opt. Photon.*, 9(3):563–719, Sep 2017.

[68] P. A. Ivanov, N. V. Vitanov, and K. Bergmann. Spontaneous emission in stimulated raman adiabatic passage. *Phys. Rev. A*, 72:053412, Nov 2005.